

D2-118470-2

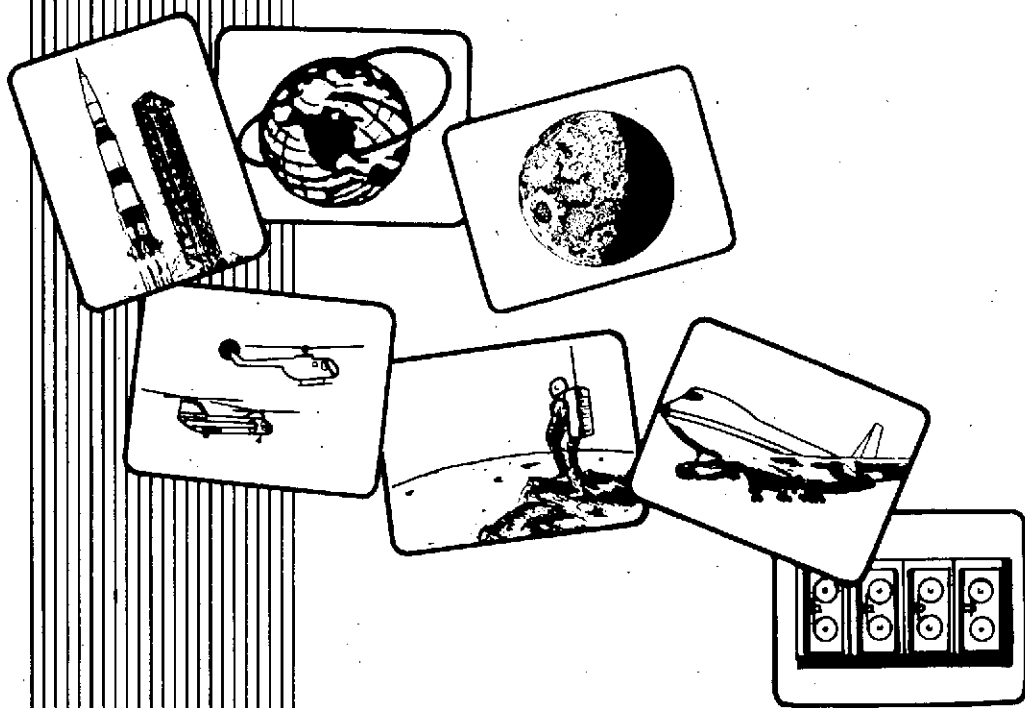
NASA CR-  
140286

ANALYSES OF THE DYNAMIC DOCKING  
TEST SYSTEM FOR ADVANCED MISSION  
DOCKING SYSTEM TEST PROGRAMS

(NASA-CR-140286) ANALYSES OF THE DYNAMIC  
DOCKING TEST SYSTEM FOR ADVANCED MISSION  
DOCKING SYSTEM TEST PROGRAMS (Boeing  
Aerospace Co., Houston, Tex.) 96 p HC  
\$8.00

N74-33775  
Unclas  
49641

CSCL 14B G3/11



THE **BOEING** COMPANY  
HOUSTON, TEXAS

August 30, 1974

DOCUMENT NO. D2-118470-2

ANALYSES OF THE DYNAMIC DOCKING TEST SYSTEM  
FOR ADVANCED MISSION DOCKING SYSTEM TEST PROGRAMS


Contract NAS 9-13136

August 30, 1974

Prepared by

R. M. Gates  
J. E. Williams

Approved by

  
\_\_\_\_\_  
R. K. Nuno  
Technical Program Manager

BOEING AEROSPACE COMPANY  
Houston, Texas

REVISIONS

REV. SYM	DESCRIPTION	DATE	APPROVED

## ABSTRACT

This document presents the results of analytical studies performed in support of the design, implementation, checkout and use of NASA's Dynamic Docking Test System (DDTS) during the period July 1, 1973 to June 30, 1974. Included are analyses of simulator components, a list of detailed operational test procedures written, a summary of simulator performance, and an analysis and comparison of docking dynamics and loads obtained by test and analysis.

This report was prepared for the National Aeronautics and Space Administration by Boeing Aerospace Company in fulfillment of the requirements of Exhibit B of Contract NAS 9-13136.

## KEY WORDS

Docking Simulator  
Dynamic Docking Test System (DDTS)  
Hydraulic Actuators  
Servosystems  
Structural Analysis  
System Analysis

## TABLE OF CONTENTS

<u>PARAGRAPH</u>		<u>PAGE</u>
	REVISIONS	ii
	ABSTRACT AND KEY WORDS	iii
	TABLE OF CONTENTS	iv
	LIST OF ILLUSTRATIONS	v
	LIST OF TABLES	vii
	REFERENCES	viii
1.0	INTRODUCTION	1
2.0	BACKGROUND INFORMATION	2
2.1	DDTS DESCRIPTION	2
2.2	APOLLO SOYUZ TEST PROJECT DOCKING SYSTEM	2
3.0	SYSTEM ANALYSES	6
3.1	STRUCTURAL ANALYSES	6
3.2	SINGLE ACTUATOR ANALYSES	8
3.3	ACTIVE TABLE ANALYSES	26
3.4	TOTAL SYSTEM STABILITY ANALYSIS	42
4.0	DETAILED OPERATIONAL TEST PROCEDURES	51
4.1	PROCEDURES DOCUMENT CONTENTS	51
4.2	TEST REQUIREMENTS AND OPERATIONAL TEST PROCEDURES	52
5.0	ANALYSIS OF DOCKING DYNAMICS AND LOADS	55
5.1	DEVELOPMENT TESTS	55
5.2	10 HZ INVESTIGATION	72
5.3	US/US QUALIFICATION TEST	80
6.0	CONCLUSIONS AND RECOMMENDATIONS	87

## ILLUSTRATIONS

<u>FIGURE</u>		<u>PAGE</u>
2-1	DDTS Simulator Facility	3
2-2	System Block Diagram of DDTS	4
2-3	ASTP Docking Mechanism	5
3-1	Single-Axis Servo Block Diagram	9
3-2	Displacement-to-Pressure Frequency Response	10
3-3	Circuit Diagram, Twin Gyrator Notch Filter	11
3-4	Twin Gyrator Notch Filter Frequency Response	12
3-5	Single Actuator Frequency Response, Displacement Open Loop	13
3-6	Single Actuator Frequency Response, Pressure Open Loop	14
3-7	Single Actuator Frequency Response, Closed Loop	16
3-8	Single Actuator Frequency Response, Including Rate Command	17
3-9	Single Actuator Closed Loop Frequency Response, Forward Loop Gain Variation	19
3-10	Single Actuator Frequency Response, Position Open Loop, Hydraulic Bleed Orifice Variation	20
3-11	Single Actuator Frequency Response, Pressure Open Loop, Hydraulic Bleed Orifice Variation	21
3-12	Rate Command First Order Lag Filter Characteristics	22
3-13	Single Actuator Frequency Response, Including Rate Command Filter A	23
3-14	Single Actuator Frequency Response, Including Rate Command Filter B	24
3-15	Rate Command Notch Filter Characteristics	25
3-16	Single Actuator Frequency Response, Including Rate Command Filter C	27
3-17	Table Displacement Frequency Response	29
3-18	Table Accelerations, Frequency Response Test	30
3-19	Actuator Accelerations, Frequency Response Test	31
3-20	Angle Limit Abort Switch	33
3-21	Table Coordinate System and Definition of Actuator Lengths	35

## ILLUSTRATIONS (Continued)

<u>FIGURE</u>		<u>PAGE</u>
3-22	TABGEOM Listing	38
3-23	Limit Switch Setting to Prevent Table Fall Through, Actuator 1, 3 and 5	41
3-24	Limit Switch Setting to Prevent Table Fall Through, Actuator 2, 4 and 6	41
3-25	Total System Block Diagram	43
3-26	Total System Stability, Near Full Extension	47
3-27	Total System Stability, Full Extension (Tension)	48
3-28	Total System Stability, Full Retract	49
5-1	Typical Test/Analysis Correlation, US-USSR Development Test, USA Active Case 3, Hot; X Force on CSM C.G.	62
5-2	Typical Test/Analysis Correlation, US-USSR Development Test, USA Active Case 3, Hot; Y Force on CSM C.G.	63
5-3	Typical Test/Analysis Correlation, US-USSR Development Test, USA Active Case 3, Hot; Z Force on CSM C.G.	64
5-4	Typical Test/Analysis Correlation, US-USSR Development Test, USA Active Case 2, Hot; X Force on CSM C.G.	65
5-5	Typical Test/Analysis Correlation, US-USSR Development Test, USA Active Case 2; Y Force on CSM C.G.	67
5-6	Typical Test/Analysis Correlation, US-USSR Development Test, USA Active Case; Z Force on CSM C.G.	69
5-7	Effect of Rate Command Gain on Load	75
5-8	Effect of Rate Gain on Peak Load, Case 16	77
5-9	Effect of Rate Gain on Peak Load, Case 3	78
5-10	Effect of Rate Gain on Peak Load, Case 5	79
5-11	Typical Test Results Without Rate Command Filter	81
5-12	Typical Test Results with Notch Filter in Rate Command Line	82
5-13	US-US Qualification Case 9 (-Y Miss, High Energy) Without Rate Command Filter (a) and With Notch Filter (b)	83

## TABLES

		<u>PAGE</u>
3-1	SINGLE ACTUATOR PARAMETERS	18
3-2	FLOOR SWIVEL JOINT LOCATIONS	40
3-3	ACTIVE TABLE SWIVEL JOINT LOCATIONS	40
5-1	US/US DEVELOPMENT TEST CONDITIONS	57
5-2	US/USSR DEVELOPMENT TEST CONDITIONS	59
5-3	LOCATION OF DOCUMENTED TEST DATA US/USSR DEVELOPMENT TEST - USSR ACTIVE	60
5-5	US/USSR DEVELOPMENT TEST DATA/MATH MODEL COMPARISON	71
5-6	US/US QUALIFICATION TEST CONDITIONS	84
5-7	US/US QUALIFICATION TEST DATA MATH MODEL COMPARISON	85



## REFERENCES

1. Boeing Document D2-118470-1, "Analysis of the Dynamic Docking Test System for Advanced Mission Docking System Test Programs," August 1973.
2. Boeing Document D2-118544-1, "Mathematical Model for the Simulation of Dynamic Docking Test System Active Table Motion," August 1974.
3. Boeing Document D2-118544-2, "Dynamic Docking Test System Active Table Motion Computer Program, NASA Advanced Docking System (NADS)," August 1974.
4. Boeing Document, D2-118546-1, "Dynamic Docking Test System Active Table Frequency Response Test Results," August 1974.
5. Boeing Document D2-118465-1, "Assembling, Integrating and Editing the Checkout Test Requirements and Detailed Test Procedures for the Dynamic Docking Test System," June 1973.
6. Boeing Document D2-118482-1, "Assembling and Editing Operational Test Procedures Utilizing Administrative Terminal System for the Dynamic Docking Test System," January 1974.
7. Boeing Document D2-118482-2, "Assembling and Editing Operational Test Procedures Utilizing Administrative Terminal System for the Dynamic Docking Test System," January 1974.
8. IED 50009-1, "Apollo Soyuz Joint Development Test Plan, Docking Systems
9. Structural Test Branch, Johnson Space Center, Houston, Texas, ES6
10. USA WG3-018, "DDTS Joint Development Test Data, USA Docking System Active," January 29, 1974.
11. USSR WG3-022, "DDTS Joint Development Test Data USSR Docking System Active," January 22, 1974.
12. Boeing Memorandum 5-2920-HOU-087, "Joint US/USSR Development Test Data/Math Model Correlation," dated August 30, 1974.

## 1.0 INTRODUCTION

This report presents the results of analytical studies performed between July 1, 1973 and June 30, 1974 to fulfill the requirements of Contract NAS 9-13136. The purpose of this R&D contract was to perform system analyses, to provide general technical support for implementation of NASA's DDTS, and to assemble detailed operational test procedures.

Included in this report are:

- a. Structural analyses of simulator components
- b. Servo actuator performance studies
- c. Active table motion analysis
- d. System stability analysis
- e. Analysis of docking dynamics and loads

This work is a continuation of the work performed between July 3, 1972 and June 29, 1973 under Contract NAS 9-13136 and documented in Reference 1.

## 2.0 BACKGROUND INFORMATION

### 2.1 DOTS DESCRIPTION

The DOTS is a large motion, real-time docking simulator built by NASA JSC for full-scale testing of advanced docking systems. Figure 2-1 illustrates the hardware configuration of the DOTS simulator. Docking motions are simulated by virtue of six linear hydraulic actuators driving the active table. Each actuator is capable of an 84-in. stroke. Note that because of the hardware geometry, table displacements can be much larger than the displacement capability of an individual actuator. Interaction forces between the docking mechanisms are measured by load cells and transmitted to a hybrid computer which contains rigid body equations of motion that predict the responses of the two docking vehicles. The real-time spacecraft motions are then transformed to equivalent actuator motions which are then transmitted as commands to the hydraulic servosystems. Figure 2-2 illustrates the sequence of events and interactions between the primary system components.

### 2.2 APOLLO SOYUZ TEST PROJECT DOCKING SYSTEM

The Apollo Soyuz Test Project (ASTP) docking mechanism is illustrated in Figure 2-3. The mechanism would be in the retracted position on the passive docking vehicle and the extended position on the active docking vehicle. The three guides on each spacecraft serve to align the spacecraft to the proper orientation. Upon docking ring contact, the capture latches are triggered, holding the passive vehicle to the active docking ring. The active docking ring is then retracted until the structural latches and body latches are activated. The body latches retain the docking ring in the retracted position while the structural latches hold the two spacecraft together.

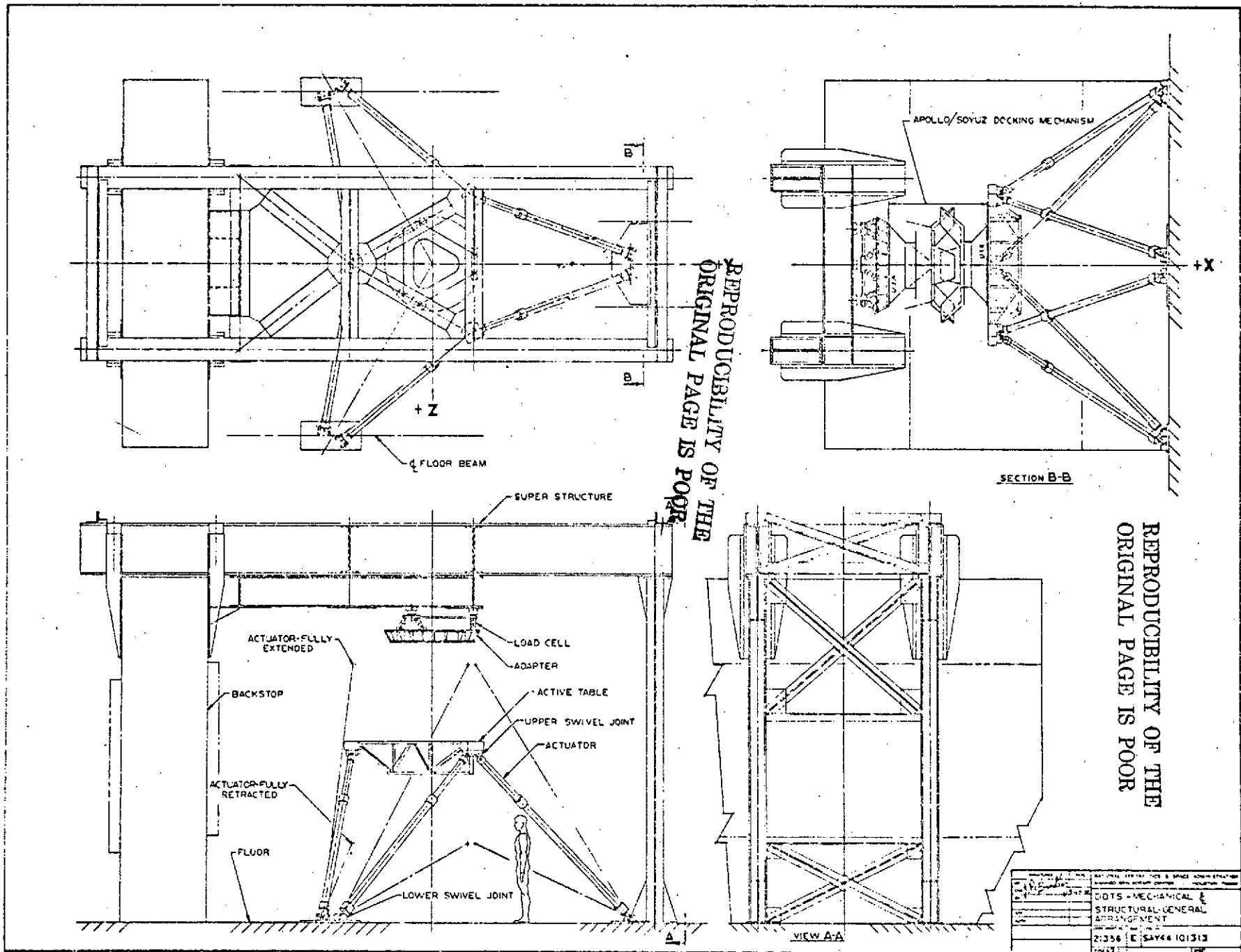


Figure 2-1. DDTs Simulator Facility

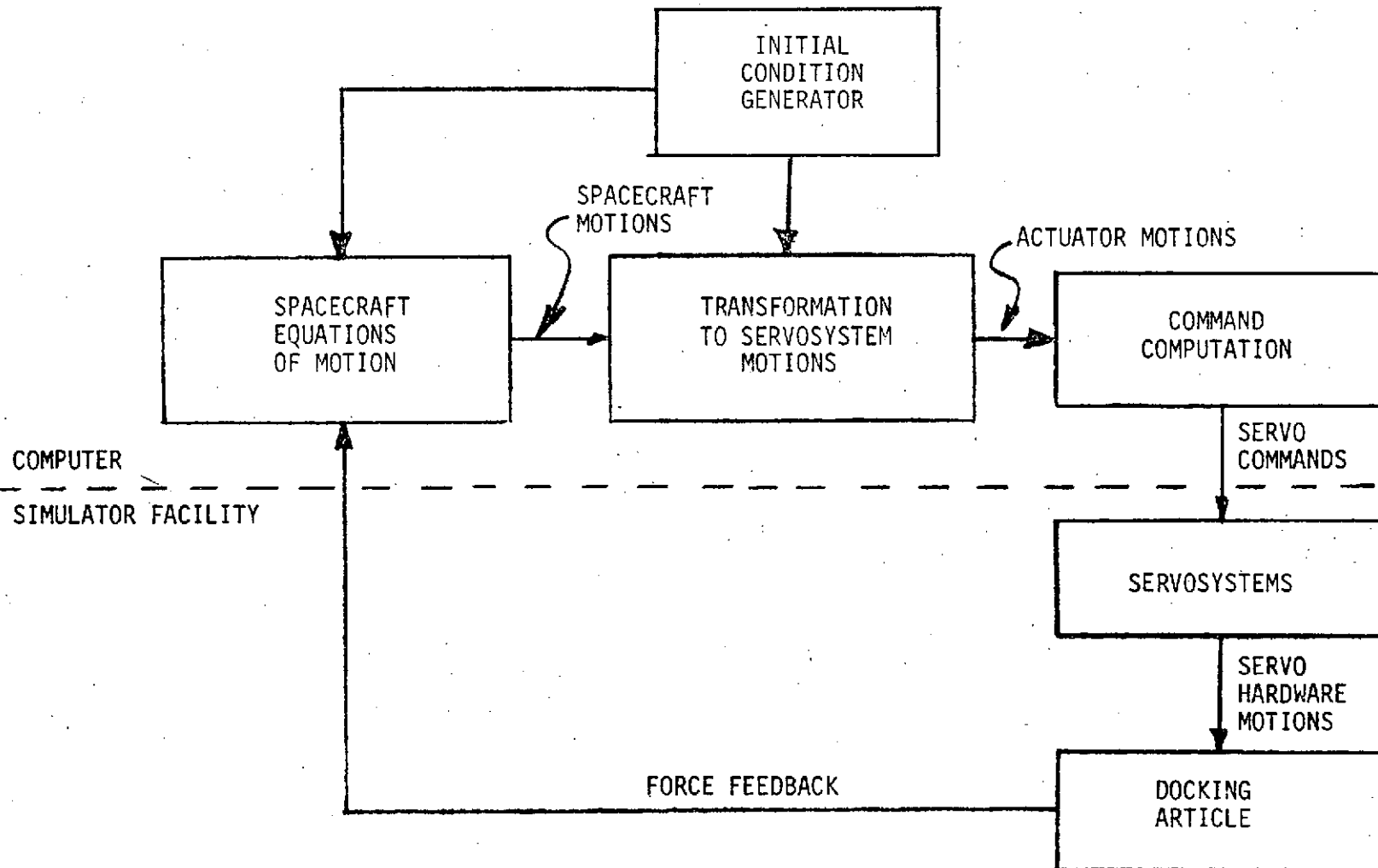
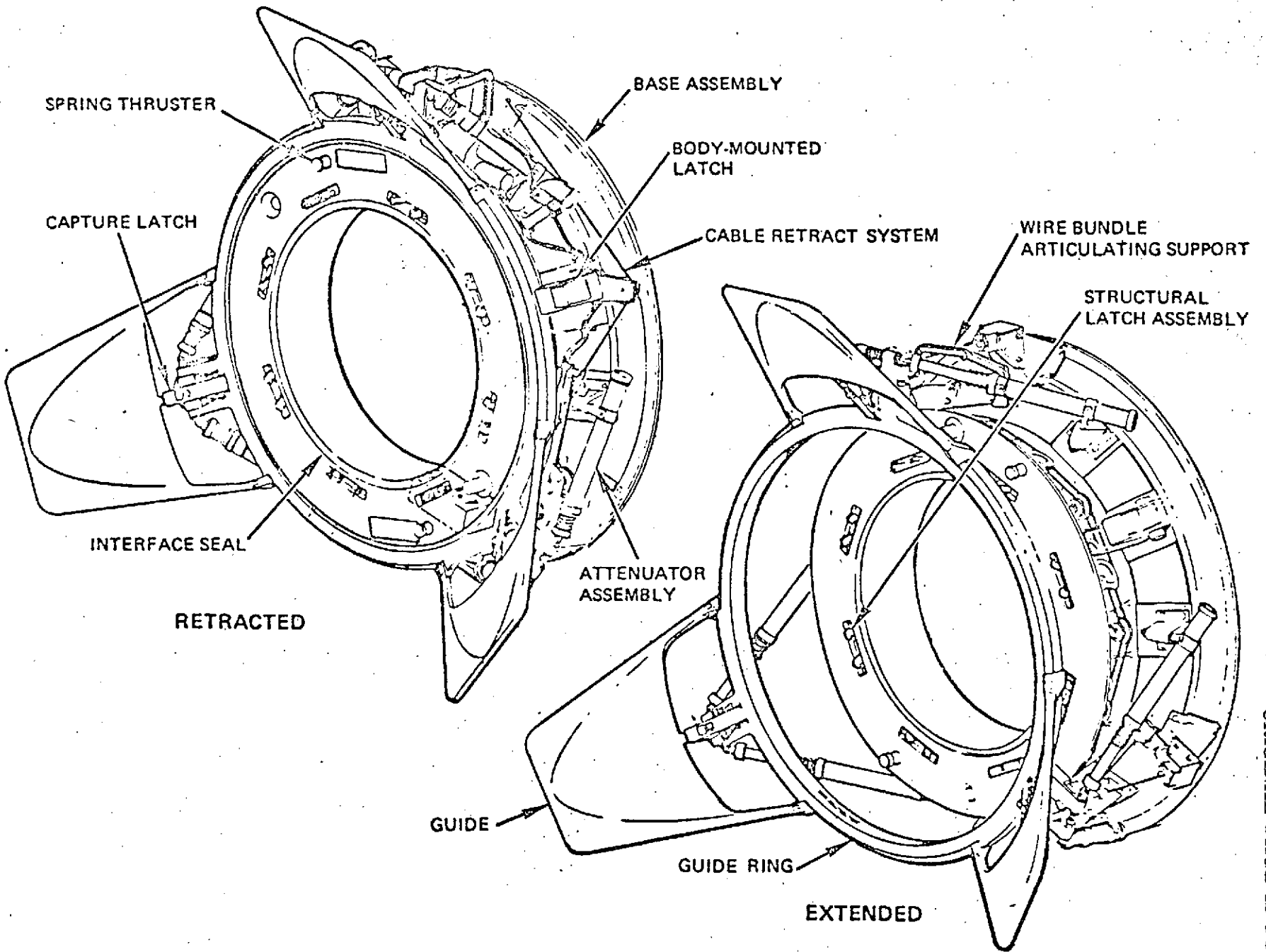


Figure 2-2. System Block Diagram of DDTS

D2-118470-2

-4-



-5-

Figure 2-3. ASTP Docking Mechanism

D2-118470-2  
 REPRODUCIBILITY OF THE ORIGINAL PAGE IS POOR

### 3.0 SYSTEM ANALYSES

#### 3.1 STRUCTURAL ANALYSES

This section contains a brief discussion of miscellaneous stress and stiffness analyses conducted to substantiate the structural adequacy of DDTS components not completed when the Reference 1 document was published. The intent of this section is not to present a formal analysis of each structural component analyzed, but to summarize the results of the analyses and verify that the structural integrity of the components was investigated and that they do comply with the design criteria established for the DDTS.

##### 3.1.1 Docking System Mass Properties Simulator

The mass properties simulator as originally designed, Dwg. SAY 44101320\* dated March 2, 1973, was found to be structurally inadequate from both a strength and stiffness standpoint. However, by adding the clamp assembly defined in Dwg. SAY 44101346 for stiffness and by adding stiffness in the cylinder-to-mass support rod attachment point area, the as-built mass properties simulator is structurally acceptable. The natural frequency of the system is estimated to be around 60 Hz and will, therefore, not couple with simulator structural dynamics. After the above-mentioned modifications were incorporated, the bending strength in the area of the attachment points was also adequate.

##### 3.1.2 Actuator Check Valve and Manifold Block

A stress analysis was performed on the manifold block, Dwg. SDF 36111292\* and check valve (modification - Teledyne Republic Modification P/N 412-1D2-6) shown in Dwg. DDTS 620.

---

\*Denote NASA-JSC drawings

## 3.1.2 (Continued)

Analysis of the manifold blocks showed that they will be structurally adequate as long as the pressurized passages are no closer than .2 inch to adjacent holes.

The modified check valve was also found structurally adequate with the following factors of safety:

Factor of Safety

	Working Pressure=3000 psi*	Proof Pressure=4500 psi*	Burst Pressure=7500 psi*
Ultimate	4.97	3.31	1.99
Yield	3.57	2.38	1.43

\*Teledyne specification

3.1.3 Adapter for USSR Docking Mechanism on DDTS

The subject adapter, Dwg. SAY 44101319, was analyzed and found to be structurally adequate.

3.1.4 DDTS Environmental Enclosure

A detailed analysis of the environmental enclosure, Dwg. SAY 44101431, indicated that all components of the structure, including the standpipe, are structurally adequate with respect to both strength and stiffness.



## 3.2 SINGLE ACTUATOR ANALYSES

The single-axis servo loop mathematical model discussed in Reference 1 was revised to include differential pressure feedback. The block diagram of this linear math model is shown in Figure 3-1. This model was used to perform open and closed loop analyses of the servo loop and to establish actuator parameters for the six-degree-of-freedom table motion model which will be discussed later.

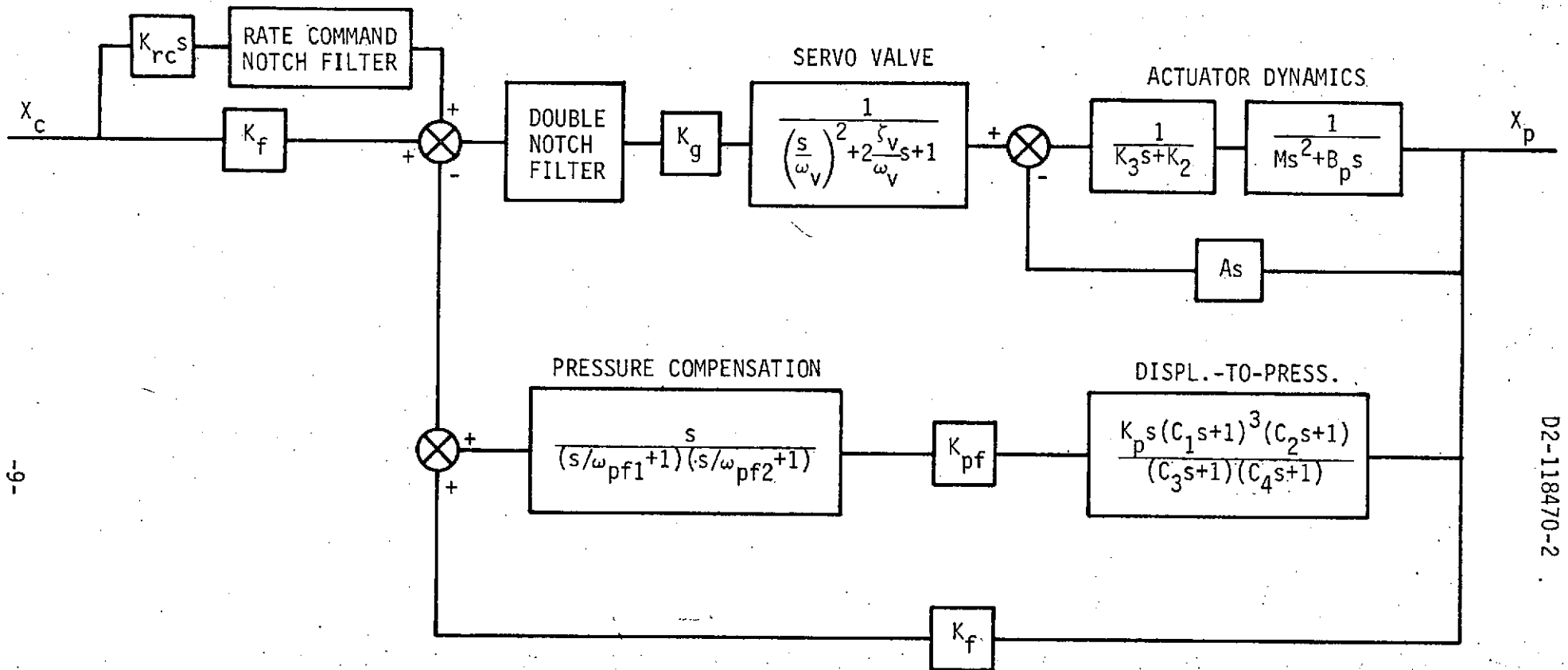
### 3.2.1 Transfer Functions

The displacement-to-pressure transfer function was derived from linearized actuator equations and modified by experimental data. Figure 3-2 shows a comparison of test and analysis data for the displacement-to-pressure transfer function.

The forward loop notch filter is a twin gyrator filter designed to attenuate the command signals at the natural frequency of the servo valves (120-150 Hz). The circuit diagram of the twin gyrator notch filter is shown in Figure 3-3. Frequency response characteristics of this filter are shown in Figure 3-4.

### 3.2.2 Open Loop Analysis

Open loop frequency response data were obtained for both the pressure and displacement feedback loops. Analytical data were obtained using the single-axis servo loop model, and test data were obtained to establish and verify analytical parameters. Test results were obtained by applying a sinusoidal signal to the valve driver in the forward loop and recording the output of the linear position potentiometer and the differential pressure transducer. Comparisons of test and analytical open loop data are shown in Figures 3-5 and 3-6, respectively.



-6-

D2-118470-2

$$\text{RATE COMMAND NOTCH FILTER} = \frac{(s/\omega_c)^2 + D_{cn}s + 1}{(s/\omega_c)^2 + D_{cd}s + 1}$$

$$K_3 = \frac{\text{Vol.}}{4 \beta_e}$$

$$\text{DOUBLE NOTCH FILTER} = \frac{(s^2 + 51680.)(s^2 + 725690.)}{(s^2 + 533.3s + 51680.)(s^2 + 533.4s + 725690.)}$$

Figure 3-1. Single-Axis Servo Block Diagram

REPRODUCIBILITY OF THE ORIGINAL PAGE IS POOR

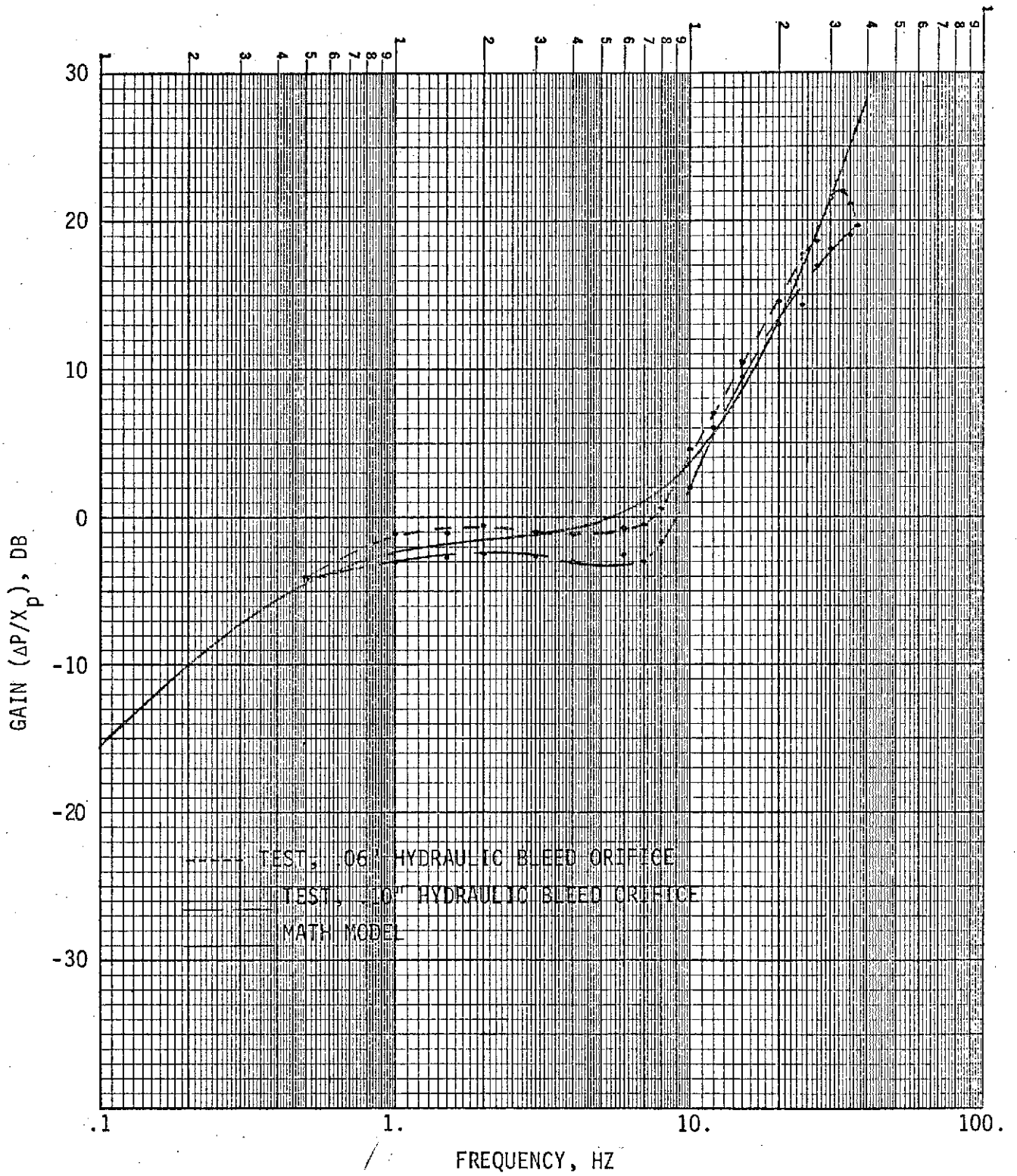


Figure 3-2. Displacement-to-Pressure Frequency Response

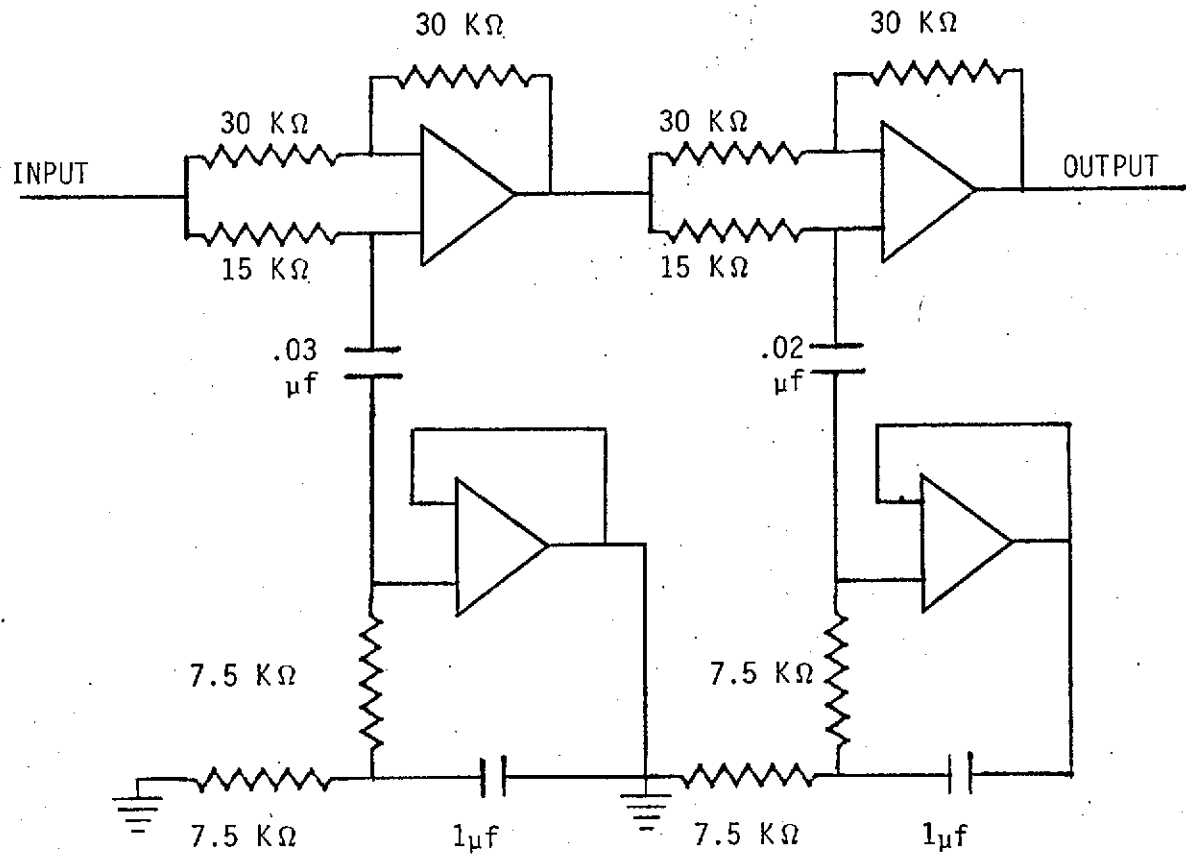


Figure 3-3. Circuit Diagram, Twin Gyration Notch Filter

REPRODUCIBILITY OF THE ORIGINAL PAGE IS POOR

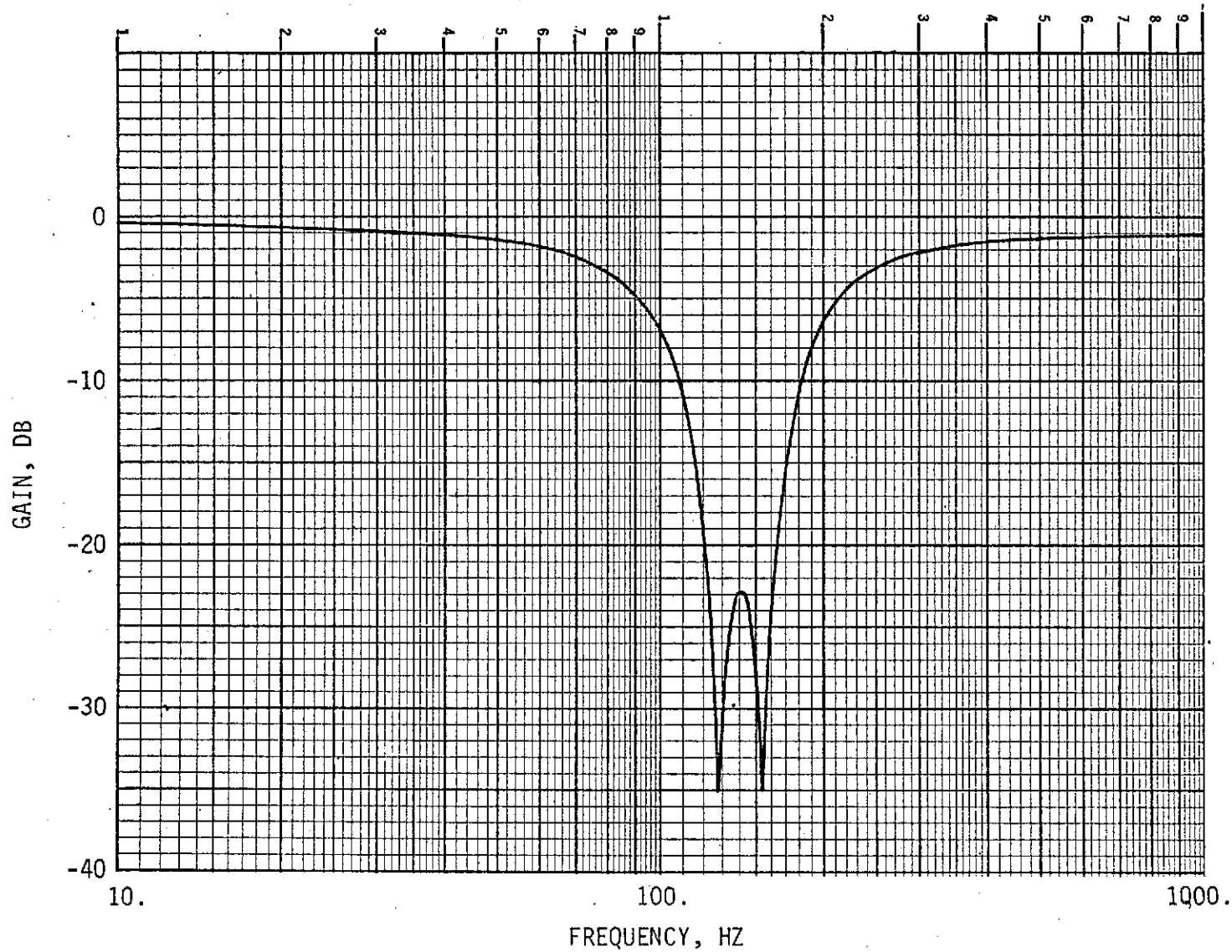


Figure 3-4. Twin Gyrotor Notch Filter Frequency Response

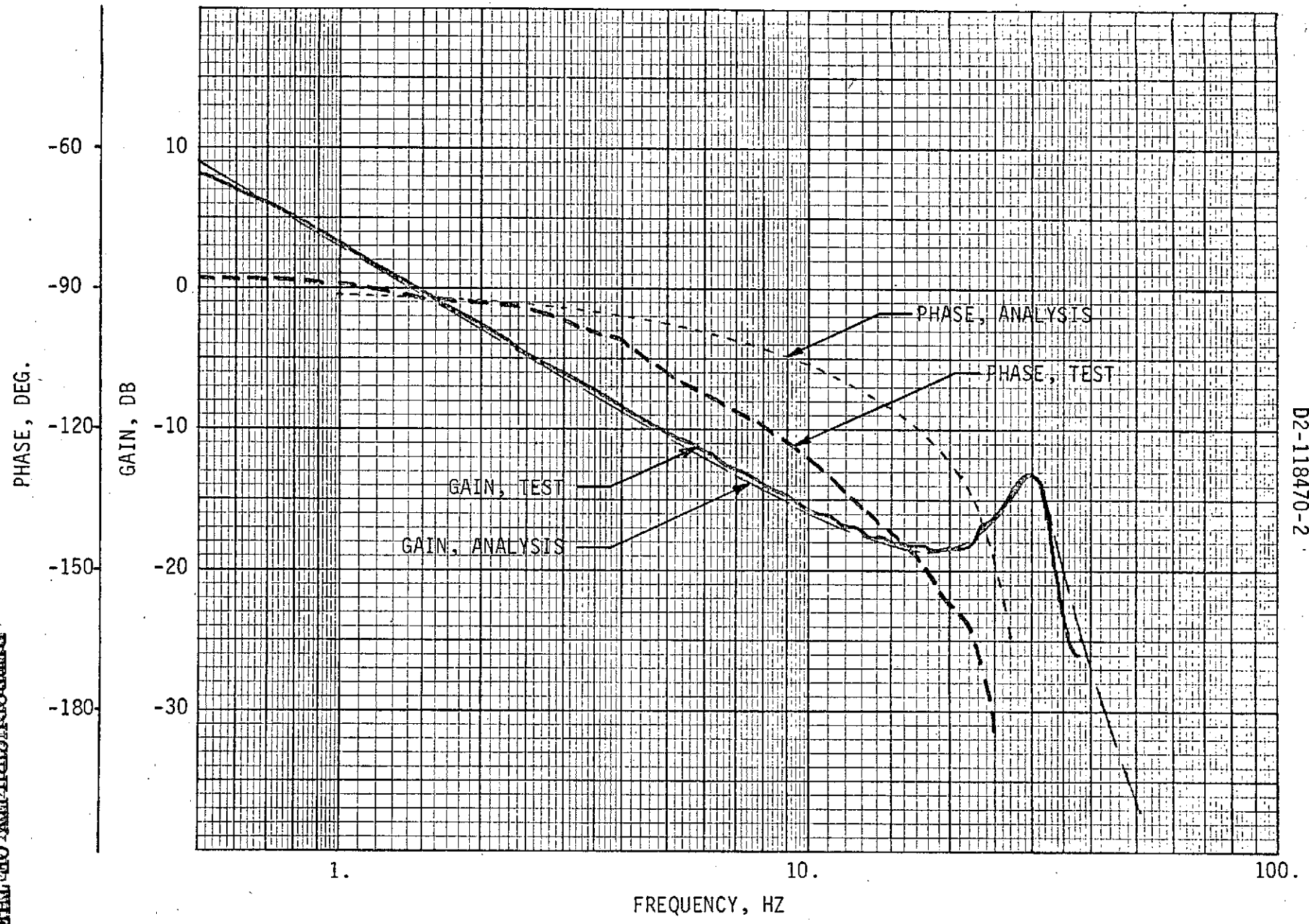


Figure 3-5. Single Actuator Frequency Response, Displacement Open Loop

REPRODUCIBILITY OF THE ORIGINAL PAGE IS POOR

REPRODUCIBILITY OF THE ORIGINAL PAGE IS POOR

-13-

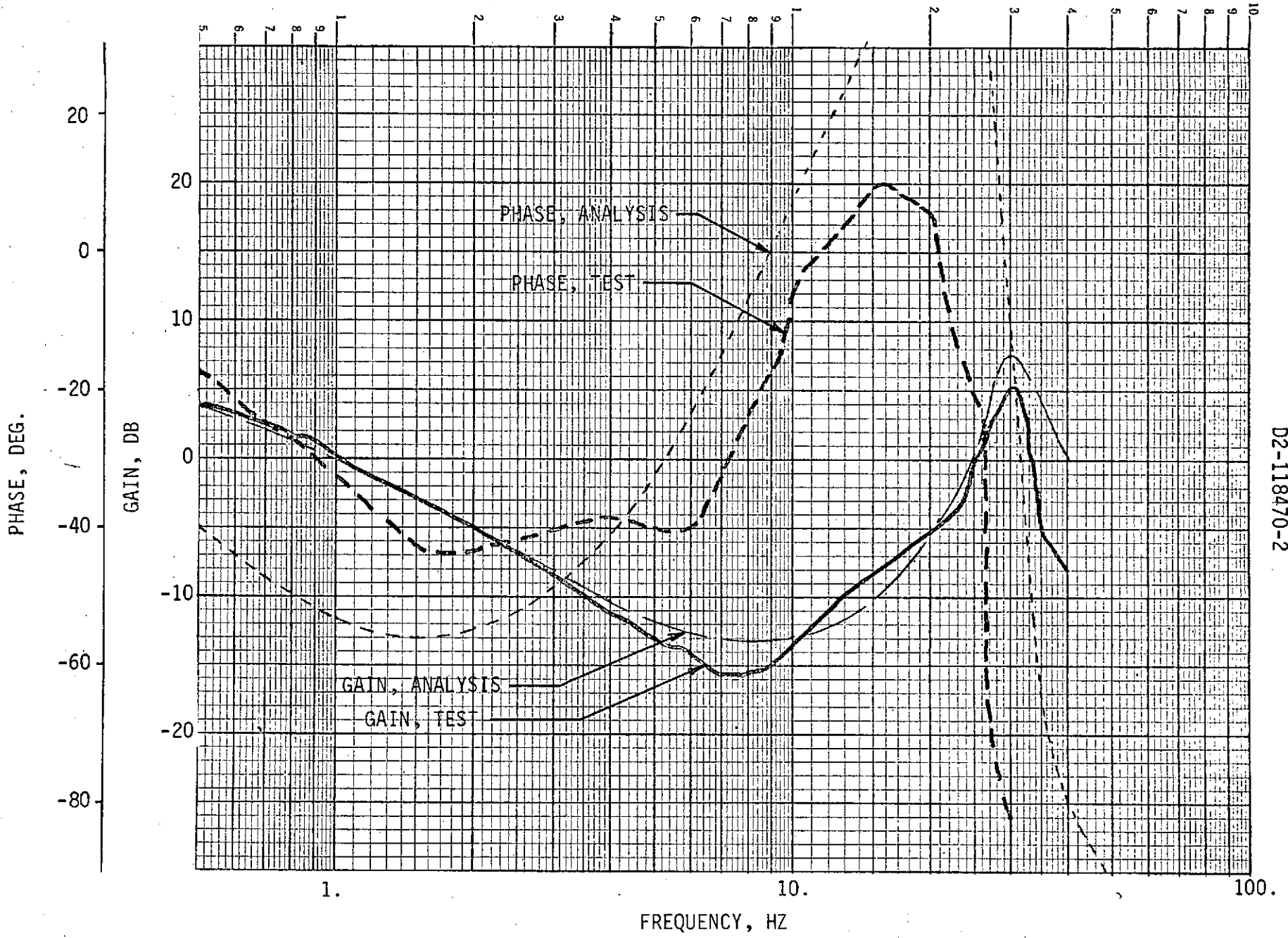


Figure 3-6. Single Actuator Frequency Response, Pressure Open Loop

### 3.2.3 Closed Loop Analysis

Using the actuator parameters obtained from the open loop analysis, the closed loop frequency response shown in Figure 3-7 was obtained. Also shown in the figure is a comparison of analytical data with test. These responses were obtained by using a sinusoidal position command only. Analytical results using both position and rate commands are shown in Figure 3-8. Actuator parameters established by this analysis are presented in Table 3-1.

Test data were also obtained for variations in forward loop gain and hydraulic bleed orifice size. Figures 3-9 through 3-11 show the results of these parameter variations.

### 3.2.4 Effect of Rate Command Filters

As a result of the development tests (see Section 5.0), various filters were incorporated in the rate command line of each actuator to eliminate unwanted 10 Hz oscillations. The effect of these filters on single actuator performance was obtained analytically.

Filter A and filter B are first order lag filters with corner frequencies of 1 Hz and 5 Hz, respectively. Frequency response characteristics of these filters are shown in Figure 3-12. Also shown in the figure are filter A characteristics with increased gain. The effects of these filters on single actuator frequency response are shown in Figures 3-13 and 3-14. Using filter A on the rate command has the effect of increasing the gain slightly at low frequencies (less than 5 or 6 Hz) and attenuating higher frequency signals. Filter B amplifies the response slightly at frequencies below 10 Hz.

Filter C is a notch filter with a notch frequency of 9.5 Hz whose characteristics are shown in Figure 3-15. Single actuator frequency response characteristics using filter C with nominal and double rate gain



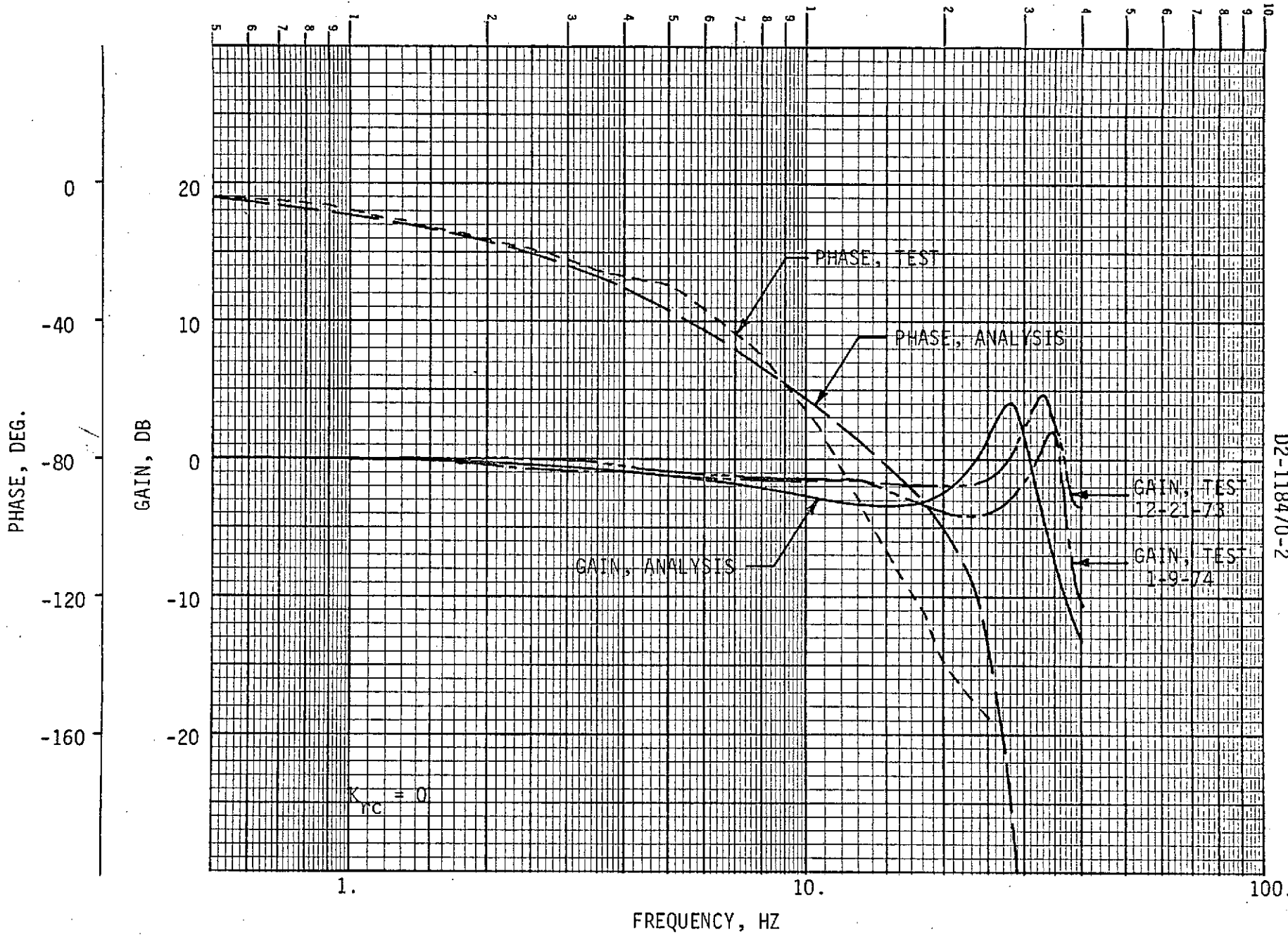


Figure 3-7. Single Actuator Frequency Response, Closed Loop

REPRODUCIBILITY OF THE ORIGINAL PAGE IS POOR

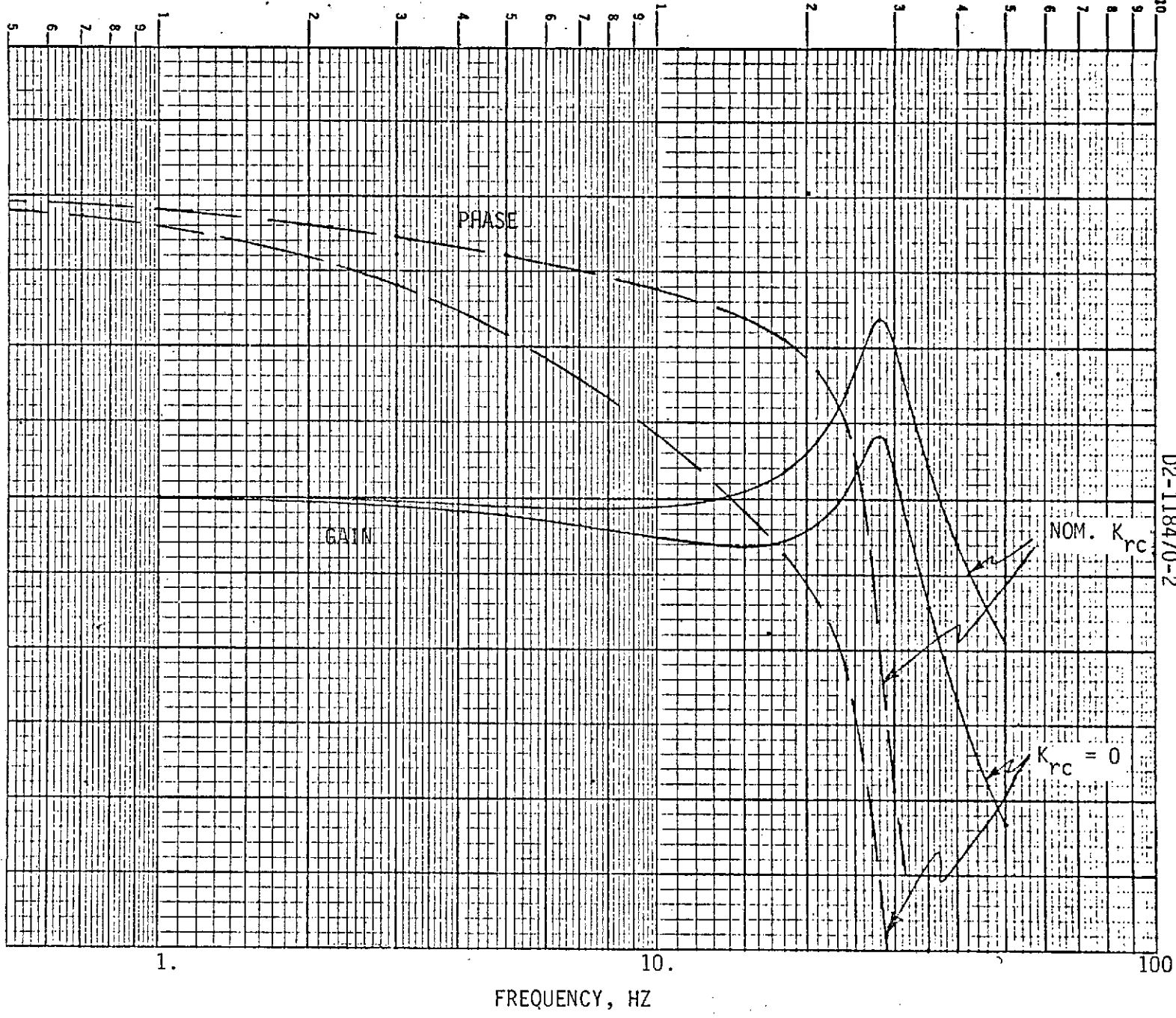
-17-

PHASE, DEG.

0  
-40  
-80  
-120  
-160

GAIN, DB

20  
10  
0  
-10  
-20



D2-118470-2

Figure 3-8. Single Actuator Frequency Response, Including Rate Command

TABLE 3-1  
SINGLE ACTUATOR PARAMETERS

PARAMETER	V A L V E				
	POSITION OPEN LOOP	PRESSURE OPEN LOOP	CLOSED LOOP		
M = effective mass	1.25	↑	↑		
AREA = average piston area	7.8				
VOL = hydraulic volume	541.				
$\beta_e$ = equivalent bulk modulus	$10^5$	↓	↓		
$B_p$ = actuator viscous damping coefficient	40.				
$K_2 = K_c + C_p$ = valve pressure flow coefficient + leakage coefficient	.0125			SAME AS POSITION OPEN LOOP	SAME AS POSITION OPEN LOOP
$\tau_v$ = servo valve equivalent viscous damping ratio	.7				
$\omega_v$ = servo valve resonant frequency	879.2				
$C_1$	.01326	↓	↓		
$C_2$ } displacement-to-	.0159				
$C_3$ } pressure transfer	.3183				
$C_4$ } function coefficients	.022				
$K_p$	.0676				
$K_g$ = forward loop gain (amplifier & servo valve)	32.7	32.7	48.46		
$K_f$ = position feedback gain	.25	0.	1.		
$K_{pf}$ = pressure feedback gain	0	1.	.015		
$\omega_{pf1}$ } pressure compensation	N.A.	N.A.	18.85		
$\omega_{pf2}$ } filter constants	N.A.	N.A.	628.32		
$K_{rc}$ = rate command gain	0	0	.0128		

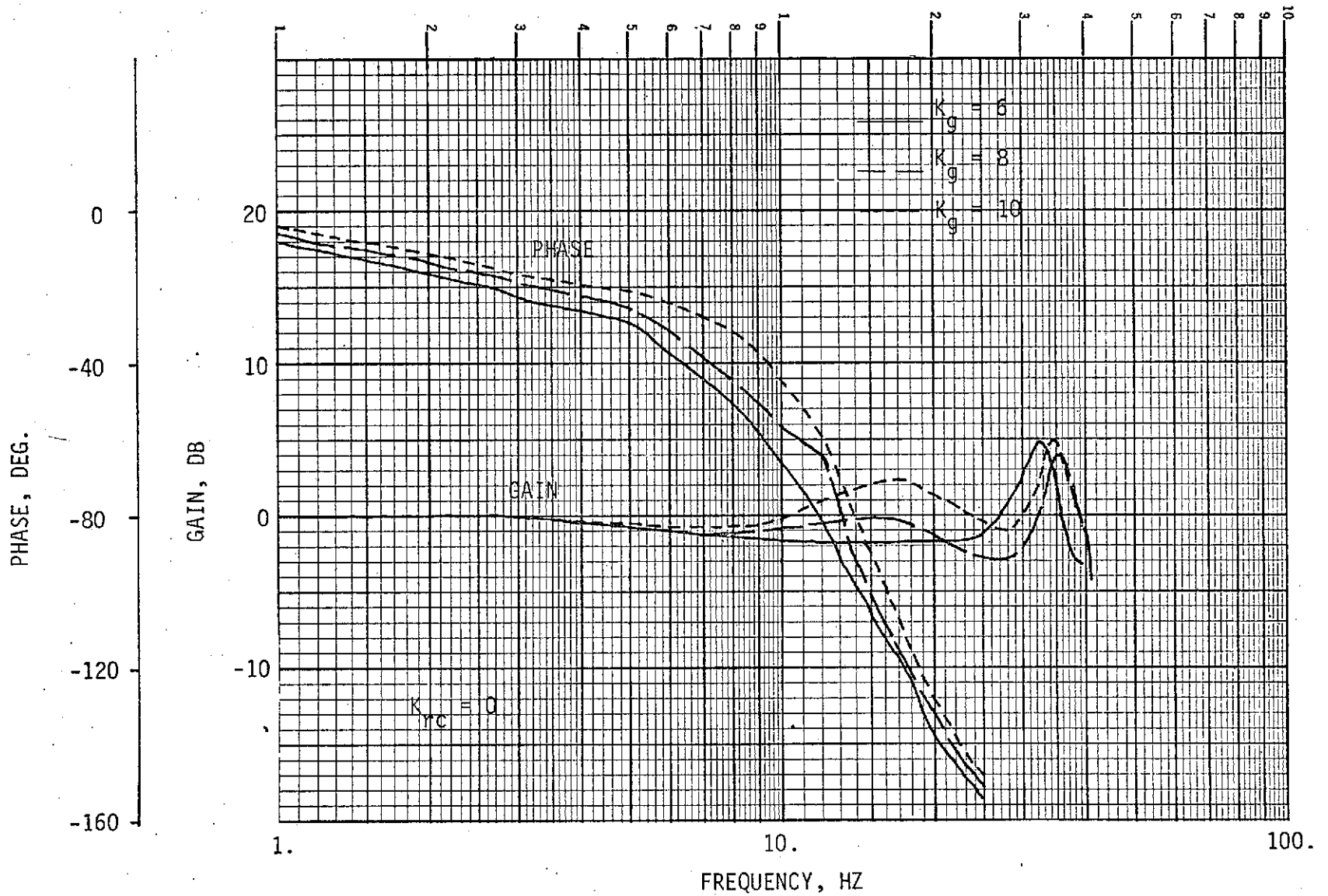


Figure 3-9. Single Actuator Closed Loop Frequency Response, Forward Loop Gain Variation

PHASE, DEG.

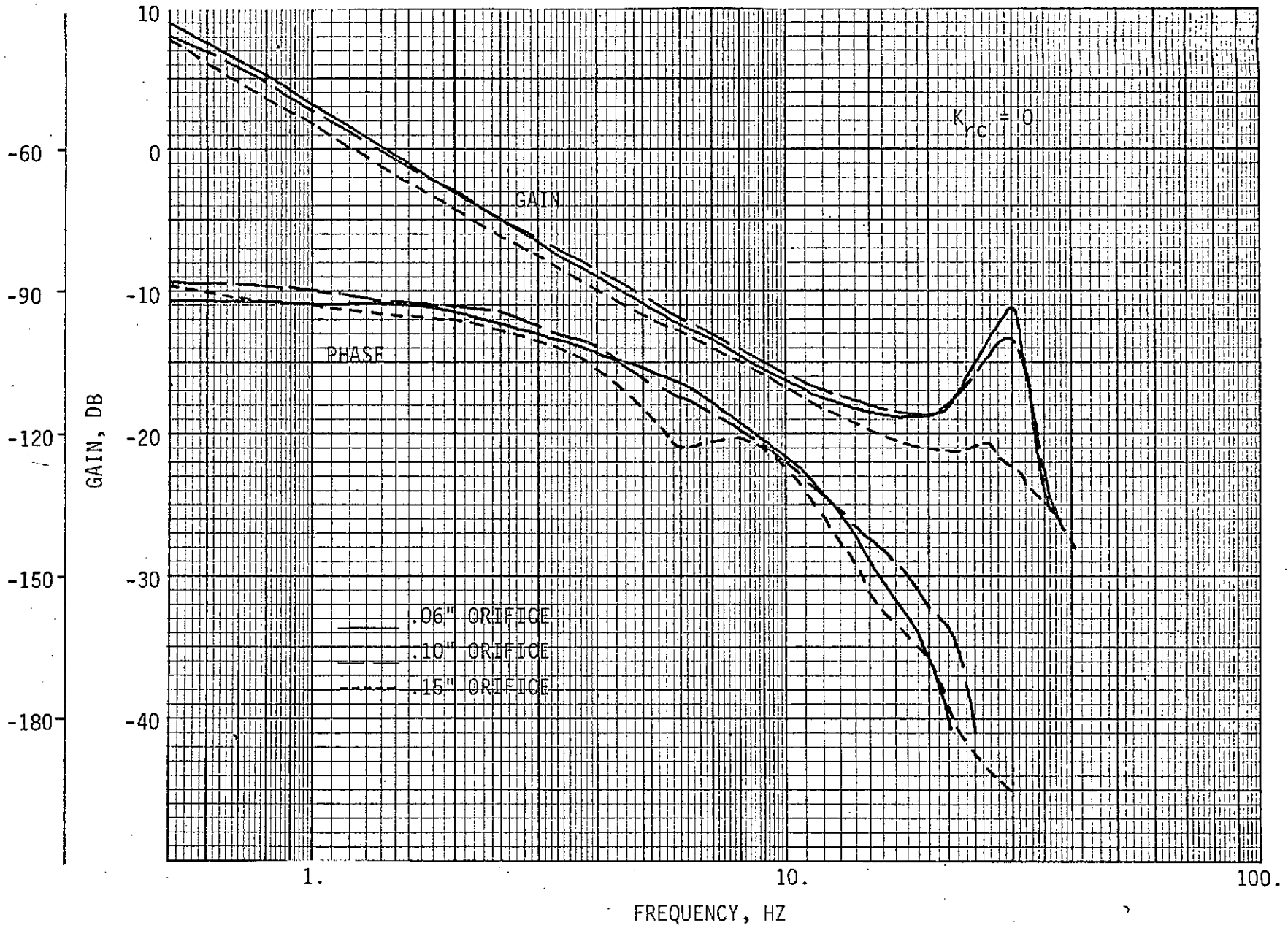


Figure 3-10. Single Actuator Frequency Response, Position Open Loop, Hydraulic Bleed Orifice Variation

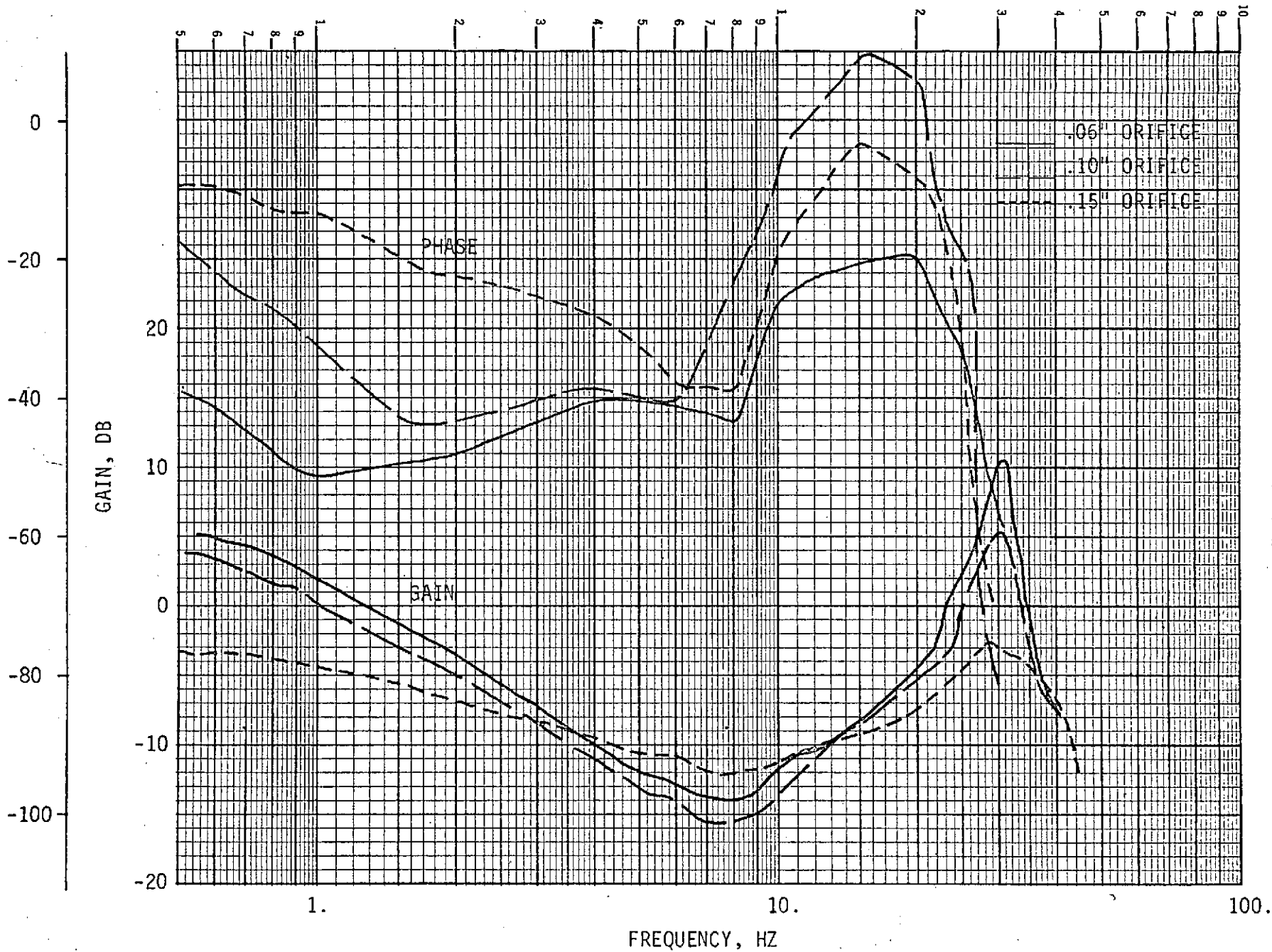


Figure 3-11. Single Actuator Frequency Response, Pressure Open Loop, Hydraulic Bleed Orifice Variation

REPRODUCIBILITY OF THE ORIGINAL PAGE IS POOR

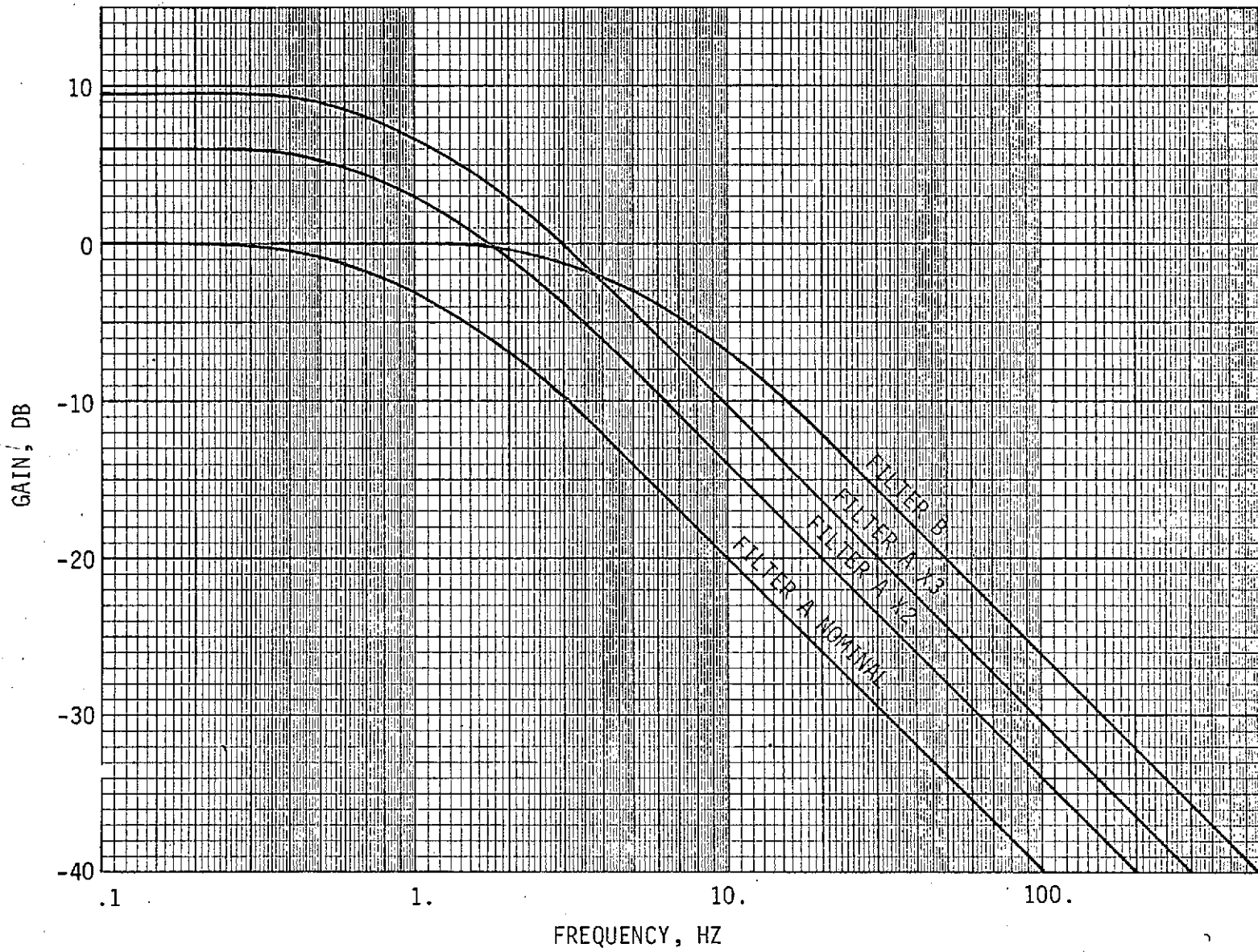


Figure 3-12. Rate Command First Order Lag Filter Characteristics.

REPRODUCIBILITY OF THE ORIGINAL PAGE IS POOR

PHASE, DEG.

0  
-40  
-80  
-120  
-160

GAIN, DB

20  
10  
0  
-10  
-20

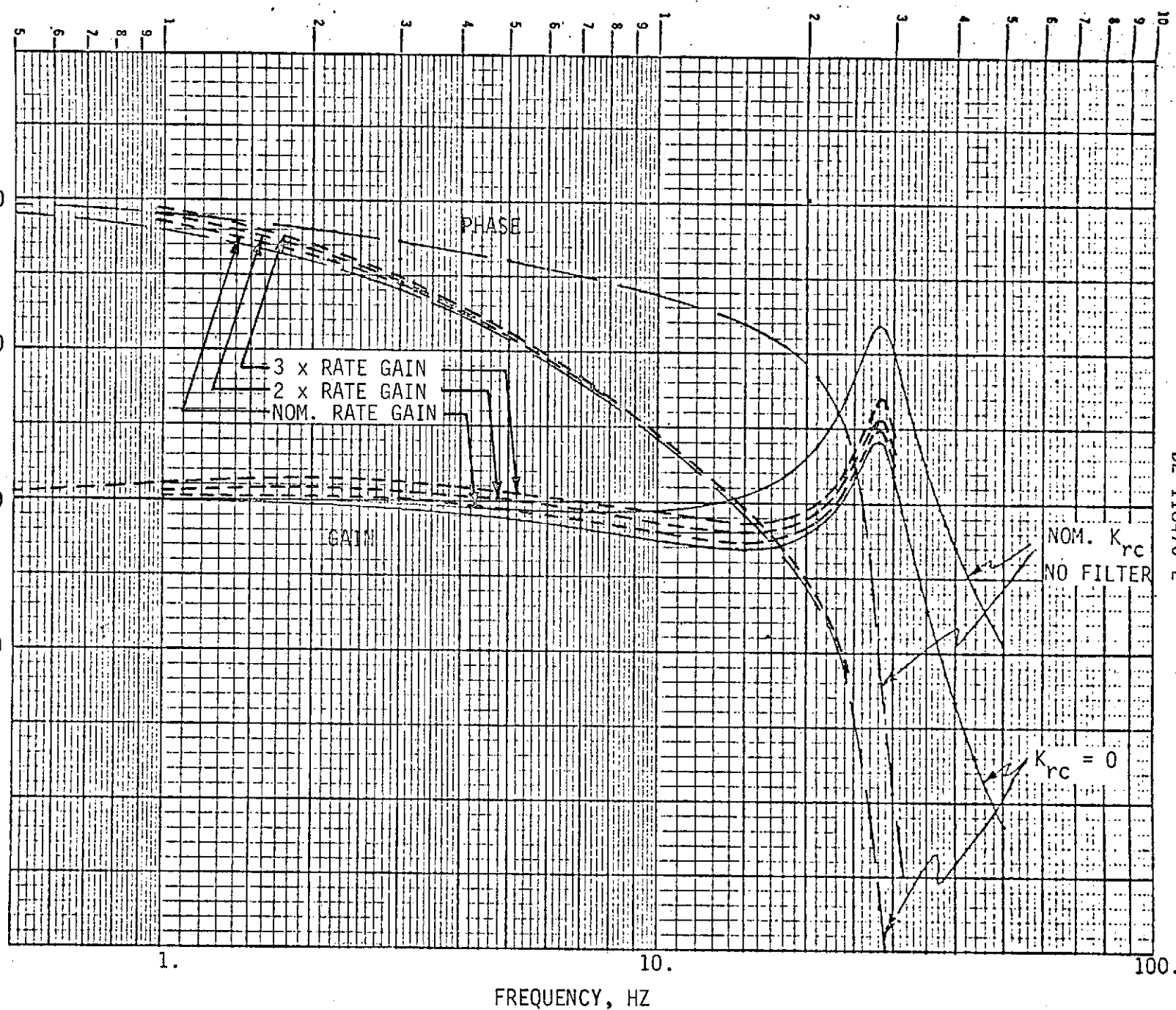


Figure 3-13. Single Actuator Frequency Response, Including Rate Command Filter A



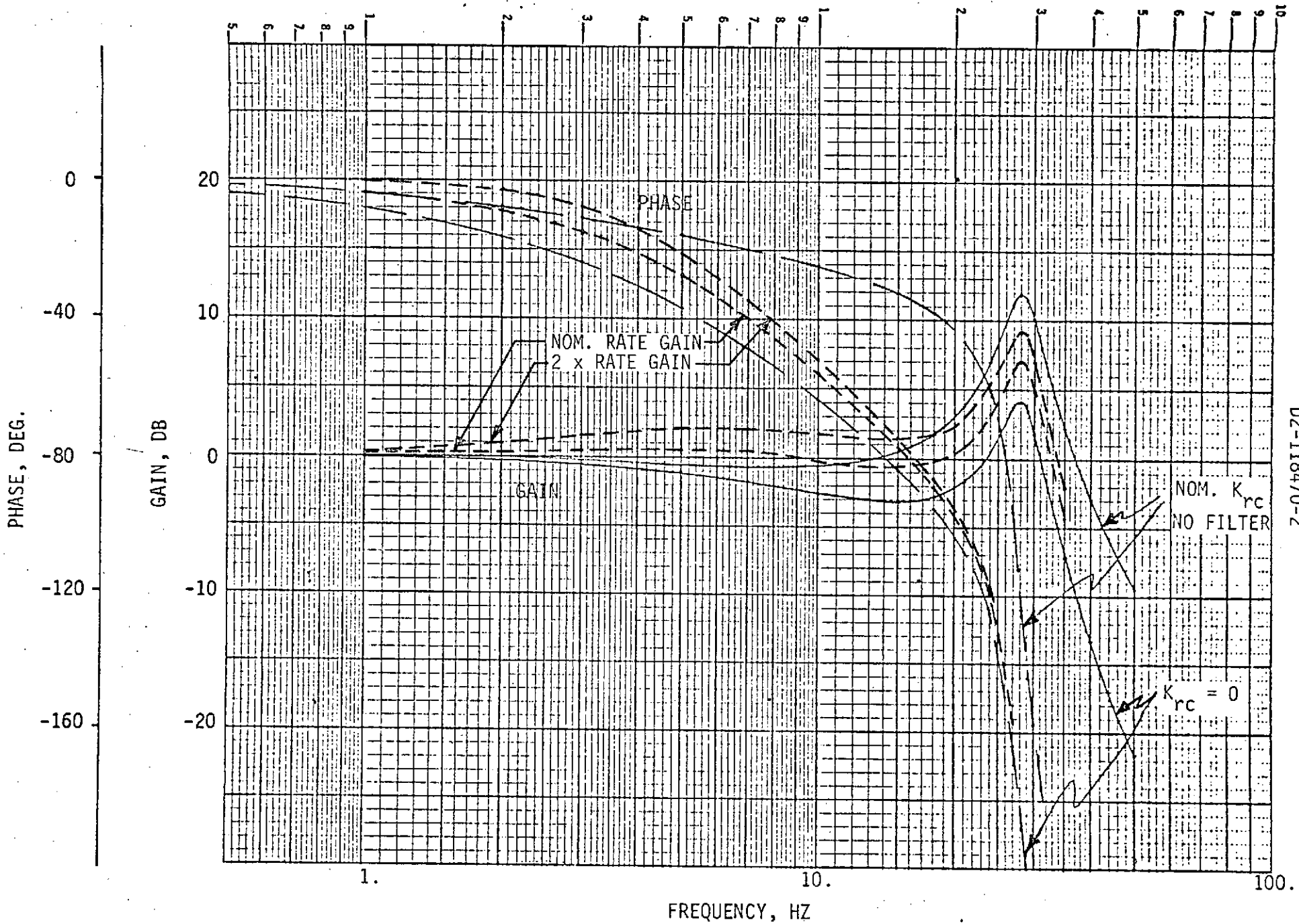


Figure 3-14. Single Actuator Frequency Response, Including Rate Command Filter B

REPRODUCIBILITY OF THE  
ORIGINAL PAGE IS POOR

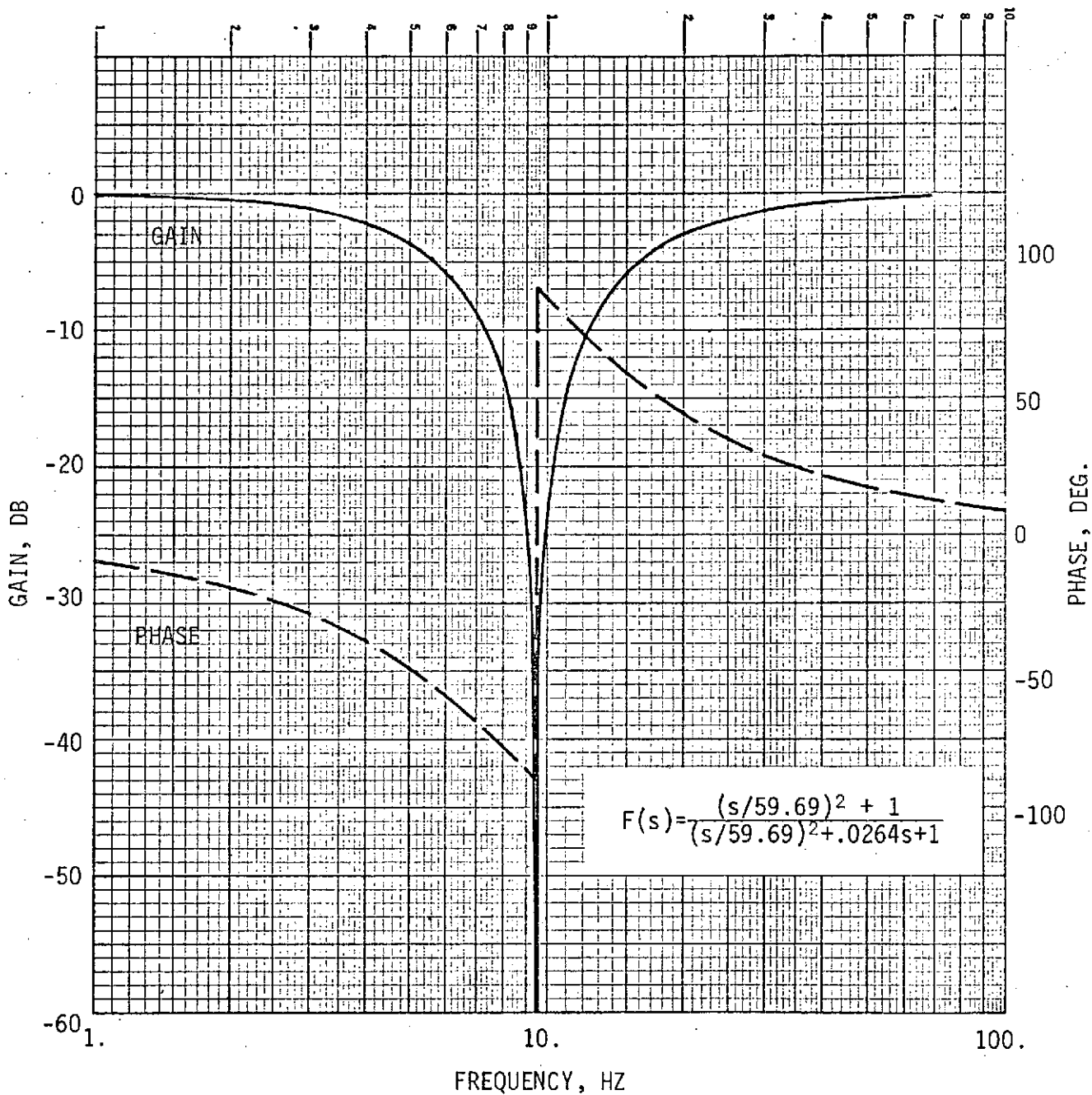


Figure 3-15. Rate Command Notch Filter Characteristics

### 3.2.4 (Continued)

are shown in Figure 3-16. With double rate gain, actuator response is amplified slightly at frequencies below 8 Hz and is attenuated at frequencies between 8 and 18 Hz. It will be shown in Section 3.3 that the active table has a resonance at approximately 11 Hz; therefore, filter C should be effective in attenuating this resonance.

## 3.3 ACTIVE TABLE ANALYSES

Analyses of the active table were performed to determine its frequency response characteristics and to study the ability of angle sensing limit switches to prevent table "fall through."

### 3.3.1 Six-Degree-of-Freedom Motion Analysis

The six-degree-of-freedom mathematical model and computer program discussed in Reference 1 were modified to include differential pressure feedback in the actuator representation. This mathematical model determines the response of the active table to motion commands. The model includes a rigid representation of the table structure and a flexible representation of each of the six actuators. The actuator model also includes servo valve dynamics, hydraulic flow and pressure equations, and the electronic control system. The math model and computer program, NASA Advanced Docking System (NADS), are described in detail in References 2 and 3, respectively. The actuator parameters determined from the single-axis actuator analysis were used in NADS to obtain active table frequency response data and to assess three-dimensional coupling effects.

Two attempts were made to obtain table frequency response test data to compare with the analytical predictions. The first frequency response test was performed using five cycles of table position and velocity command at each frequency. The command was limited to five cycles at .125 inch to minimize the dynamic environment on the linear potentiometers. Discrete

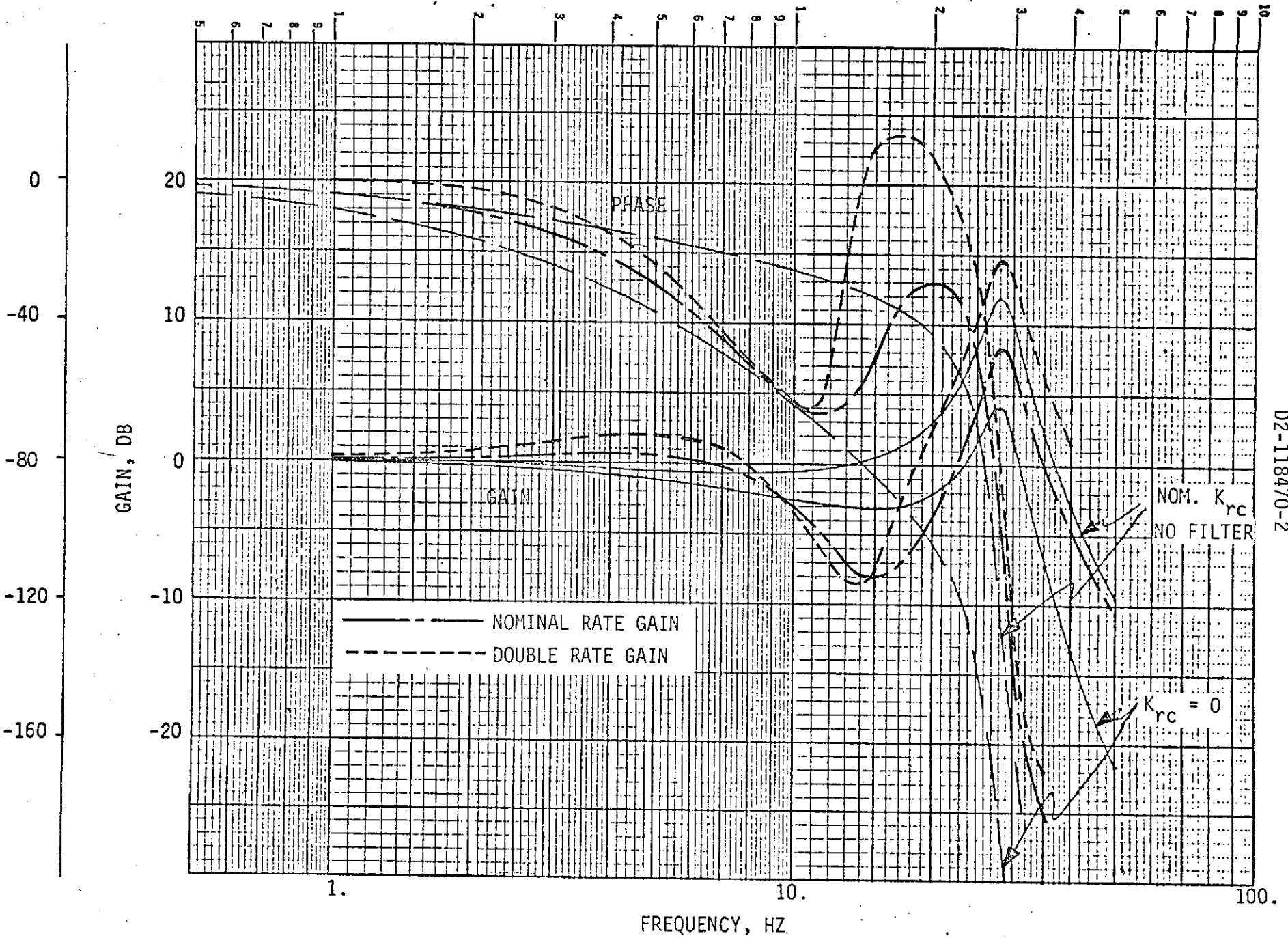


Figure 3-16. Single Actuator Frequency Response, Including Rate Command Filter C

## 3.3.1 (Continued)

frequencies were used due to the need for both position and velocity command signals. The tests in all axes were curtailed due to excessive table response at frequencies in the vicinity of 10 Hz. The severity of the starting transient at each frequency was considered to be the cause of the excessive dynamic response. There was also considerable drift in the sinusoidal command signal.

A second table frequency response test was attempted with a reduced input command signal. This test used a 0.05 inch sinusoidal position command signal in each of the X, Y and Z directions. The velocity command gain,  $K_{rc}$ , was set to zero. This permitted the use of the automatic frequency sweeping signal generator. The frequency sweep was begun at 1.0 Hz and incremented by 1.0 Hz after 15 cycles at each frequency.

Using the actuator parameters listed in Table 3-1, frequency response characteristics of the table for position commands in the X, Y and Z directions were obtained using NADS computer program. The table frequency response exhibits two resonances--one at the hydraulic resonance ( $\sim 30$  Hz) and another which corresponds to the bending frequency of the actuators ( $\sim 11$  Hz). In the lateral directions, the hydraulic resonance occurs at 22 Hz due to increased effective mass in the lateral direction. Table and actuator acceleration response predictions were also obtained. Based on these predictions, a table acceleration limit of  $\pm 3.0$  g was established to preclude possible damage to the table or actuators. Accelerometers on the table and actuator 6 were monitored during the test, and an automatic abort capability was utilized.

Each of the tests was aborted automatically due to excessive accelerations at 9 Hz in the lateral direction and 11 Hz in the vertical direction. Comparisons of predicted and experimentally derived table displacements are shown in Figure 3-17. Predicted table accelerations are compared with measured table accelerations in Figure 3-18. Lateral accelerations measured at the upper end of the actuator 6 cylinder are compared with pretest predictions in Figure 3-19.

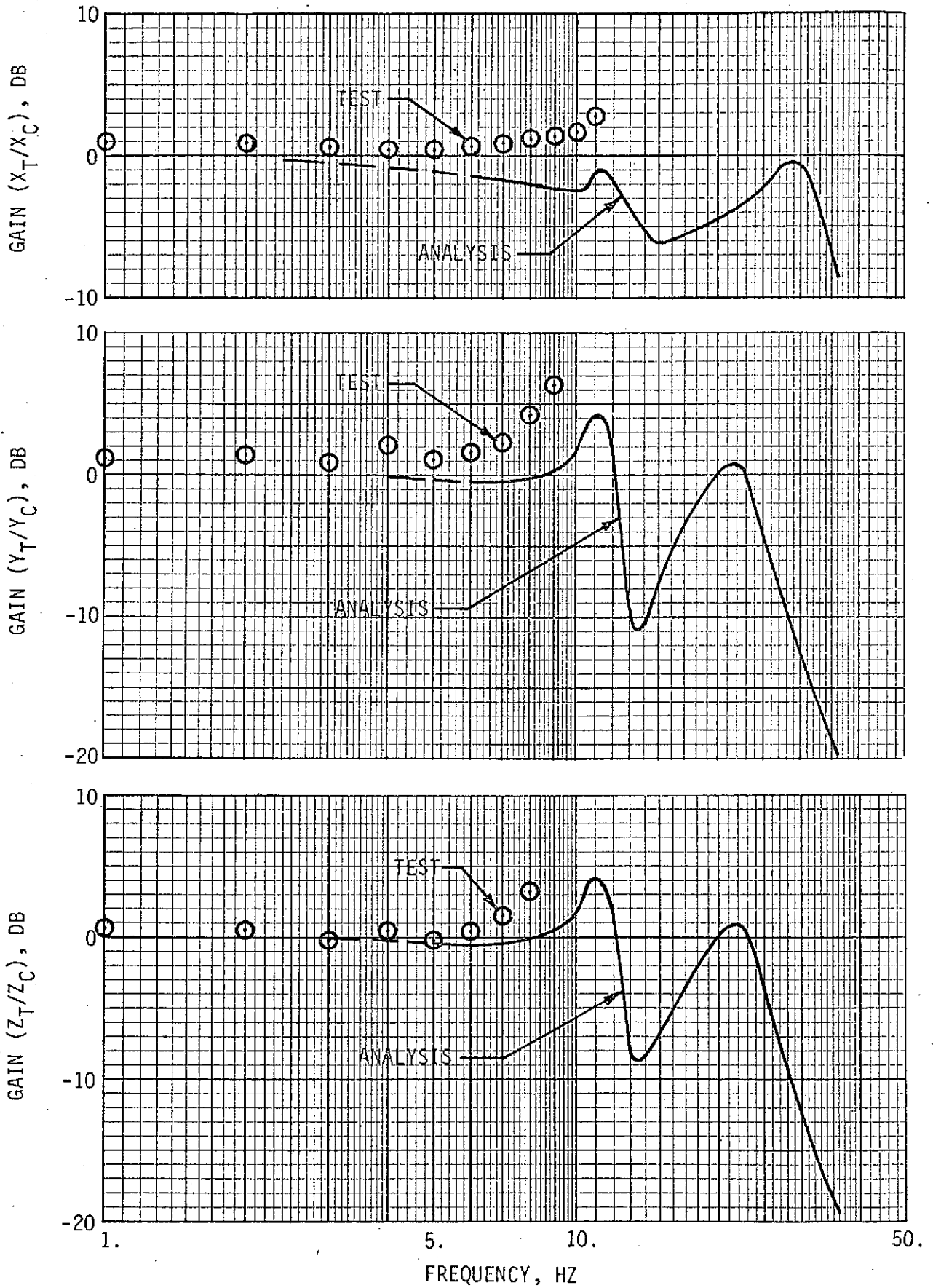


Figure 3-17. Table Displacement Frequency Response

REPRODUCIBILITY OF THE ORIGINAL PAGE IS POOR.

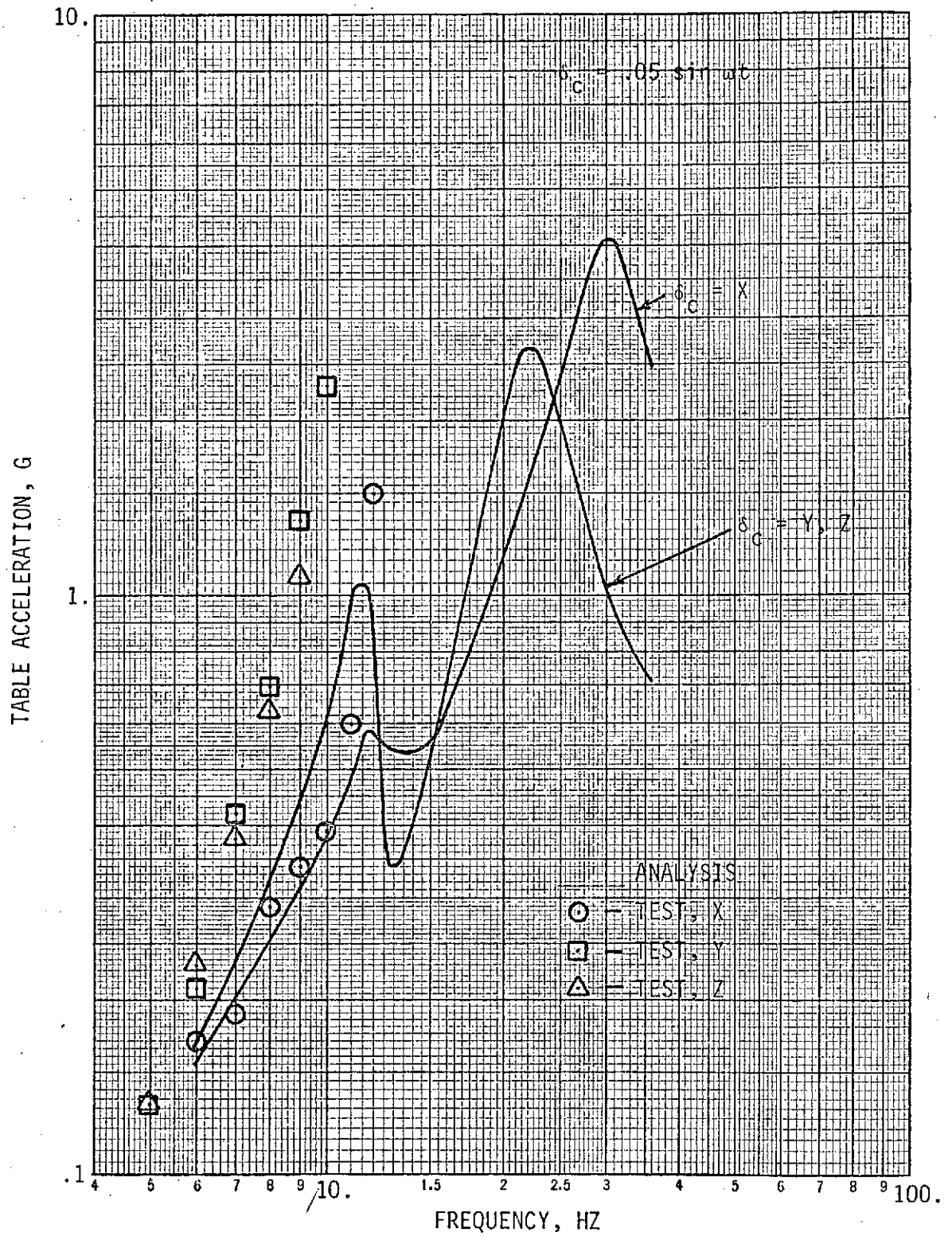


Figure 3-18. Table Accelerations, Frequency Response Test

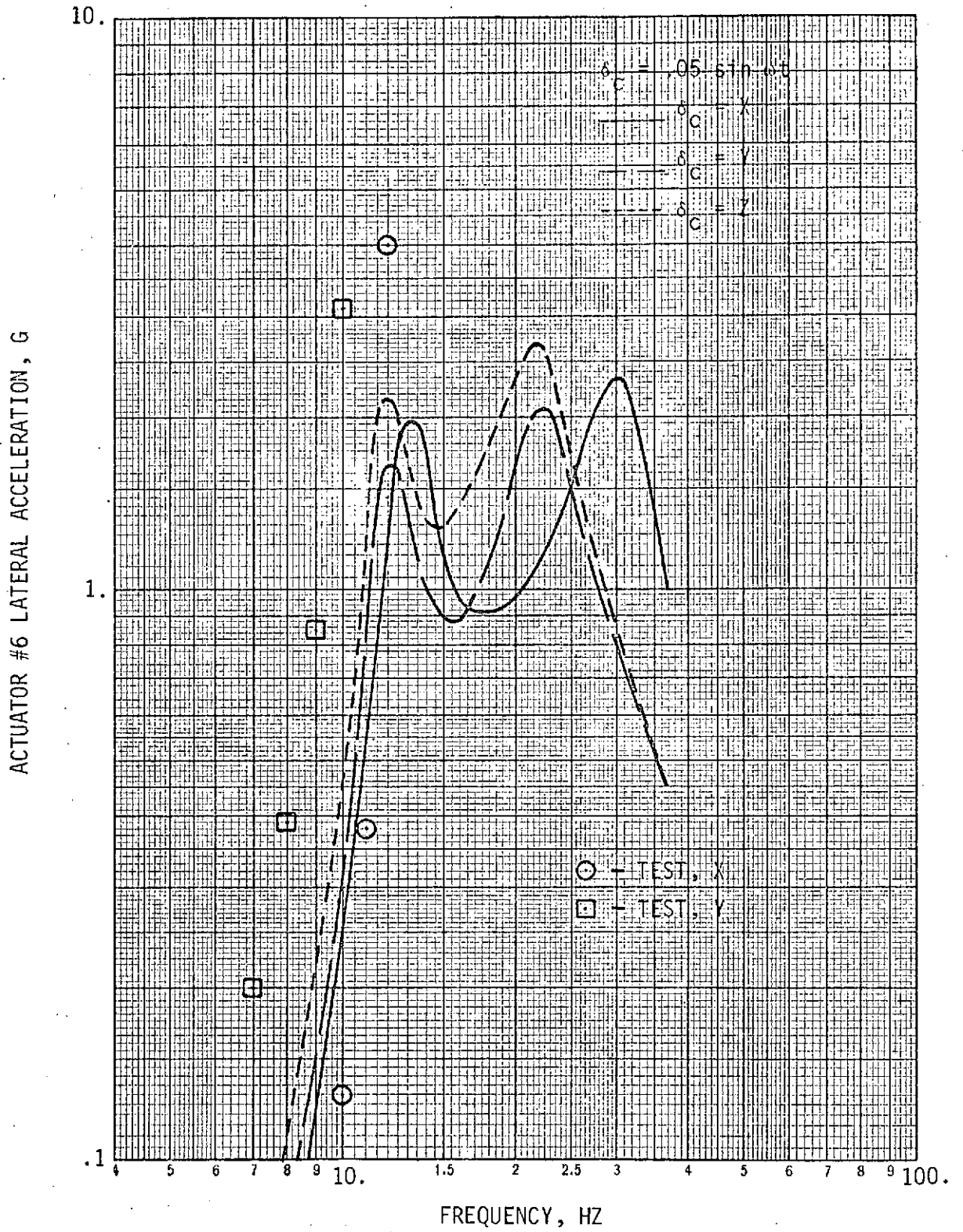


Figure 3-19. Actuator Accelerations, Frequency Response Test



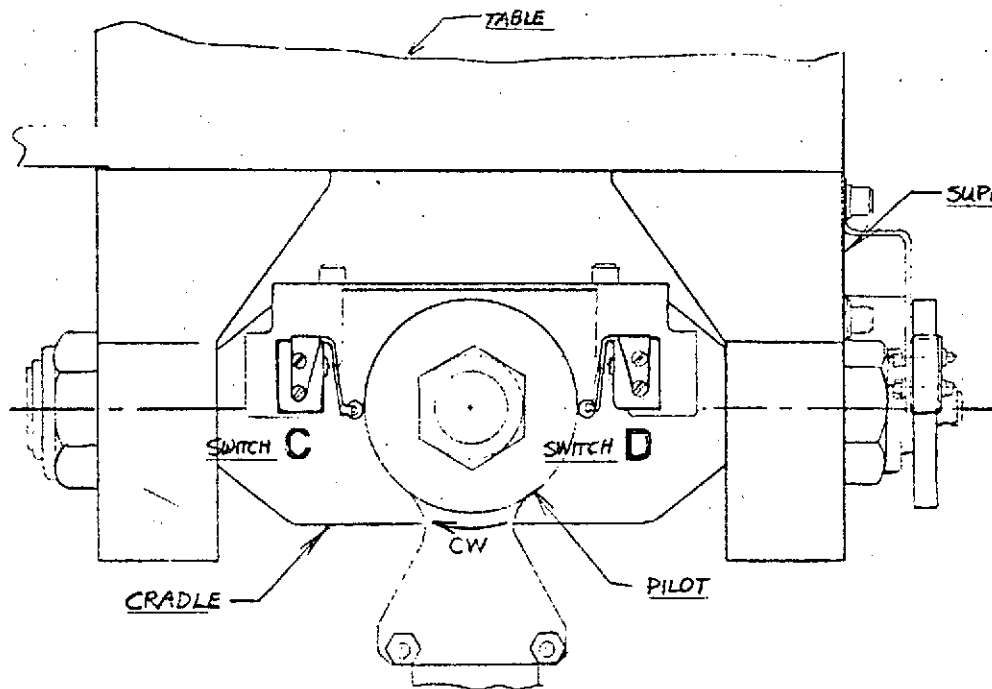
### 3.3.1 (Continued)

It is apparent that the active table exhibits considerably higher dynamic characteristics than were predicted; however, the cause of this discrepancy has not been identified. Reducing the damping associated with actuator flexibility did not increase analytical table response significantly.

Analysis of the analytical frequency response predictions shows that insignificant coupling between table responses in the commanded direction and responses in other directions exists. During the frequency response test, however, some coupling was observed. In general, the off-axis motion was less than 30 percent of the commanded table motion at frequencies below 10 Hz. The highest coupling occurred during the X-axis test at frequencies of 10 and 11 Hz (the test was aborted at 11 Hz). Detailed frequency response test results are documented in Reference 4.

### 3.3.2 Angle Abort Limit Analysis

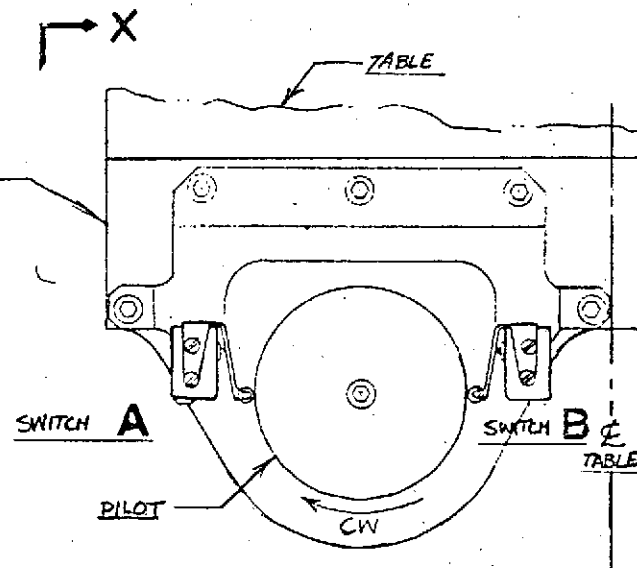
Four angle sensors were installed at the upper swivel of each actuator. Each sensor consisted of a fixed "microswitch" with a roller-leaf actuating lever bearing on a rotating pilot disc having adjustable cams. The cams were designed to actuate the switches for both clockwise and counterclockwise rotation. These four switches, designated A, B, C, and D, were situated so that switches A and B measured rotations in a vertical plane while switches C and D indicated rotations predominantly in a horizontal plane (see Figure 3-20). A swivel angle limit abort plan was developed to utilize these switches to prevent damage to the simulator and docking hardware due to table "fall through" and to limit the horizontal envelope of the table motion within the environmental enclosure. "Fall through" is a term used to refer to a condition that is possible because of the relationship between table and actuator geometry. If the table becomes rotated to the point that it is in a plane with adjacent pairs of actuators joining at a table corner, no vertical support is provided by these actuators; thus, permitting this corner of the table to travel vertically as the two actuators rotate about their base.



VIEW X-X

ACTUATOR / CRADLE ANGLES

TYPICAL OF ACTUATORS 1, 3 AND 5  
 (ACTUATORS 2, 4 AND 6 MIRROR IMAGE -  
 I.E. SWITCH 'C' CLOSEST TO CENTER  
 OF TABLE - SWITCH 'D' OUTBOARD)



VIEW LOOKING TOWARD  
 CENTER OF TABLE

CRADLE / TABLE ANGLES

TYPICAL OF ACTUATORS 1, 3 AND 5  
 (ACTUATORS 2, 4 AND 6 MIRROR IMAGE -  
 I.E. SWITCH 'A' RIGHT OF 'B' LOOKING  
 TOWARD CENTER OF TABLE)

Figure 3-20. Angle Limit Abort Switch

## 3.3.2 (Continued)

The angle setting for which these cams must be set in order to satisfy the objectives can be determined once the relationship between table translation and rotation and sensor rotations is known.

Let  $\Delta\rho$  define the "horizontal" angle change measured with switches C and D when the table moves; let  $\Delta\beta$  be the "vertical" angle change associated with switches A and B. Define  $\rho_j$  and  $\beta_j$  as the angle measured in the plane of the switches of actuator  $j$  as follows

$$\rho_j = \tan^{-1} \frac{\sqrt{x_j^2 + z_j^2}}{-y_j}$$

$$\beta_j = \tan^{-1} \frac{x_j}{z_j}$$

Where  $x_j$ ,  $y_j$  and  $z_j$  are actuator lengths as defined isometrically in Figure 3-21 for  $j = 2$ .

To determine the value of  $\rho_j$  and  $\beta_j$  for all actuators and all locations of the table, define the following parameters:

[RA] = A 3 x 6 matrix of table coordinates at the upper end of the actuator

[RF] = A 3 x 6 matrix of inertial coordinates of the actuator floor attach points

$\left. \begin{array}{l} x_I \\ y_I \\ z_I \end{array} \right\} = \text{Inertial position of table c.g.}$

$\left. \begin{array}{l} \theta \\ \phi \\ \psi \end{array} \right\} = \text{Euler angles}$

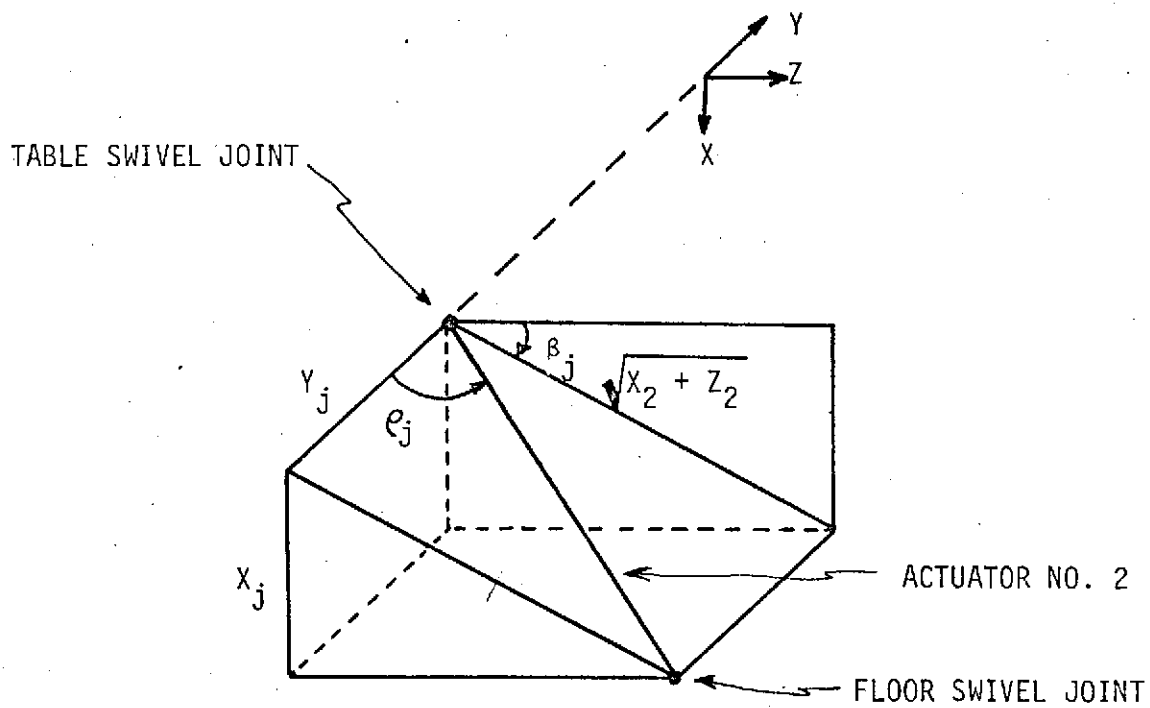
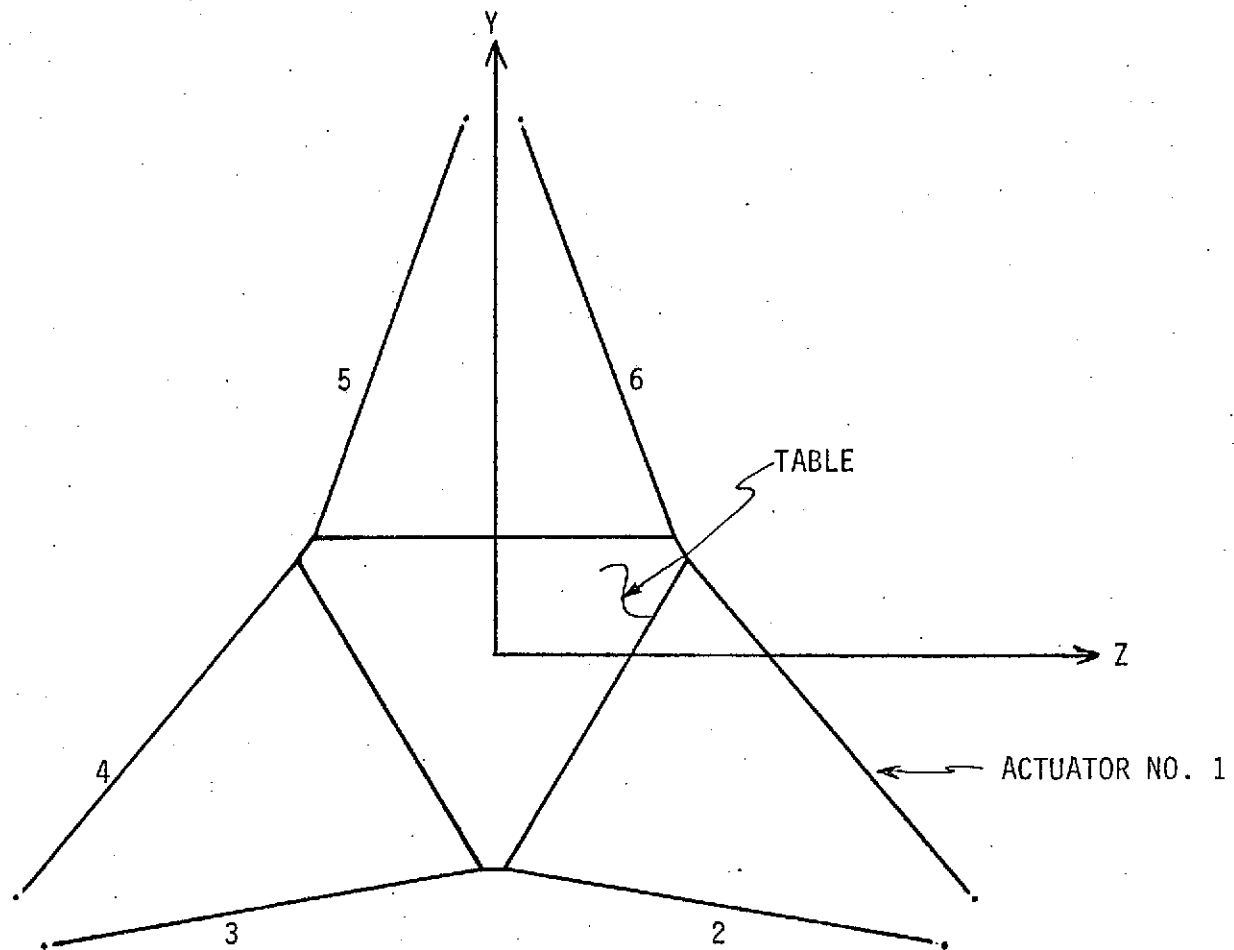


Figure 3-21. Table Coordinate System and Definition of Actuator Lengths

## 3.3.2 (Continued)

The 3 x 6 matrix of floor attachment locations expressed in table coordinates [RFT], is given by

$$[RFT] = [A]^T \left[ [RF] - \begin{Bmatrix} x_I \\ y_I \\ z_I \end{Bmatrix} [1 \ 1 \ 1 \ 1 \ 1 \ 1] \right]$$

and the 3 x 6 matrix of components of actuator length in table coordinates is given by

$$[ALT] = [RFT] - [RA]$$

The values of the  $x_j$ ,  $y_j$  and  $z_j$  are then defined by the use of geometry as

$$x_j = ALT(1,j)$$

$$y_1 = ALT(3,1)*.86603+ALT(2,1)*.5$$

$$y_2 = -ALT(2,2)$$

$$y_3 = -ALT(2,3)$$

$$y_4 = -ALT(3,4)*.86603+ALT(2,4)*.5$$

$$y_5 = -ALT(3,5)*.86603+ALT(2,5)*.5$$

$$y_6 = ALT(3,6)*.86603+ALT(2,6)*.5$$

$$z_1 = -ALT(2,1)*.86603+ALT(3,1)*.5$$

$$z_2 = ALT(3,2)$$

$$z_3 = -ALT(3,3)$$

$$z_4 = -ALT(2,4)*.86603-ALT(3,4)*.5$$

$$z_5 = ALT(2,5)*.86603+ALT(3,5)*.5$$

$$z_6 = ALT(2,6)*.86603-ALT(3,6)*.5$$

### 3.3.2 (Continued)

A listing of the computer program, TABGEOM, developed to perform the calculations is reproduced in Figure 3-22. The values of the constants, [RA] and [RF] used in the analysis are shown in Table 3-2 and Table 3-3, respectively.

Analyses were performed for several table heights with various combinations of translations and rotations to establish limit switch settings that would satisfy the original objectives. The resulting recommended limit switch settings to prevent table "fall through" are shown in Figures 3-23 and 3-24.

Implementation of the limit switches for the constraint of lateral motion was found to be impractical since large lateral motion which results from small angle changes could not be controlled accurately enough with the setting fidelity of the angular readings available on the switches; and because unlimited translation could occur with the proper combination of table rotation. For example, unlimited -Y translation can be obtained if a + rotation about the Z axis is added continually so that no change in the indicated angle on the limit switch occurs with Y translation. Therefore, the system did not provide a "foolproof" abort system for lateral table motion.

The lateral constraint desired was obtained by implementing computer aborts that sensed motion outside of a specified conical frustrum within the environmental enclosure; thus, satisfying the original objective of no interference with the environmental enclosure. The conical frustrum required to satisfy the abort objectives is defined by the following coordinates:

At table height,  $X = 70.4$  in. the abort radius is 38.5 in.

At table height,  $X = 159.461$  in. the abort radius is 28.6 in.

REPRODUCIBILITY OF THE  
ORIGINAL PAGE IS POOR

C>P TABGEOM FORTRAN

```

      DIMENSION RA(3,6),RF(3,6),A(3,3),RFT(3,6),
      1 ALT(3,6),AL(6),Y(6),Z(6),BETA(6),RHO(6),
      2 THETA(6),RS(3,6),XYZ(3)
      DATA RA/0.,25.102,49.5,0.,-55.419,3.,0.,-55.419,-3.,
      1 0.,25.102,-49.5,0.,30.298,-46.5,0.,30.298,46.5/
      DATA RF/210.407,-64.311,123.178,210.429,-76.38,116.124,
      1 210.422,-74.573,-116.819,210.417,-62.412,-123.683,
      2 210.410,138.463,-5.975,210.369,138.389,8.005/
10  READ(5,901,END=100,ERR=100) (XYZ(I),I=1,3),THTA,PSI,PHI
      THTA=THTA/57.29578
      PHI=PHI/57.29578
      PSI=PSI/57.29578
      CT=COS(THTA)
      CS=COS(PSI)
      CP=COS(PHI)
      ST=SIN(THTA)
      SS=SIN(PSI)
      SP=SIN(PHI)
      A(1,1) = CT*CS
      A(1,2) = -CP*CT*SS+ST*SP
      A(1,3) = SP*CT*SS+CP*ST
      A(2,1) = SS
      A(2,2) = CP*CS
      A(2,3) = -SP*CS
      A(3,1) = -ST*CS
      A(3,2) = CP*ST*SS+SP*CT
      A(3,3) = -SP*ST*SS+CP*CT
C   CALCULATE ACTUATOR FLOOR ATTACHMENT LOCATIONS IN
C   TABLE COORDINATES
      DO 20 I=1,3
      DO 20 J=1,6
      RFT(I,J)=0.
      DO 20 K=1,3
20  RFT(I,J)=RFT(I,J)+A(K,I)*(RF(K,J)-XYZ(K))
C   COMPONENTS OF ACTUATOR LENGTHS IN TABLE COORDINATES
      DO 30 I=1,3
      DO 30 J=1,6
30  ALT(I,J)=RFT(I,J)-RA(I,J)
C   CALCULATE ACTUATOR LENGTHS
      DO 50 I=1,6
      AL(I)=0.
      DO 40 J=1,3
40  AL(I)=AL(I)+ALT(J,I)*ALT(J,I)
50  AL(I)=SQRT(AL(I))

```

Figure 3-22. TABGEOM Listing

REPRODUCIBILITY OF THE  
ORIGINAL PAGE IS POOR

```

Y(1)=ALT(3,1)*.86603+ALT(2,1)*.5
Y(2)=-ALT(2,2)
Y(3)=-ALT(2,3)
Y(4)=-ALT(3,4)*.86603+ALT(2,4)*.5
Y(5)=-ALT(3,5)*.86603+ALT(2,5)*.5
Y(6)=ALT(3,6)*.86603+ALT(2,6)*.5
Z(1)=-ALT(2,1)*.86603+ALT(3,1)*.5
Z(2)=ALT(3,2)
Z(3)=-ALT(3,3)
Z(4)=-ALT(2,4)*.86603-ALT(3,4)*.5
Z(5)=ALT(2,5)*.86603+ALT(3,5)*.5
Z(6)=ALT(2,6)*.86603-ALT(3,6)*.5
DO 60 I=1,6
  BETA(I)=ATAN(ALT(1,I)/Z(I))
  RHO(I)=ATAN(SQRT(ALT(1,I)**2+Z(I)**2)/Y(I))
  BETA(I)=BETA(I)*57.29578
60 RHO(I)=RHO(I)*57.29578
  DO 80 I=1,3
    DO 80 J=1,6
      RS(I,J)=0.
    DO 70 K=1,3
      70 RS(I,J)=RS(I,J)+A(I,K)*RA(K,J)
      80 RS(I,J)=RS(I,J)-RF(I,J)+XYZ(I)
    DO 90 I=1,6
      THETA(I)=ATAN(RS(1,I)/SQRT(RS(2,I)**2+RS(3,I)**2))
  90 THETA(I)=THETA(I)*57.29578
901 FORMAT(6E12.6)
902 FORMAT(/10X'A',(T15,3E15.6))
  WRITE(6,903) AL
903 FORMAT(/10X'ACTUATOR LENGTHS',(T26,3E15.6))
  WRITE(6,904) (I,RHO(I),BETA(I),THETA(I),I=1,6)
904 FORMAT(/10X'RHO, BETA, THETA FOR ACTUATORS'/(10X15,3E15.6))
905 FORMAT(/10X'RS',(T15,3E15.6))
  GO TO 10
100 STOP
  END

```

Figure 3-22. TABGEOM Listing (continued)



TABLE 3-2  
FLOOR SWIVEL JOINT LOCATIONS\*

<u>ACTUATOR No.</u>	<u><math>x_f</math> (in.)</u>	<u><math>y_f</math> (in.)</u>	<u><math>z_f</math> (in.)</u>
1	210.407	- 64.311	123.178
2	210.429	- 76.380	116.124
3	210.422	- 74.573	-116.819
4	210.417	- 62.412	-123.683
5	210.410	138.463	- 5.975
6	210.369	138.389	8.005

\*(Center of lower swivel axes referenced to the  
DDTS load cell pair axes intersections, measured)

TABLE 3-3  
ACTIVE TABLE SWIVEL JOINT LOCATIONS\*

<u>ACTUATOR No.</u>	<u><math>x_a</math> (in.)</u>	<u><math>y_a</math> (in.)</u>	<u><math>z_a</math> (in.)</u>
1	0.0	25.102	49.500
2	0.0	-55.419	3.000
3	0.0	-55.419	- 3.000
4	0.0	25.102	-49.500
5	0.0	30.298	-46.500
6	0.0	30.298	46.500

\*(Body 2 coordinates of top swivel joints, from  
drawing)

REPRODUCIBILITY OF THE ORIGINAL PAGE IS POOR

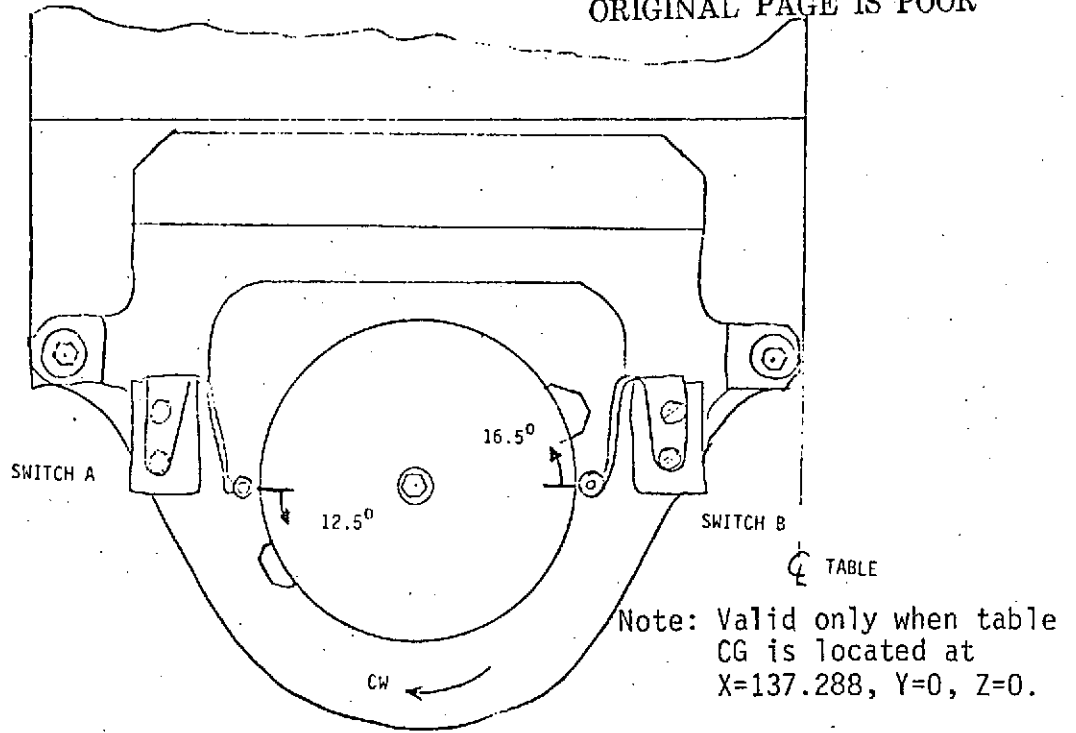


Figure 3-23. Limit Switch Setting to Prevent Table Fall Through, Actuator 1, 3 and 5

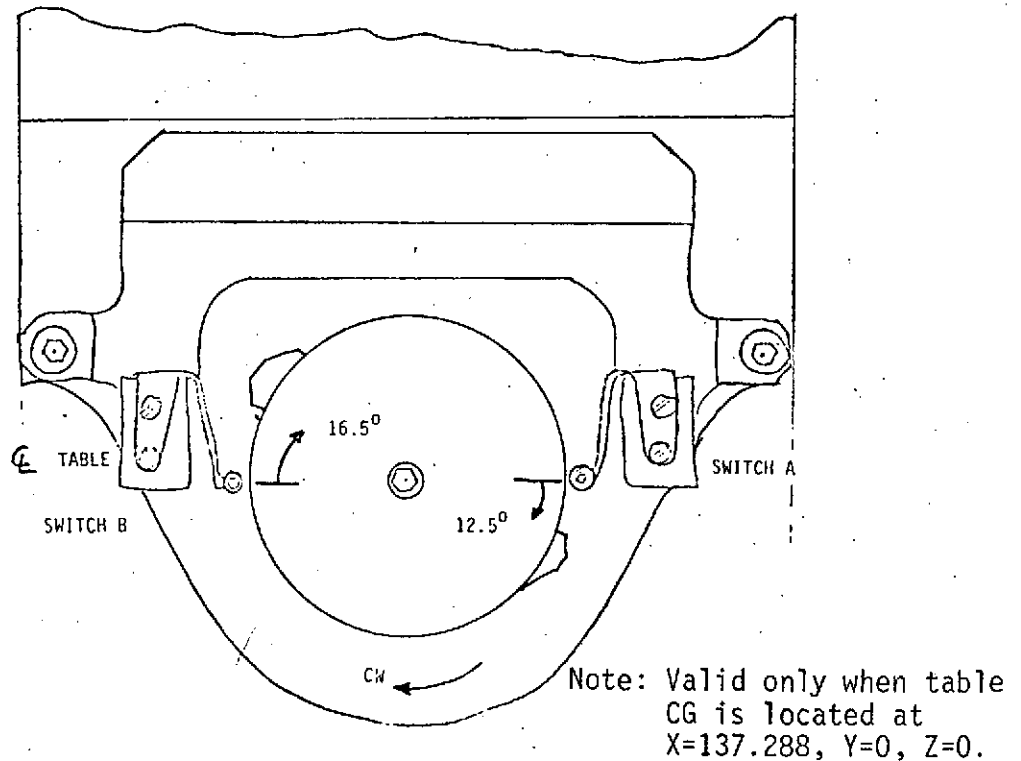


Figure 3-24. Limit Switch Setting to Prevent Table Fall Through, Actuator 2, 4 and 6

### 3.4 TOTAL SYSTEM STABILITY ANALYSIS

Math models were developed for each of the components in the total DDTS (Figure 3-25) from test or analysis to assess total loop stability. Each component will be discussed separately in the following paragraphs. Due to the complexity of the simulation, only X-axis stability was investigated.

#### 3.4.1 Load Cells

Relative motion between the two simulated spacecraft results in interaction forces which are measured by the six load cells in the stationary portion of the simulator. The dynamic load measuring capability of the load cell system was assumed to be characterized by a first order transfer function:

$$T_{LC} = \frac{F_{LC}}{F_{DH}} = \frac{1}{s/\omega_{LC} + 1}$$

Where  $F_{LC}$  is the force output of the load cells and  $F_{DH}$  is the docking hardware force measured by the load cells. Assuming a phase lag of 6 degrees at 20 Hz, the load cell transfer function becomes:

$$T_{LC} = \frac{1}{s/1257. + 1}$$

#### 3.4.2 Transmission Lines

The transmission lines carry the load cell voltages from the simulator in Building 13 to the hybrid computer in Building 16 and also the actuator commands from the computer to the simulator. Tests performed on the

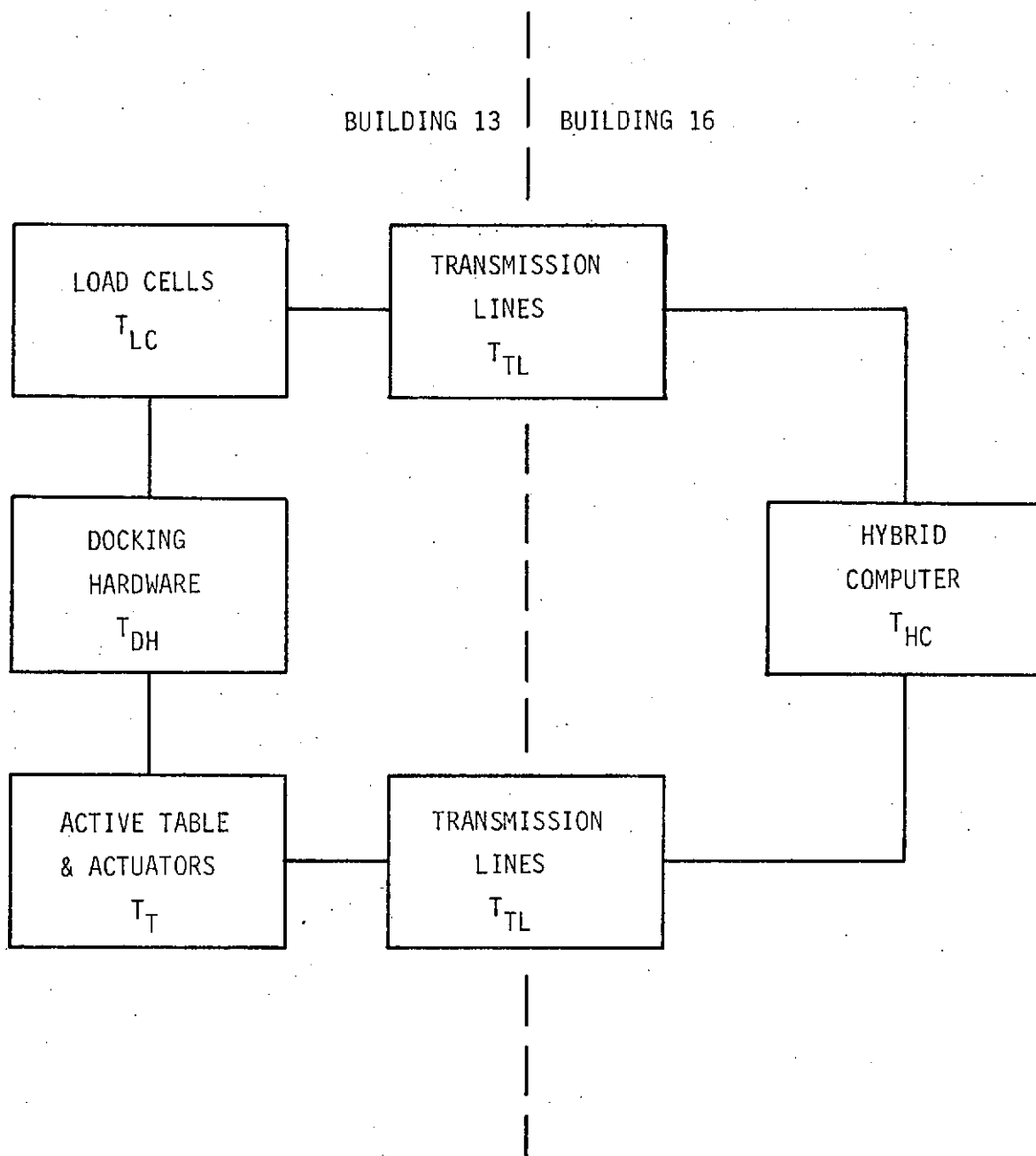


Figure 3-25. Total System Block Diagram

## 3.4.2 (Continued)

transmission lines showed very low noise levels and negligible phase shift in the dynamic range of the DDTS. Therefore, a unity transfer function was assumed for the transmission lines.

3.4.3 Hybrid Computer

The load cell voltages received by the hybrid computer are converted to total interaction forces between the spacecraft. The relative motion of the spacecraft is calculated in the computer by integrating the equations of motion under the influence of these forces. The relative motions are then transformed into DDTS hydraulic actuator position and rate commands.

A frequency response test of the hybrid computer was performed by inputting a sinusoidal voltage representing a force in the X-direction. The actuator commands generated by the computer were displayed on an oscilloscope and photographed. It was found that the wave form of the relative motions calculated began to be distorted at frequencies above 8 Hz. This distortion is caused by limitations of the TRICE, a real-time digital computer used to integrate the translational equations of motion. The TRICE is configured to provide very precise calculation of relative translational positions which are required to insure that proper docking initial conditions are obtained. This, however, results in reduced dynamic capability.

These test data show that the computer phase shift on commanded actuator length is approximately -8.6 degrees at 8 Hz. Assuming that this lag can be simulated as a first order lag filter, the hybrid computer transfer function is:

$$T_{HC} = \frac{L_C}{F_{LC}} = \frac{K_{HC}}{S^2 (S/\omega_{HC} + 1)}$$

## 3.4.3 (Continued)

where  $l_c$  is the commanded actuator length,  $F_{LC}$  is the force output of the load cells, and  $K_{HC}$  is a constant which reflects the mass associated with the simplified X-axis translation equation and the transformation between relative body motion and actuator length. With a phase lag of 8.6 degrees at 8 Hz, this transfer function becomes:

$$T_{HC} = \frac{.0285}{s^2 (s/335. + 1)}$$

3.4.4 Hydraulic Actuators

The transfer function for the hydraulic actuator,  $T_{HA}$ , was determined from the single axis servo model previously described in Paragraph 3.2. Table frequency response,  $T_T$ , was assumed to be similar to the single actuator frequency response

$$T_T = T_{HA} \quad \frac{\Delta X_T}{\Delta l_p} = \frac{l_p}{l_c} \cdot \frac{\Delta T}{\Delta l_p}$$

where  $\Delta X_T / \Delta l_p$  is the change in table position due to a change in actuator length. With the actuators at mid-stroke (the approximate position at docking contact):

$$\frac{\Delta X_T}{\Delta l_p} = 1.38$$

### 3.4.5 Docking Hardware

The docking hardware is the most difficult component of the DDTS to model since docking hardware attenuators exhibit nonlinear force transmission characteristics. Equivalent linear stiffness and damping were calculated for various positions of the attenuators including a "full retract" case where the two docking mechanisms are hard docked. The linearized transfer function for the docking hardware is made up of a spring force term and a damping force term:

$$T_{DH} = \frac{F_{DH}}{X_T} = K_{DH} + K_{DDH} S$$

Values of stiffness,  $K_{DH}$ , and damping,  $K_{DDH}$ , calculated for various conditions are tabulated below.

Condition	$K_{DH}$	$K_{DDH}$
Near full extension (compression)	6.65	.455
Full extension (tension)	$1.103 \times 10^5$	167.6
Full retract (hard docked)	$3.75 \times 10^6$	977.1

### 3.4.6 Stability Analysis

An open loop stability study was performed using the transfer functions developed. The Bode plots obtained for the three docking hardware conditions are shown in Figures 3-26 through 3-28. All cases analyzed are stable

REPRODUCIBILITY OF THE ORIGINAL PAGE IS POOR

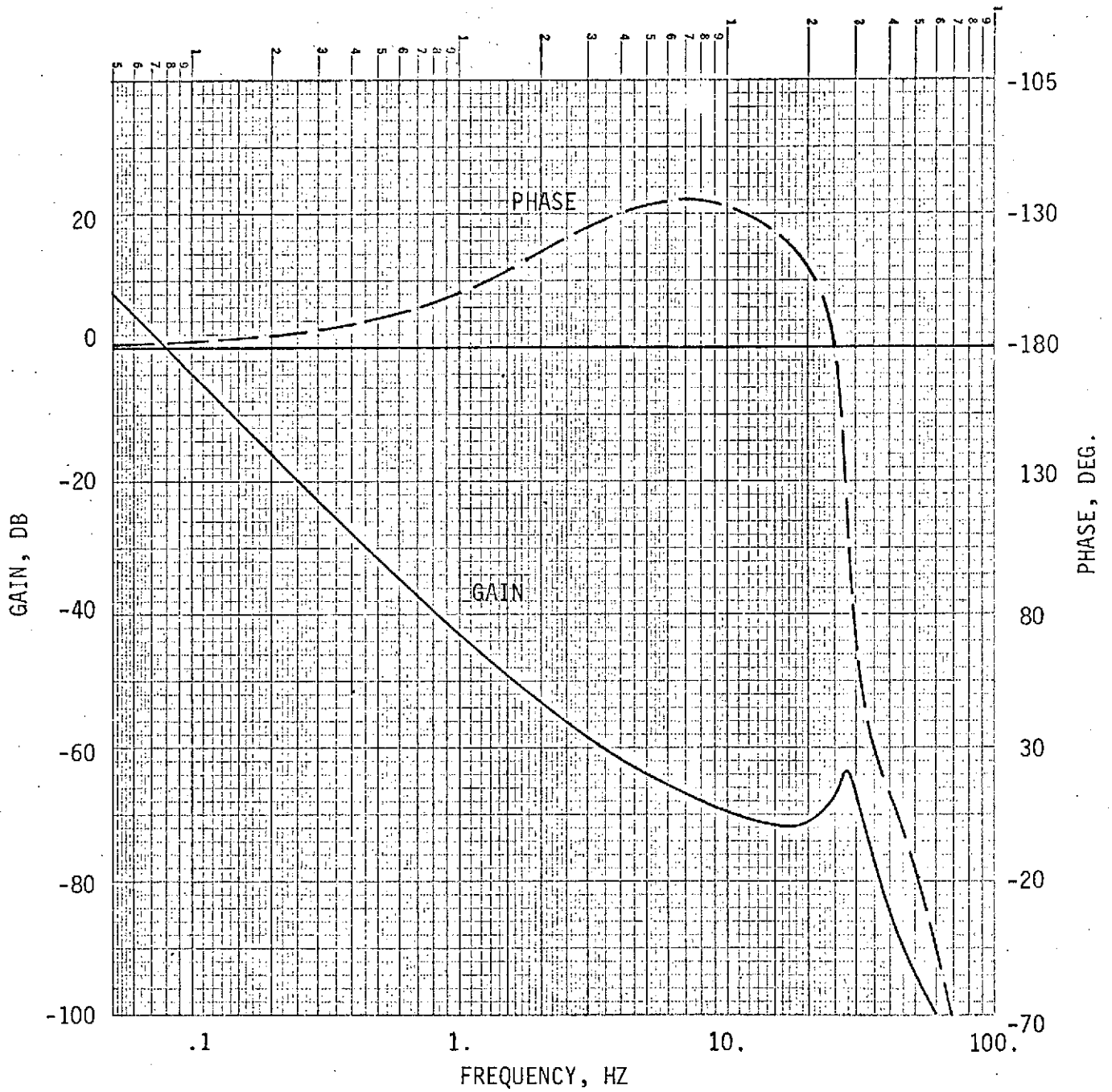


Figure 3-26. Total System Stability, Near Full Extension



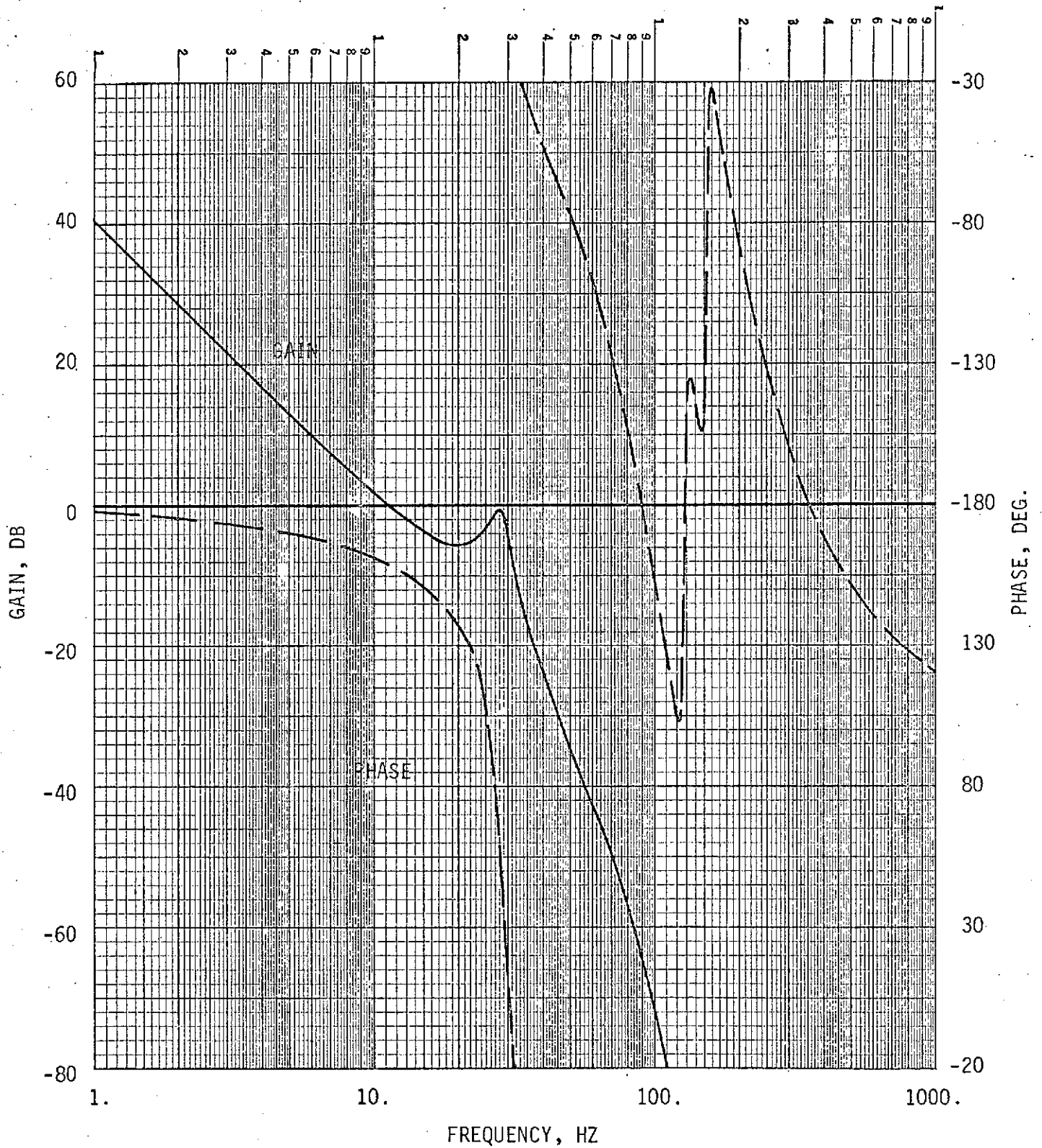


Figure 3-27. Total System Stability, Full Extension (Tension)

REPRODUCIBILITY OF THE ORIGINAL PAGE IS POOR

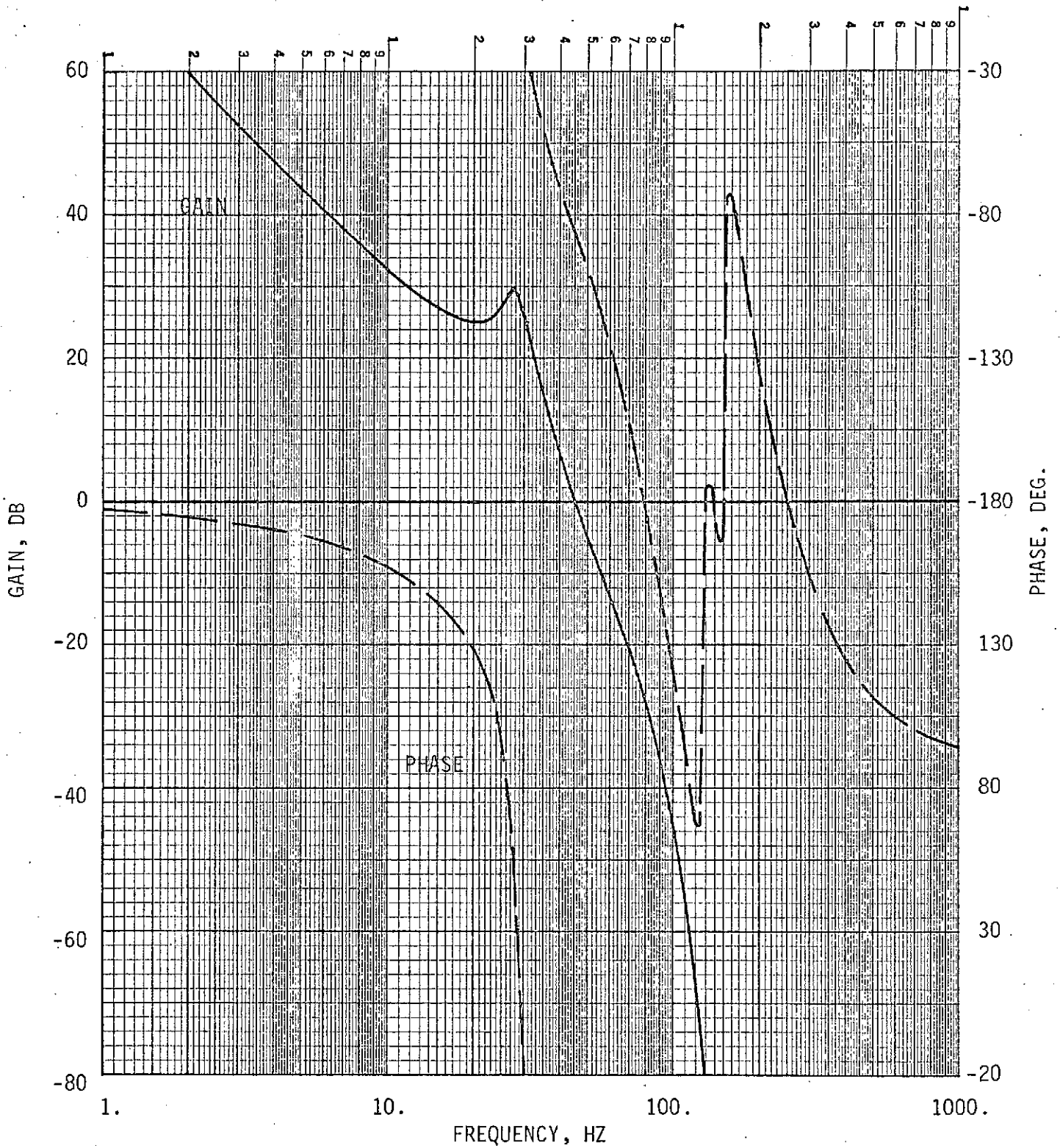


Figure 3-28. Total System Stability, Full Retract

## 3.4.6 (Continued)

including a condition at full retract with no phase shift in the load cells and hybrid computer. The stability margins obtained from this study are shown below.

Condition	Gain Margin (DB)	Phase Margin (DEG.)
Near full extension (compression)	-67	2
Full extension (tension)	-63	21
Full retract (hard docked)	-26	95
Full retract (with ideal load cells and hybrid computer)	-48	143

In the full retract cases, the stiffness and damping of the load cell system was substituted for the docking hardware system stiffness.

#### 4.0 DETAILED OPERATIONAL TEST PROCEDURES

The detailed test procedures (DTP's) for each manned operation station used in the DDTS tests were assembled, integrated, and edited for each major test program. The NASA Administrative Terminal System was used in generating these procedural documents via a remote computer terminal located in Building 13. Preliminary, review, and final copies of the DTP's were furnished for review and approval by JSC.

#### 4.1 PROCEDURES DOCUMENT CONTENTS

The DTP's were divided into the following six sections:

- a. General Information
- b. Test Procedures
- c. Test Data Sheets
- d. Post-Test Verification and Acceptance
- e. Test Rules
- f. Emergency Procedures

The General Information section contains the introduction, test objectives, references, abbreviations and acronyms, test configuration, communication and test team organization, and test instrumentation necessary to perform a complex docking test.

The Test Procedures section contains the pretest, countdown, abort backout, recycle, and shutdown procedural sequences necessary to operate each manned station. These procedural sequences include the sequence number, the commands, and the responses necessary to operate the test equipment and to control the environment. The Test Conductor (TC) sequences contain the main line of events for the docking tests. The Simulator Operator (SO), Instrumentation Technician in Building 16 (IT-1), Instrumentation Technician in Building 13 (IT-2), USA Docking Simulator Operator (DS01), and the USSR Docking Simulator Operator (DS02) test sequences are keyed for action into the TC sequences at the appropriate location and time.

## 4.1 (Continued)

The Test Data Sheets section contains the necessary tables for recording the data required for each docking test. The Post-Test Verification and Acceptance section provides space for signatures of the persons responsible for the test and its results. The Test Rules section provides the pre-planned actions that should be performed if an off-normal condition or malfunction occurs. In addition, the mandatory instrumentation is defined. The Emergency Procedures section contains the recommended procedures to be used in the event that fire or medical assistance is needed.

## 4.2 TEST REQUIREMENTS AND OPERATIONAL TEST PROCEDURES

Collections of test requirements (TRQ's) and DTP's were published in References 5 through 7. The tests for which TRQ's and/or DTP's were written are listed below along with the individual document numbers.

## Reference 5 (D2-118465-1)

Hybrid Computer Subsystem Test, TRQ-1-13/16-73

Hydraulic Supply Subsystem Test, TRQ-2-13-73

Electrical/Electronic Subsystem Test, TRQ-3-13-73

Load Cell Subsystem Test, TRQ-4-13-73

Transmission Line Subsystem Test, TRQ-5-13/16-73

Data Acquisition Subsystem Test, TRQ-6-13/16-73

Servo Actuator Unit Test, TRQ-7-13-73

Data Reduction Verification Test, TRQ-8-13/16-73

Motion Simulator Test, TRQ-9-13-73

Gravity Compensation Subsystem Test, TRQ-10-13-73

Thermal Environment Subsystem Test, TRQ-11-13-73

Hybrid Computer Subsystem Test, DTP-1-13/16-73

Hydraulic Supply Subsystem Test, DTP-2-13-73

4.2 (Continued)

Electrical/Electronic Subsystem Test, DTP-3-13-73

Part I, Instrumentation

Part II, Force Measuring System

Part III, Comcor Line Driver Checkout

Part IV, Simulator Control Panel

Part V, Servo Amplifier and Abort Card Test

Part VI, Analog Computer Checkout (AD-80)

Part VII, Local Computer Control Checkout

Part VIII, Interface Verification

Part IX, Differential Measuring System

Part X, Electronic System Checkout

Load Cell Subsystem Test, DTP-4-13-73

Load Cell Subsystem Test, DTP-4-13-73 (Rev. A)

Transmission Line Subsystem Test, DTP-5-13/16-73

Data Acquisition Subsystem Test, DTP-6-13/16-73

Servo Actuator Unit Test, DTP-7-13-73

Data Reduction Verification Test, DTP-8-13/16-73

Motion Simulator Test, DTP-9-13-73

Gravity Compensation Subsystem Test, DTP-10-13-73

Thermal Environment Subsystem Test, DTP-11-13-73

Reference 6 (D2-118482-1)

Hydraulic Supply Subsystem Test, DTP-2-13-73, Rev. A

Electrical/Electronic Subsystem Test, DTP-3-13-73

Part VI, Analog Computer Checkout (AD-80)

Part IX, Pressure Abort System Verification

4.2 (Continued)

Servo Actuator Unit Test, DTP-7-13-73, Rev. A

Motion Simulator Test, DTP-9-13-73

Gravity Compensation Subsystem Test, DTP-10-13-73

Thermal Environmental Subsystem Test, DTP-11-13-73

Probe and Drogue Test, DTP-12-13-73

DDTS Integration and Open Loop Test, DTP-14-13-73

USA Development Test, TOP-2-13-73

Reference 7 (D2-118482-2)

USA/USSR Joint Dynamic Development Test, TOP, USA WG3-009

USA/USSR Joint Dynamic Development Test, TOP, USA WG3-009A, Rev. A

USA/USSR Joint Dynamic Development Test, TOP, USA WG3-009B, Rev. B

Verification of Docking System Kinematic Envelopes on the Dynamic Docking Test System, TOP USA WG3-012

USA/USSR Joint Dynamic Qualification Test, TOP, USA WG3-020, Review Copy

## 5.0 ANALYSIS OF DOCKING DYNAMICS AND LOADS

This section discusses the results of the US/US development tests, the US/USSR development tests, and the 10 Hz investigation conducted to evaluate proposed "fixes" to the 10 Hz anomaly that arose during the development tests. The subsequent US/US qualification testing performed using these fixes is also discussed.

### 5.1 DEVELOPMENT TESTS

The development test program was conducted to "prove that the USA and USSR docking system can withstand the maximum loads and perform all required functions under design conditions" (Reference 8). The DDT-S served as the instrument to provide this proof. The function of the DDT-S was to:

- a. Provide the desired relative docking initial conditions to the docking hardware.
- b. Simulate the subsequent relative dynamic motion of the two spacecraft.
- c. Supply as output
  - (1) Design hardware loads
  - (2) Capture characteristics

Items b and c were also obtained analytically. Results from the two sources - test and analysis - were then compared and an assessment made.

The following assessment of the US/US and the US/USSR development tests can be made:

- a. Desired initial contact conditions were achieved with a high degree of accuracy.
- b. Good correlation between analytically predicted capture and experimental results was obtained.



## 5.1 (Continued)

- c. Good agreement was obtained between analytical and experimental load and motion signatures (especially during the time span from contact through capture and maximum loads).
- d. In general, peak loads were within 10 percent of analytically predicted results.

### 5.1.1 US/US Development Tests

This series of tests was conducted prior to the joint US/USSR development test. The test article consisted of the active US docking hardware on one side of the DDTS and the passive US docking system on the other. The simulation was modeled so that the mass properties of the US passive system represented the Soyuz mass properties. This series of tests, then, simulated the joint US/USSR tests to be conducted later with the USSR passive system. For this reason, a detailed presentation of US/US development test data and analysis results is not included as part of this report. Only a summary is presented.

Tests were conducted with the initial docking contact conditions shown in Table 5-1. Only ambient temperature tests were performed and cases 7, 8, 11 and 12 were omitted. The test data obtained are documented on microfilm and can be obtained from Reference 9.

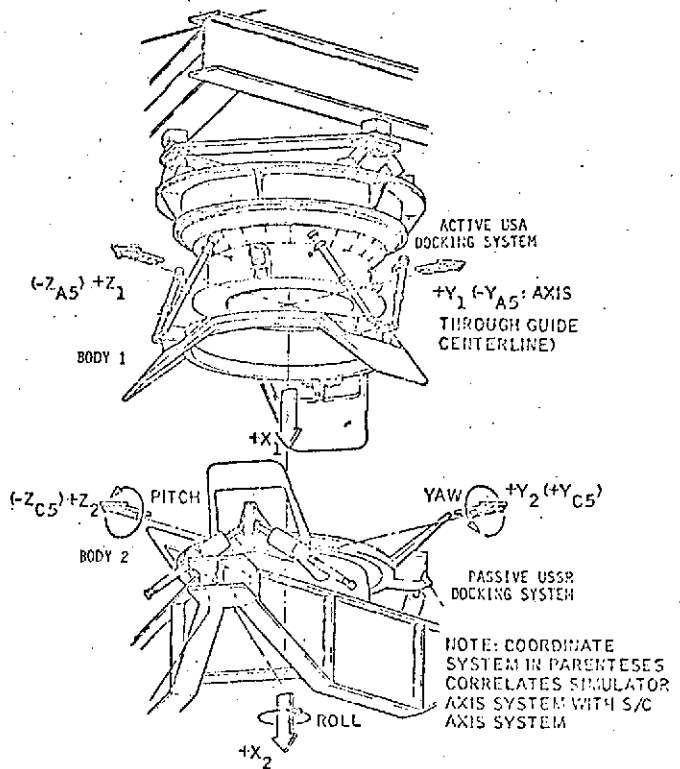
### 5.1.2 US/USSR Development Tests

Joint US/USSR development tests were performed with both the USA and the USSR docking hardware in the active mode. The discussion of test results that follows, however, will be primarily devoted to tests conducted with the USA system active since no USSR active system analytical results are available for comparison purposes.

TABLE 5-1 US/US DEVELOPMENT TEST CONDITIONS

CASE	3CLOSING VELOCITY		3LATERAL VELOCITY				4MISS DISTANCE				5ANGULAR RATE			6ANGULAR ATTITUDE			TEMP	REMARKS
			Y		Z		Ym		Zm		Roll	Pitch	Yaw	Roll	Pitch	Yaw		
	(mps)	(fps)	(mps)	(fps)	(mps)	(fps)	(m)	(ft)	(m)	(ft)	(deg/sec)	(deg/sec)	(deg/sec)	(deg)	(deg)	(deg)		
1	.05	.164	0.0	0.0	0.0	0.0	0.0	0.0	0.0	0.0	0.0	0.0	0.0	0.0	0.0	0.0	amb	Straight-in low energy
2	.0915	.3	0.0	0.0	0.0	0.0	0.0	0.0	0.0	0.0	0.0	0.0	0.0	0.0	0.0	0.0	↑	Straight-in nominal
3	.3	.985	0.0	0.0	0.0	0.0	0.0	0.0	0.0	0.0	0.0	0.0	0.0	0.0	0.0	0.0		Straight-in high energy
4	.05	.164	-.05	-.164	0.0	0.0	-.3	-.985	0.0	0.0	0.0	-1.0	0.0	0.0	-3.0	0.0		-Y miss low energy
5	.0915	.3	-.05	-.164	0.0	0.0	-.3	-.985	0.0	0.0	0.0	-1.0	0.0	0.0	-3.0	0.0		-Y miss nominal
6	.3	.985	-.1	-.328	0.0	0.0	-.3	-.985	0.0	0.0	0.0	-1.0	0.0	0.0	-7.0	0.0		-Y miss high energy
7	.05	.164	.05	.164	0.0	0.0	.3	.985	0.0	0.0	0.0	+1.0	0.0	0.0	3.0	0.0		+Y miss low energy
8	.3	.985	.1	.328	0.0	0.0	.3	.985	0.0	0.0	0.0	1.0	0.0	0.0	7.0	0.0		+Y miss high energy
9	.05	.164	-.05	-.164	0.0	0.0	-.212	-.696	-.212	-.696	0.0	-1.0	0.0	0.0	-3.0	0.0		-Y; -Z miss low energy
10	.3	.985	-.1	-.328	0.0	0.0	-.212	-.696	-.212	-.696	-1.0	-1.0	0.0	0.0	-7.0	0.0		-Y; -Z miss high energy
11	.05	.164	0.0	0.0	.05	.164	0.0	0.0	.3	.985	-5	0.0	-1.0	0.0	0.0	-3.0		+Z miss low energy
12	.3	.985	0.0	0.0	.1	.328	0.0	0.0	.3	.985	-1.0	0.0	-1.0	0.0	0.0	-7.0		+Z miss high energy
13	.05	.164	-.025	-.080	-.05	-.164	0.0	0.0	0.0	0.0	0.0	0.0	0.0	0.0	-.3	.6		Pitch-yaw miss low energy
14	.05	.164	0.0	0.0	0.0	0.0	0.0	0.0	0.0	0.0	-5	0.0	0.0	-7.0	0.0	0.0		Roll miss low energy
15	.0915	.3	0.0	0.0	0.0	0.0	0.0	0.0	0.0	0.0	-1.0	0.0	0.0	-7.0	0.0	0.0		Roll miss nominal
16	.3	.985	0.0	0.0	0.0	0.0	0.0	0.0	0.0	0.0	-1.0	0.0	0.0	-7.0	0.0	0.0		Roll miss high energy
17	.05	.164	-.05	-.164	0.0	0.0	0.0	0.0	0.0	0.0	1.0	0.0	0.0	7.0	0.0	0.0		Jack knife low energy
18	.0915	.3	-.05	-.164	0.0	0.0	0.0	0.0	0.0	0.0	1.0	0.0	0.0	7.0	0.0	0.0	↓	Jack knife nominal
19	.3	.985	-.1	-.328	0.0	0.0	0.0	0.0	0.0	0.0	1.0	0.0	0.0	7.0	0.0	0.0	amb	Jack knife high energy

- The spacecraft with the active and passive docking systems are designated as body 1 and body 2, respectively.
- Spacecraft control system operations are defined in IED50016.
- Closing and Lateral Velocities (X, Y, Z)  
Translational velocity components (expressed in the body 2 system) of the body 1 c.g. with respect to the body 2 c.g.
- Miss Distance (Ym, Zm)  
Coordinates (expressed in the body 2 system) of the point defined by the intersection of the X<sub>1</sub> axis and the plane passing through the forwardmost part of the body 1 docking system guides.
- Angular Rates (Roll, Pitch, Yaw)  
Relative rotational velocity components of body 1 relative to body 2 (expressed in the body 1 system) using the right-hand rule for direction of rotations about the X<sub>1</sub>, Z<sub>1</sub>, and Y<sub>1</sub> axes, respectively.
- Angular Attitude (Roll, Pitch, Yaw)  
Roll attitude is the included angle (measured in the Y-Z plane of the body 2 system) from the X-Y plane of body 2 to the X-Y plane of body 1, using the right-hand rule for direction of rotation about the X<sub>2</sub> axis. Pitch and yaw attitudes are the components of the included angle (expressed in the body 2 system) from the body 2 X-axis to the body 1 X-axis, using the right-hand rule for pitch attitude about the Z<sub>2</sub> axis and yaw attitude about the Y<sub>2</sub> axis.



## 5.1.2 (Continued)

Test cases used in the joint development test are shown in Table 5-2. These conditions were chosen to demonstrate docking capability at various temperatures (ambient, high, and low). Some cases represent high energy cases chosen to produce design docking hardware loads, and other cases are low energy cases which could lead to capture difficulties. The test data obtained with the USA system as the active spacecraft are documented in Reference 10; the USSR active test data are in Reference 11. Since these test reports consist of 14 volumes and 35 volumes of data, respectively, the tables of contents are included in this report as Tables 5-3 and 5-4 so that specific data might be found more easily.

As mentioned in Paragraph 5.1, the test results obtained with the USA docking hardware in the active mode agreed closely with the pretest analytical results obtained with the JSC "Ring Finger Docking Dynamics Program." Test versus analysis correlation results for each test case are documented in Reference 12. Some typical plots from Reference 12 are shown in Figures 5-1 through 5-6. A summary of the comparison of peak loads obtained in the high energy cases is tabulated in Table 5-5.

Figures 5-1 through 5-6 demonstrate the good agreement that was obtained for two high energy cases shown in Table 5-2. Also indicated in these figures is a 9-10 Hz dynamic phenomenon that is not considered to be representative of the docking hardware. These oscillations can be classified as:

- a. 10 Hz oscillations
- b. 10 Hz instability following capture

These phenomena were observed in test results with either the USA or the USSR docking system in the active mode.

The general 10 Hz oscillation was present in most test runs. However, it was usually of such low amplitude that it presented no major concern. In some cases, the 10 Hz content was large enough to cause questions to be

REPRODUCIBILITY OF THE ORIGINAL PAGE IS POOR

TABLE 5-2 US/USSR DEVELOPMENT TEST CONDITIONS

CASE	CLOSING VELOCITY			LATERAL VELOCITY			MISS DISTANCE		ANGULAR RATE			ANGULAR ATTITUDE			TEMPERATURE	REMARKS
	X (mps)	Y (mps)	Z (mps)	Ym (m)	Zm (m)	Roll (deg/sec)	Pitch (deg/sec)	Yaw (deg/sec)	Roll (deg)	Pitch (deg)	Yaw (deg)					
1	0.3	0.0	0.0	0.0	0.0	0.0	0.0	0.0	0.0	0.0	0.0	0.0	0.0	high, low	Straight-in high energy	
2	0.3	-0.1	0.0	-0.3	0.0	0.0	-1.0	0.0	0.0	0.0	-7.0	0.0	0.0	high, low	-Y miss, high energy	
3	0.3	0.0	0.1	0.0	0.3	-1.0	0.0	-1.0	0.0	0.0	0.0	-7.0	0.0	high, low	+Z miss, high energy	
4	0.3	-0.1	0.0	-0.212	-0.212	-1.0	-1.0	0.0	0.0	0.0	-7.0	0.0	0.0	high, low	-Y; -Z miss, high energy	
5	0.05	-0.05	0.0	-0.3	0.0	0.0	-1.0	0.0	0.0	0.0	-3.0	0.0	0.0	low	-Y miss, low energy	
6	0.05	-0.05	0.0	-0.212	-0.212	-1.0	-1.0	0.0	0.0	0.0	-3.0	0.0	0.0	low	-Y; -Z miss, low energy	
7	0.05	0.0	0.05	0.0	0.3	0.0	0.0	-1.0	0.0	0.0	0.0	-3.0	0.0	low	+Z miss, low energy	
8	0.05	0.0	0.0	0.0	0.0	-1.0	0.0	0.0	0.0	-7.0	0.0	0.0	0.0	low	Roll miss, low energy	
9	0.3	-0.1	0.0	-0.3	0.0	0.0	-1.0	0.0	0.0	7.0	0.0	0.0	high, low	Max Soyuz guide load		
10	0.3	0.0	0.0	0.0	0.0	1.0	0.0	0.0	7.0	0.0	0.0	0.0	high, low	Roll, high energy		
11	0.05	-0.05	0.0	-0.3	0.0	0.0	-1.0	0.0	0.0	7.0	0.0	0.0	0.0	low	-Y, Max. Ang. Miss, low energy	
12	0.05	-0.05	0.0	-0.3	0.0	-1.0	-1.0	0.0	-7.0	7.0	0.0	0.0	0.0	low	-Y, Max. Ang. Miss, roll, low energy	

- The spacecraft with the active and passive docking systems are designated as body 1 and body 2, respectively.
- Spacecraft control system operations are defined in IED50016.
- Closing and Lateral Velocities (X, Y, Z)  
Translational velocity components (expressed in the body 2 system) of the body 1 c.g. with respect to the body 2 c.g.
- Miss Distance (Ym, Zm)  
Coordinates (expressed in the body 2 system) of the point defined by the intersection of the X<sub>1</sub> axis and the plane passing through the forwardmost part of the body 1 docking system guides.
- Angular Rates (Roll, Pitch, Yaw)  
Relative rotational velocity components of body 1 relative to body 2 (expressed in the body 1 system) using the right-hand rule for direction of rotations about the X<sub>1</sub>, Z<sub>1</sub>, and Y<sub>1</sub> axes, respectively.
- Angular Attitude (Roll, Pitch, Yaw)  
Roll attitude is the included angle (measured in the Y-Z plane of the body 2 system) from the X-Y plane of body 2 to the X-Y plane of body 1, using the right-hand rule for direction of rotation about the X<sub>2</sub> axis. Pitch and yaw attitudes are the components of the included angle (expressed in the body 2 system) from the body 2 X-axis to the body 1 X-axis, using the right-hand rule for pitch attitude about the Z<sub>2</sub> axis and yaw attitude about the Y<sub>2</sub> axis.

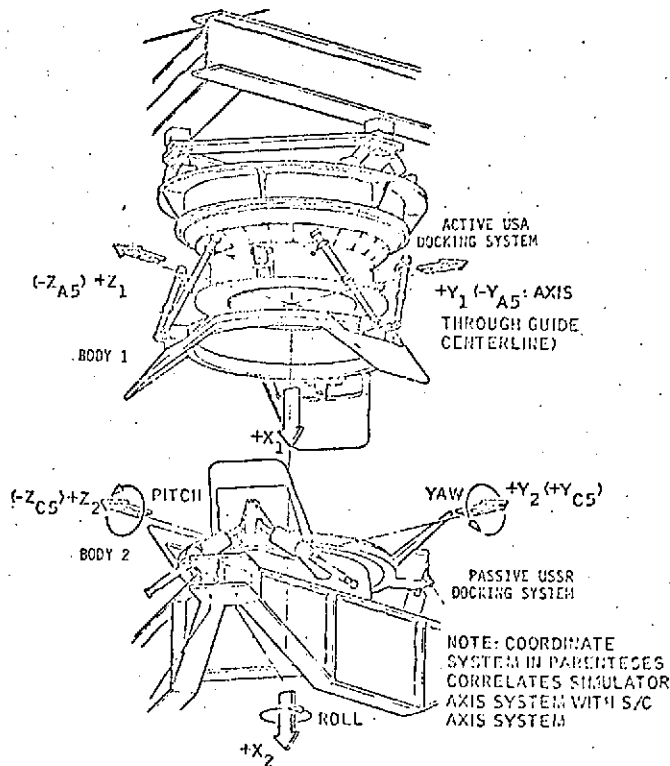


TABLE 5-3

LOCATION OF DOCUMENTED TEST DATA  
US/USSR DEVELOPMENT TEST - US ACTIVE



<u>VOLUME</u>	<u>TEST CASE</u>	<u>TEMPERATURE</u>	<u>TEST IDENTIFICATION</u>
<u>Category I</u>			
1	5	ambient	101931400051
2	6	"	101931400061
3	1	cold	103031600011
3	2	"	110231600021
4	3	"	110231600031
4	4	"	110231600042
4	5	"	102931600051
5	6	"	102931600061
6	7	"	110231600071
6	8	"	110231600081
7	9	"	110231600091
7	10	"	110231600102
8	11	"	102931600111
8	12	"	103031600121
9	1	hot	102631500011
9	2	"	120731500021
9	3	"	102631500031
10	4	"	120731500041
11	9	"	102631500091
11	10	"	102631500101
<u>Category II</u>			
12	3	ambient	120631400031
12	9	"	120631400091
13	10	"	120631400101
13	11 (SCS + retract)	"	120631410011
14	3 (DAP)	"	120731410031
14	9 (DAP)	"	120731410091
14	10 (DAP)	"	120731410101
14	1 (DAP + retract)	"	120731410011
②	2	hot	120731500041
	4	"	120731500021


① Volume number of Document USA WG3-018.

② Included in the Category I listing above.

TABLE 5-4

LOCATION OF DOCUMENTED TEST DATA  
 US/USSR DEVELOPMENT TEST - USSR ACTIVE

<u>VOLUME</u> 	<u>TEST</u>	<u>VOLUME</u> 	<u>TEST</u>
<u>Category I</u>		<u>Category II (continued)</u>	
1	111731700051	17	112731700071
	111731700061		112731700081
2	111731800011	18	112731700122
	111731800021		112731701214
3	111731800031	19	112731700091
	111731800041	20	112731700911
4	111731800052		112731700611
	111731800061	21	112731700711
	111731800101	22	112731700461
5	112031900011	23	112731700621
	112131900012	24	112731700631
	112031900013	25	112831700911
	112131900021		112831701221
6	112131900031	26	112831701641
	112131900041		112831700642
	112131900051		112831711221
7	112131900062	27	112831710031
	112131900071		112831700101
8	112031900082	28	112931700721
	112131900091	29	112931701111
	112131900101	30	112931710031
	112131900111		112931710092
9	112131900121	31	112931710101
<u>Category II</u>			112931710102
10	112331910041	32	120331900041
	112331910411		120331900411
	112331910421		120331900422
11	112331910432	33	120331900431
	112331910442		120331900011
12	112631700041		120331910011
	112631700412	34	120331910012
13	112631700421		120331900101
	112631700431		120331910014
14	112631700451		120331910015
15	112631700111	35	120531700011
16	112631701111		120531710011
	112731701111		120531710101
17	112731700121		120531700101

 Volume number of Document USSR WG3-022.

REPRODUCIBILITY OF THE ORIGINAL PAGE IS POOR

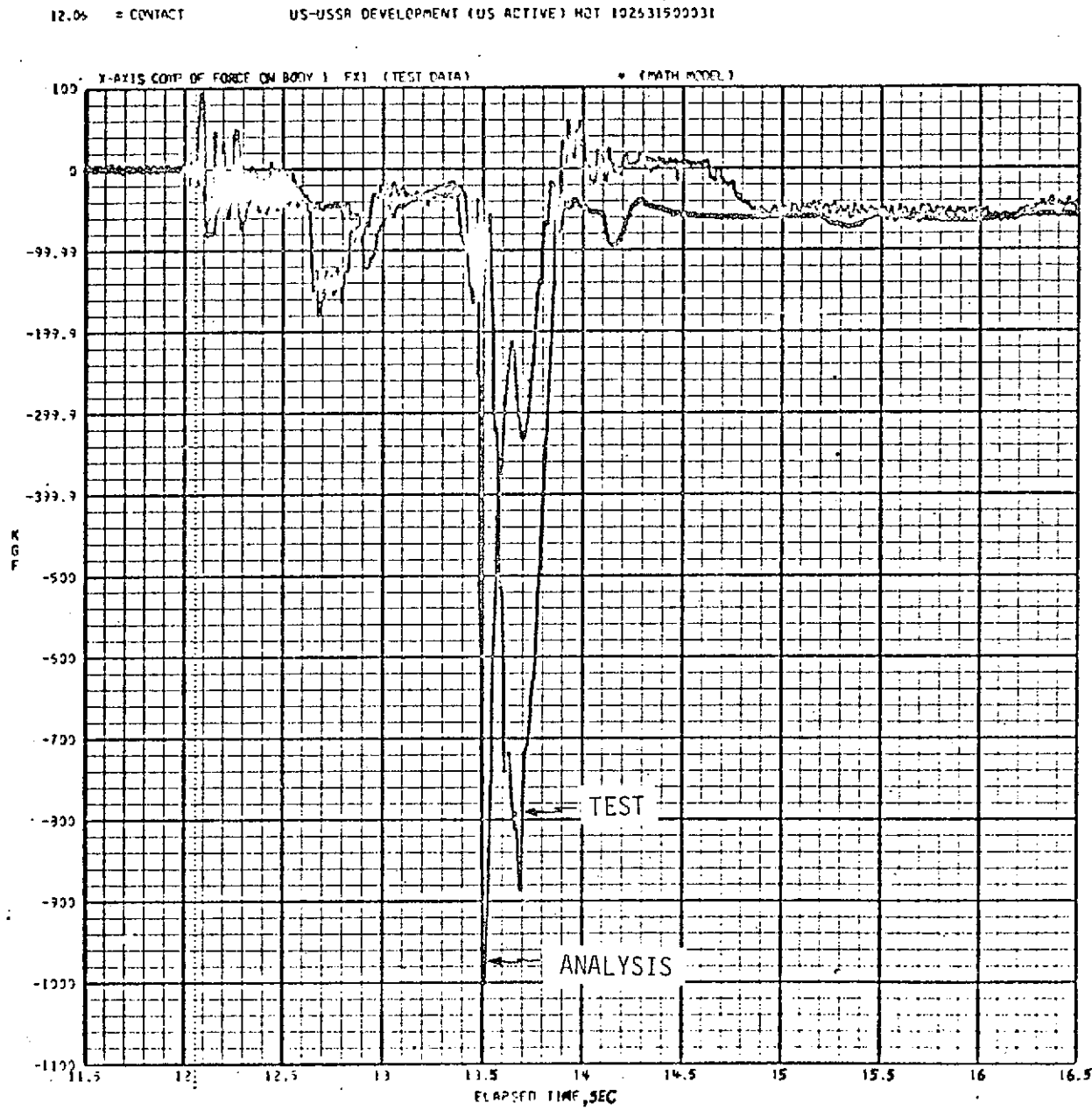


Figure 5-1. Typical Test/Analysis Correlation, US-USSR Development Test, USA Active Case 3, Hot; X Force on CSM C.G.

REPRODUCIBILITY OF THE  
ORIGINAL PAGE IS POOR

12.96 = CONTACT

US-USSR DEVELOPMENT (US ACTIVE) HOT 102531500031



Figure 5-2. Typical Test/Analysis Correlation, US-USSR  
Development Test, USA Active Case 3, Hot;  
Y Force on CSM C.G.



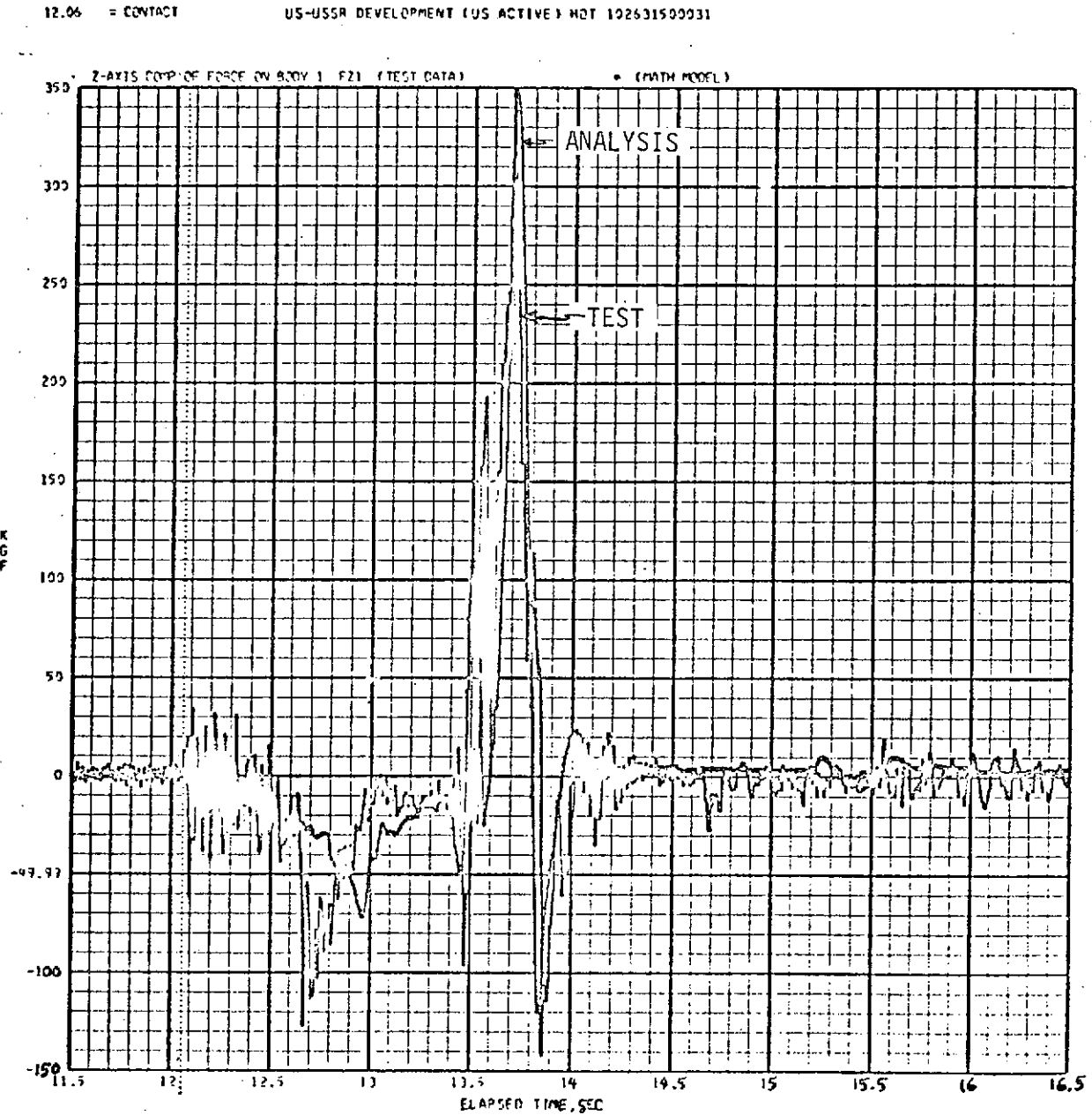


Figure 5-3. Typical Test/Analysis Correlation, US-USSR Development Test, USA Active Case 3, Hot; Z Force on CSM C.G.

12.06 = CONTACT  
 12.08 = NO PARTURE  
 12.09 = MM TAPE A01619

US-USSR DEVELOPMENT (US ACTIVE) HOT 120731500021

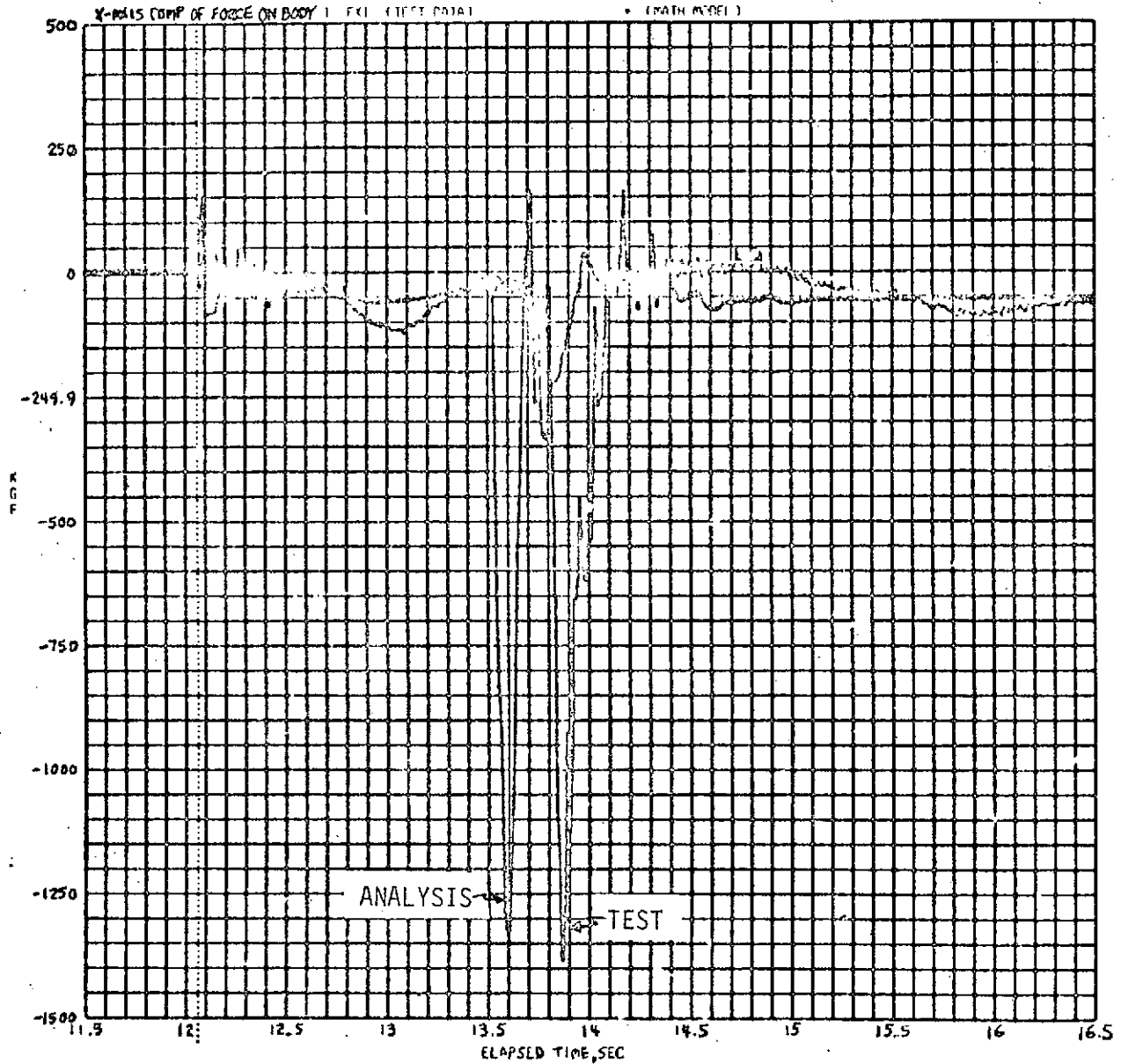


Figure 5-4. Typical Test/Analysis Correlation, US-USSR Development Test, USA Active Case 2, Hot; X Force on CSM C.G.

REPRODUCIBILITY OF THE ORIGINAL PAGE IS POOR

US-USSR DEVELOPMENT (US ACTIVE) HOT 120731500021

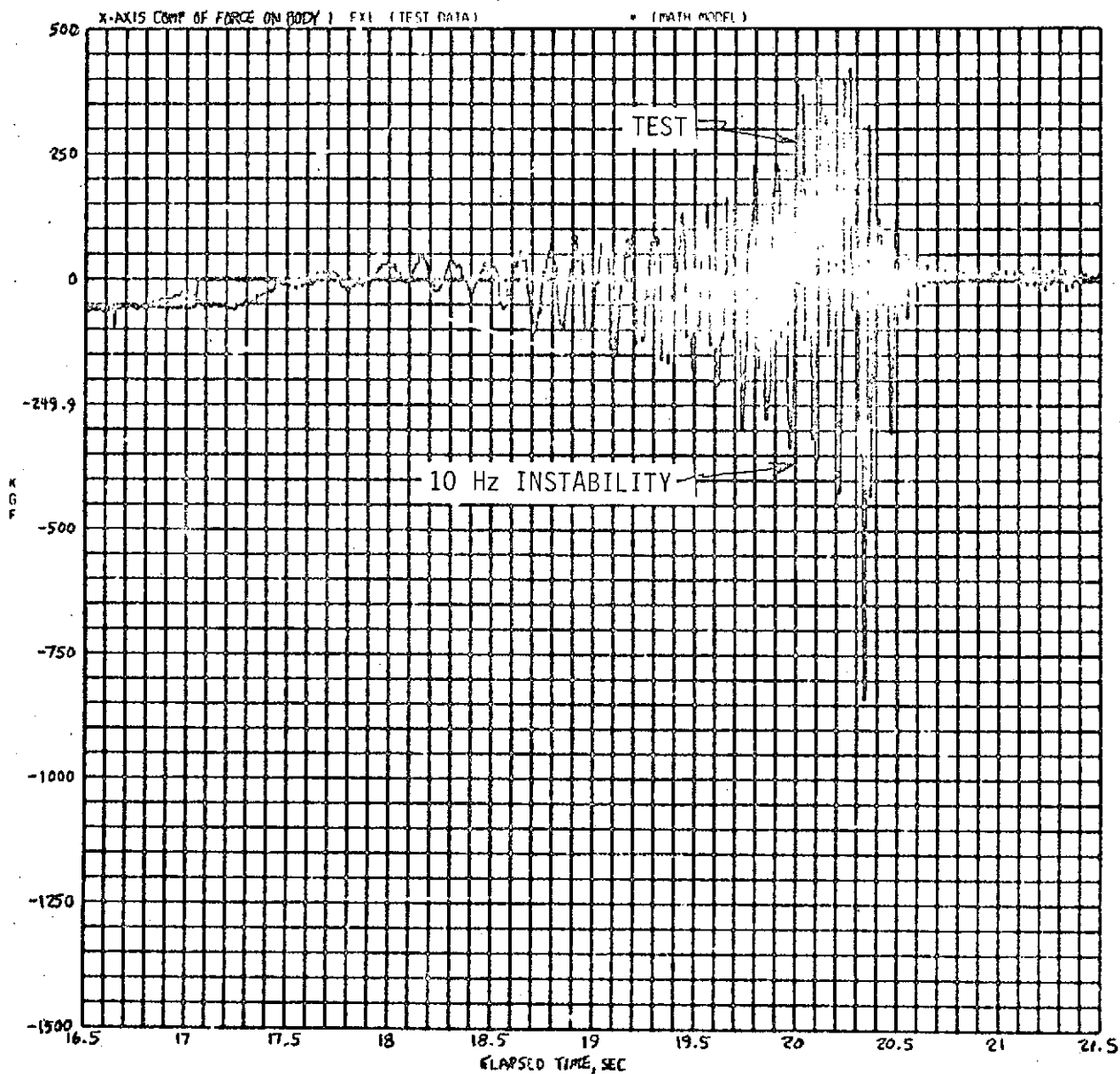


Figure 5-4. Typical Test/Analysis Correlation, US-USSR Development Test, USA Active Case 2, Hot; X Force on CSM C.G. (continued)

REPRODUCIBILITY OF THE ORIGINAL PAGE IS POOR

12.06 = CONTACT  
 12.05 = NO CAPTURE  
 12.06 = M/M TAPE R01519

US-USSR DEVELOPMENT (US ACTIVE) HOT 120731500021

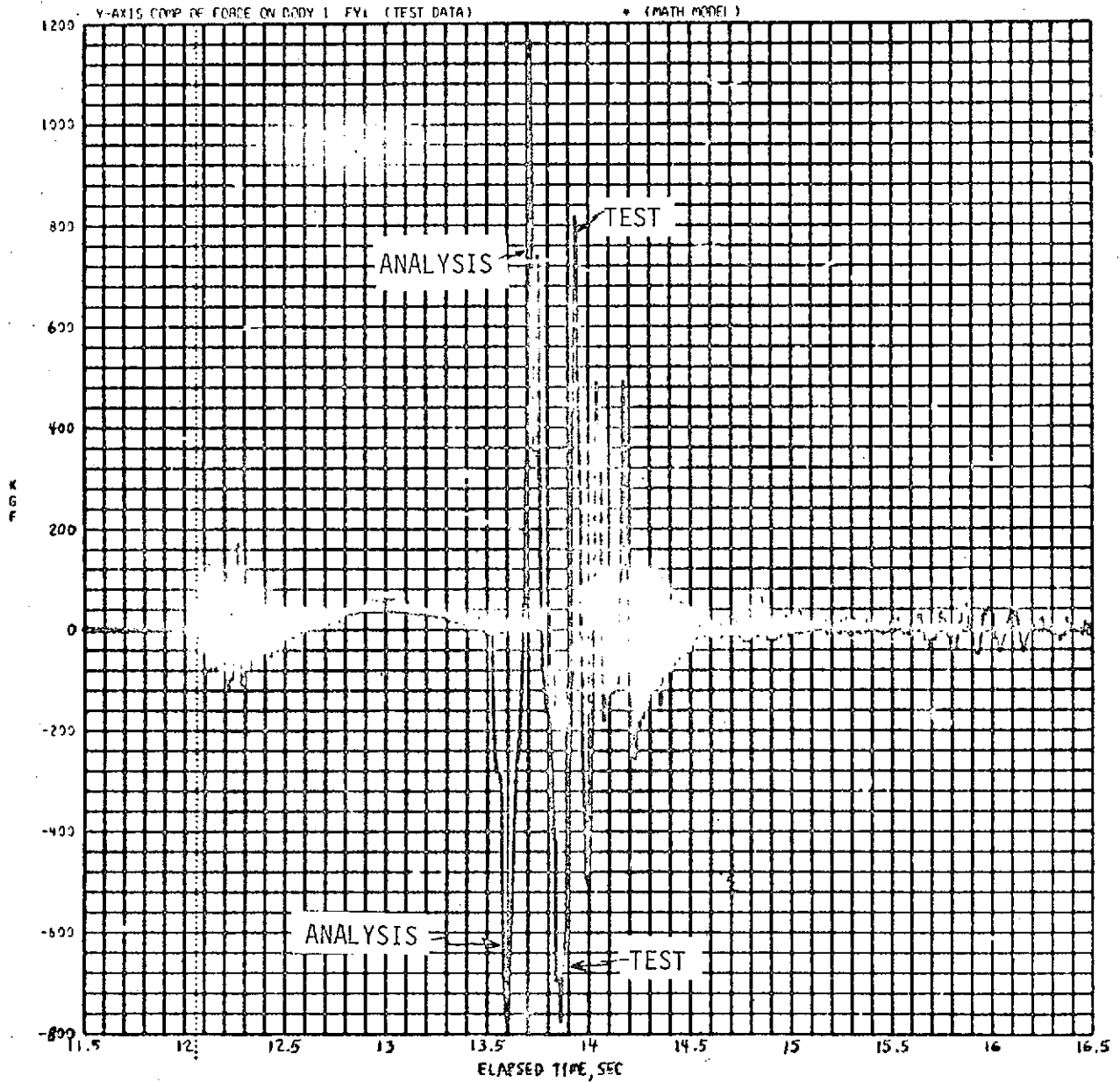


Figure 5-5. Typical Test/Analysis Correlation, US-USSR Development Test, USA Active Case 2; Y Force on CSM C.G.

US-USSR DEVELOPMENT (US ACTIVE) HOT 120731500021

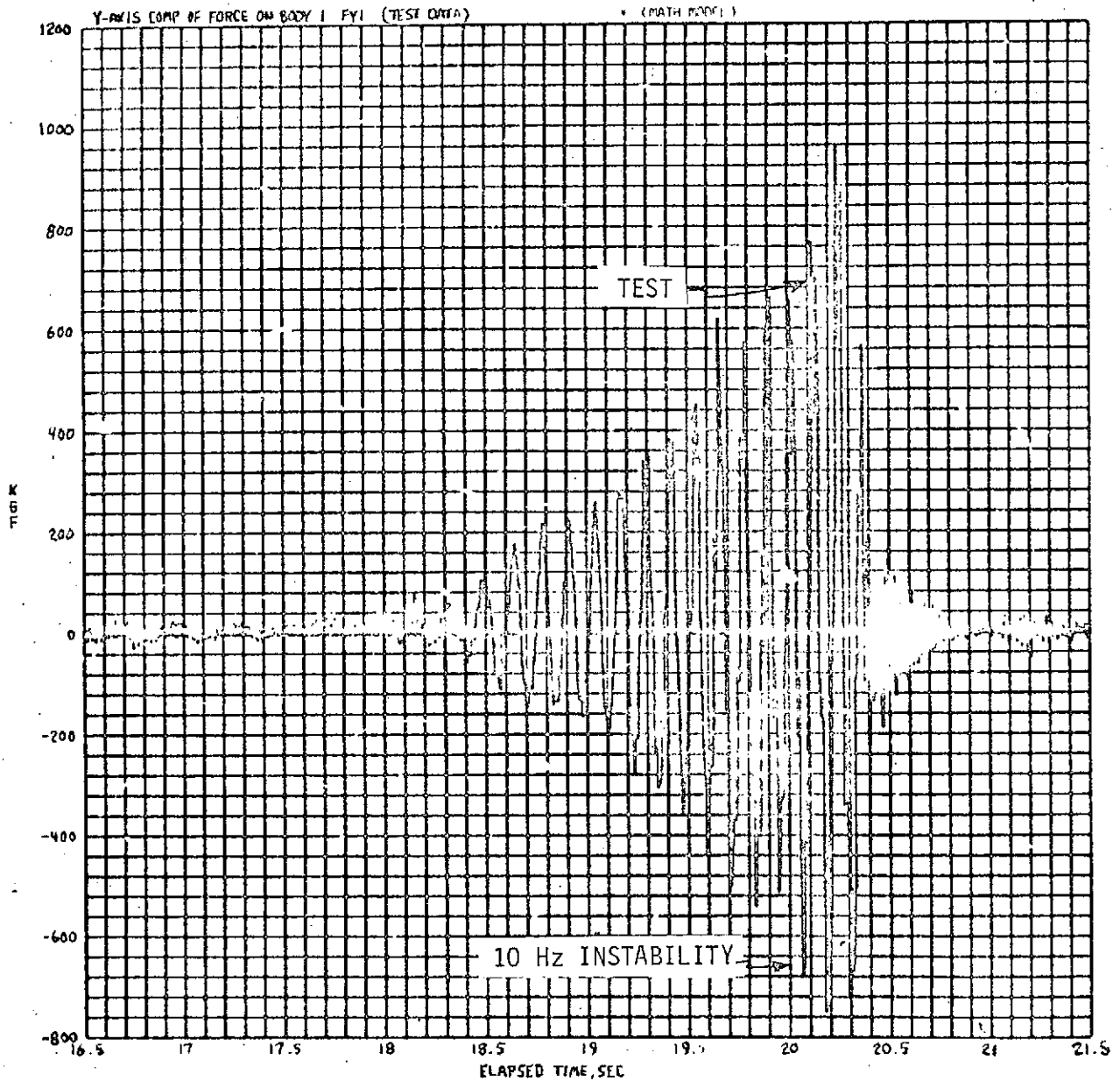


Figure 5-5. Typical Test/Analysis Correlation, US-USSR Development Test, USA Active Case 2; Y Force on CSM C.G. (continued)

12.74 2.000000  
12.74 2.000000  
12.74 2.000000

US-USSR DEVELOPMENT (US ACTIVE) HOT 120731500021

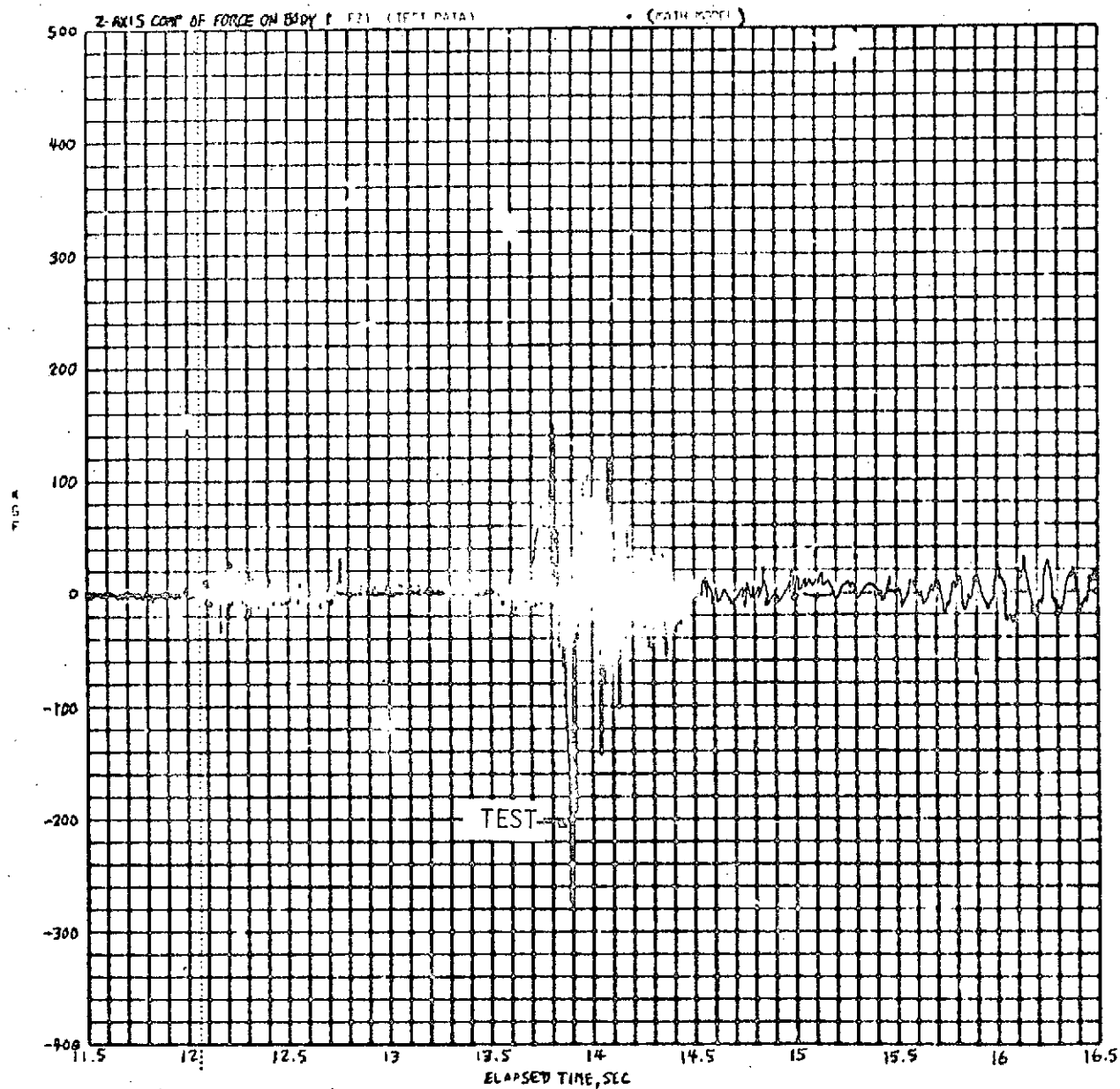


Figure 5-6. Typical Test/Analysis Correlation, US-USSR Development Test, USA Active Case 2; Z Force on CSM C.G.

REPRODUCIBILITY OF THE ORIGINAL PAGE IS POOR

US-USSR DEVELOPMENT (US ACTIVE) HOT 120731500021

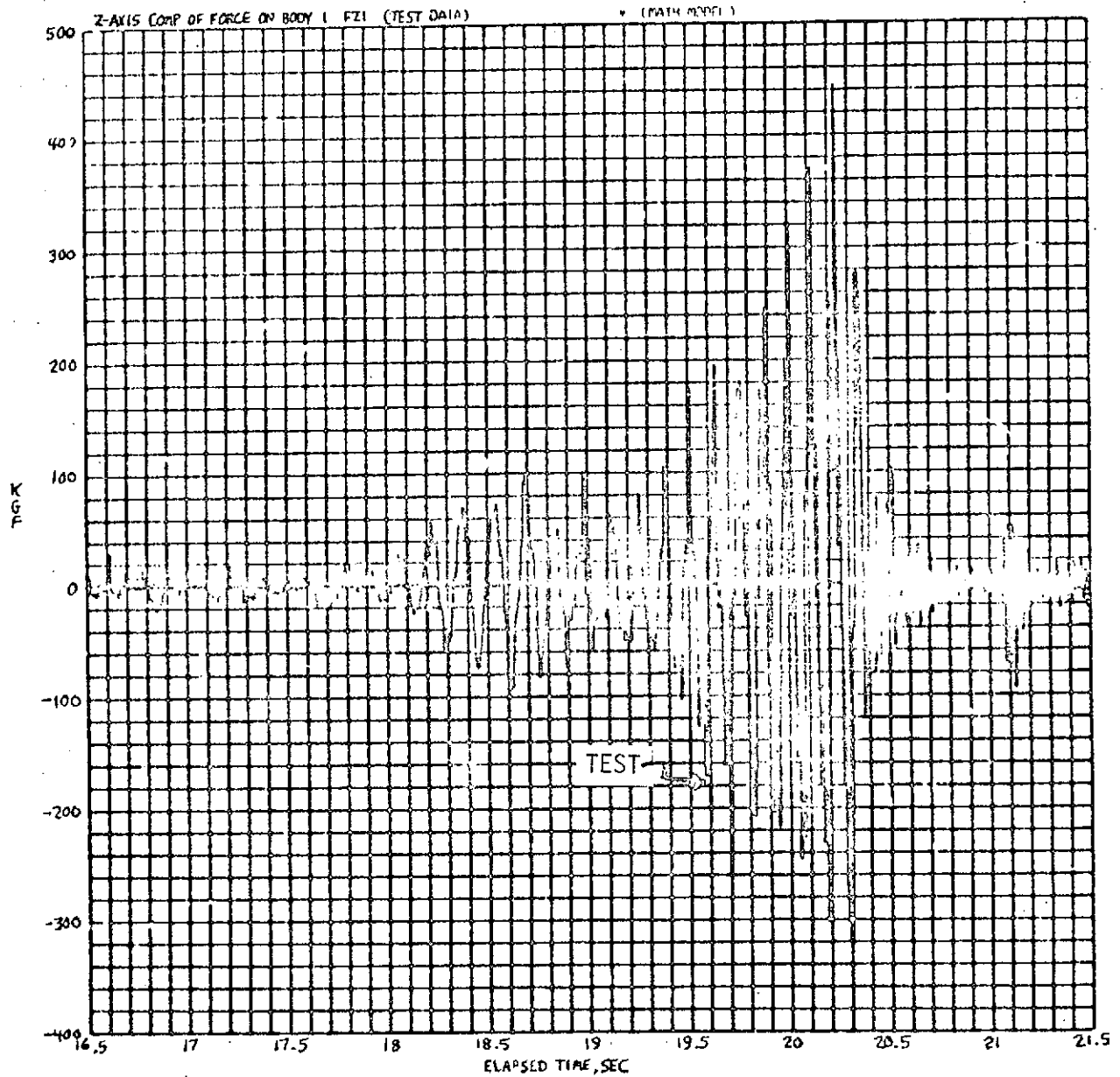


Figure 5-6. Typical Test/Analysis Correlation, US-USSR Development Test, USA Active Case 2; Z Force on CSM C.G. (continued)

TABLE 5-5

## US/USSR DEVELOPMENT TEST DATA/MATH MODEL COMPARISON

CASE	TYPE CONDITION	RUN NUMBER	TEMP. (°C)	AXIAL LOAD <sup>1</sup>		LATERAL LOAD <sup>2</sup>		CAPTURE LATCH LOAD		CAPTURE TIME	
				TEST	MODEL	TEST	MODEL	TEST <sup>3</sup>	MODEL <sup>4</sup>	TEST	MODEL
1	STRAIGHT-IN, HIGH ENERGY	102631500011 103031600011	+70. -50.	+455. +530.	+400. +590.	+49. -59.	+3. +12.	+10. +31.	+1. +13.	0.02 0.02	0.0 0.0
2	-Y MISS, HIGH ENERGY	120731500021 110231600021	+70. -50.	+1500. +800.	+1450. +930.	+500. +320.	+480. +360.	+270. +65.	+870. +336.	NO CAP. <sup>5</sup> NO CAP.	2.74 NO CAP.
4	-Y -Z MISS, HIGH ENERGY	120731500041 110231600042	+70. -50.	+1140. +730.	+820. +970.	+500. -330.	+380. -360.	+168. +250.	-356. +107.	NO CAP. NO CAP.	NO CAP. NO CAP.
9	-Y MISS, JACK- KNIFE, HIGH ENERGY	102631500091 110231600091	+70. -50.	+1030. +860.	+835. +750.	+465. +200.	+200. +175.	+193. +210.	+390. +406.	1.67 1.73	1.59 1.57
10	ROLL, HIGH ENERGY	102631500101 110231600102	+70. -50.	+624. +437.	+628. +532.	+110. -236.	+30. +0.0	+80. +216.	+1. +1.	0.57 0.62	0.59 0.60

## NOTES:

1. AXIAL LOAD =  $F_x$ .
2. LATERAL LOAD =  $F_y$  or  $F_z$  DEPENDING ON WHICH IS MAXIMUM.
3. LATCH LOAD = LATCH NO. 1, 2, or 3 DEPENDING ON WHICH IS MAXIMUM SUM OF TWO HOOKS.
4. MATH MODEL LATCH LOADS ARE CONSERVATIVE.
5. RUN NUMBER 120731500021 INDICATED CAPTURE AT 4.77 SAC BUT LATCH NO. 1 DID NOT LOAD UP.

REPRODUCIBILITY OF THE  
ORIGINAL PAGE IS POOR



### 5.1.2 (Continued)

raised concerning the validity of the peak docking loads; especially during testing with the USSR system in the active mode since lateral motion can change the axial stiffness properties of their docking hardware. Unstable oscillations, in the Y axis, at 10 Hz appeared in some of the docking cases following capture. This instability did occur, however, after peak loads were obtained; and it is believed that the value of the peak load was not affected.

Both the general low level 10 Hz oscillation and the 10 Hz instability following capture were attributed to the dynamic response of the DDTS since the hydraulic actuators possess a bending frequency in the range of 10-14 Hz. However, it is believed that the 10 Hz oscillations, although undesirable, did not prevent an adequate evaluation of joint docking loads and capture performance.

The next section discusses a study performed in order to evaluate methods of eliminating this 10 Hz oscillation.

## 5.2 10 HZ INVESTIGATION

An experimental parameter study was performed in an effort to eliminate the 10 Hz oscillations and the 10 Hz instability, and thus evaluate the effects of the oscillations on measured peak loads and capture performance.

The rate command term in the simulation was chosen as the most likely quantity to suspect as being potentially responsible because (a) a portion of the rate command signal is summed with a position signal to make up each actuator motion command; (b) if the hydraulic actuator bending dynamics were causing the problem, the rate command could be "feeding" the oscillations; and (c) it was evident that large rate command oscillations occurred when the 10 Hz dynamics were noticeable. The following variations to the rate command signal were investigated:

## 5.2 (Continued)

- a. Rate command gain variation
- b. First order lag filter on rate command signal
  - (1) With a 1 Hz corner frequency (filter A)
  - (2) With a 5 Hz corner frequency (filter B)
- c. Notch filter on rate command signal (filter C)

Rate command gain variations were performed using the joint development hardware with the USSR as the active system. Case 1 (straight-in, high energy) and Case 10 (roll, high energy) initial conditions were used. Case 1 was chosen because peak axial experimental loads were higher than expected. Case 10 was chosen because of a 10 Hz instability in the Y axis after peak load had occurred.

The results of these studies using Case 1 initial conditions show:

- a. As the rate command gain is decreased from nominal, the load increases. The 10 Hz oscillation is eliminated; however, a 2 Hz limit cycle load oscillation occurs immediately after peak load.
- b. When the rate command gain is doubled, identical load traces are obtained during peak loading. The 10 Hz oscillation in axial load is not altered during peak loading; however, the oscillation damps out sooner.

The results of the parameter studies using Case 10 initial contact conditions show that:

- a. Eliminating the rate command increased the load and removed the 10 Hz oscillations; however, a 2 Hz instability occurred approximately 20 seconds after contact.

## 5.2 (Continued)

- b. Reducing the rate command gain to one-half the nominal value also increased the load slightly but eliminated the instability that had existed previously.
- c. Doubling the rate command caused severe divergence following a slightly smaller peak load.

The results of varying the rate command gain can be generalized as shown in Figure 5-7. The conclusion concerning the rate command gain is that

- a. Rate command is required for structural dynamics because without it, loads are too high.
- b. The rate command gain required to yield proper loads encourages simulator instability.

First order lag filters described in Paragraph 3.2.4 were then installed in the rate command line in an attempt to attenuate the 10 Hz oscillations. Rate command gain was then varied with the first order lag filter having a 1 Hz corner frequency (filter A) and again with a 5 Hz corner frequency (filter B). US/US development hardware was used for this study. The following test cases were studied:

- a. Straight-in - high energy
- b. Roll miss - high energy
- c. -Y miss - low energy
- d. -Y miss - nominal energy

Using filter A, the first two cases performed well with double rate command gain; there were no 10 Hz oscillations and no significant change in the value of peak load from previously tested cases without the filter. A value of triple the nominal rate command gain was required in order to obtain these results for the third case above. The fourth case exhibited severe 5 Hz oscillations in the lateral Y direction with amplification in

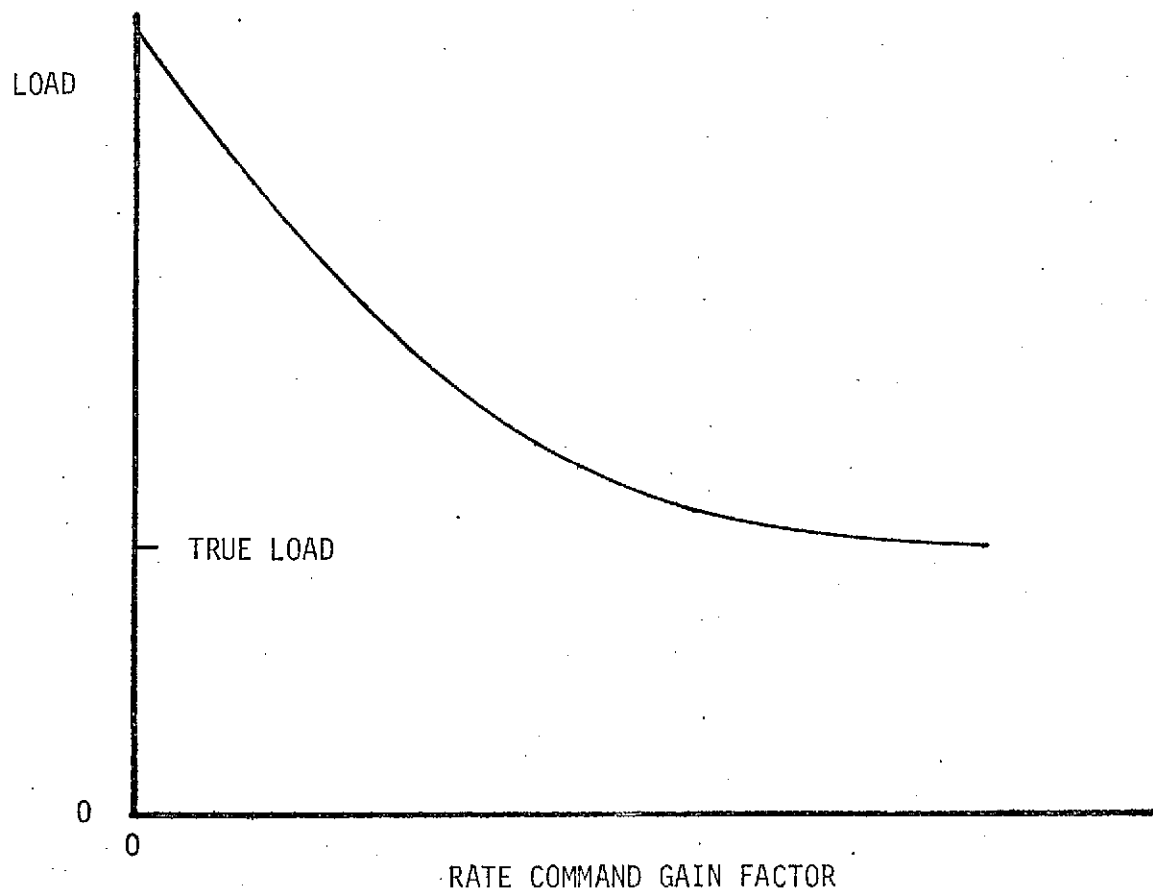


Figure 5-7. Effect of Rate Command Gain on Load

## 5.2 (Continued)

the magnitude of the lateral load. The use of filter B was not as acceptable as filter A.

The conclusion at the end of this study was that the use of a filter was a step in the right direction since it appeared to be the solution to the problem for some cases. However, US/US development case -Y miss, nominal energy was unstable for any value of the rate command gain when either of the aforementioned filters was in the line. Since the frequency of the docking dynamics was higher (5 Hz) in this case than in other cases, the lag filter was not providing the gain required. A filter which would provide sufficient gain throughout the docking structure natural frequencies yet provide attenuation at the 10 Hz frequency associated with the actuators was required.

A notch filter (filter C) was designed and installed on the rate command line of each actuator. An experimental parameter study was conducted on the rate command gain using the notch filter and the US/US development hardware. The following cases were investigated:

- a. Straight-in - high energy
- b. Roll miss - high energy
- c. -Y miss - nominal energy

All three cases were successfully tested using the notch filter. The first two cases represent the cases that had been a problem during development testing. The third case was the case that could not be successfully completed with the lag filters.

The effect of the value of rate command gain on the axial load for these three cases is shown in Figures 5-8, 5-9, and 5-10. In all these cases, the 10 Hz oscillation was eliminated and no simulator instability existed.

REPRODUCIBILITY OF THE ORIGINAL PAGE IS POOR

CASE 16 (US/US), ROLL MISS, HIGH ENERGY

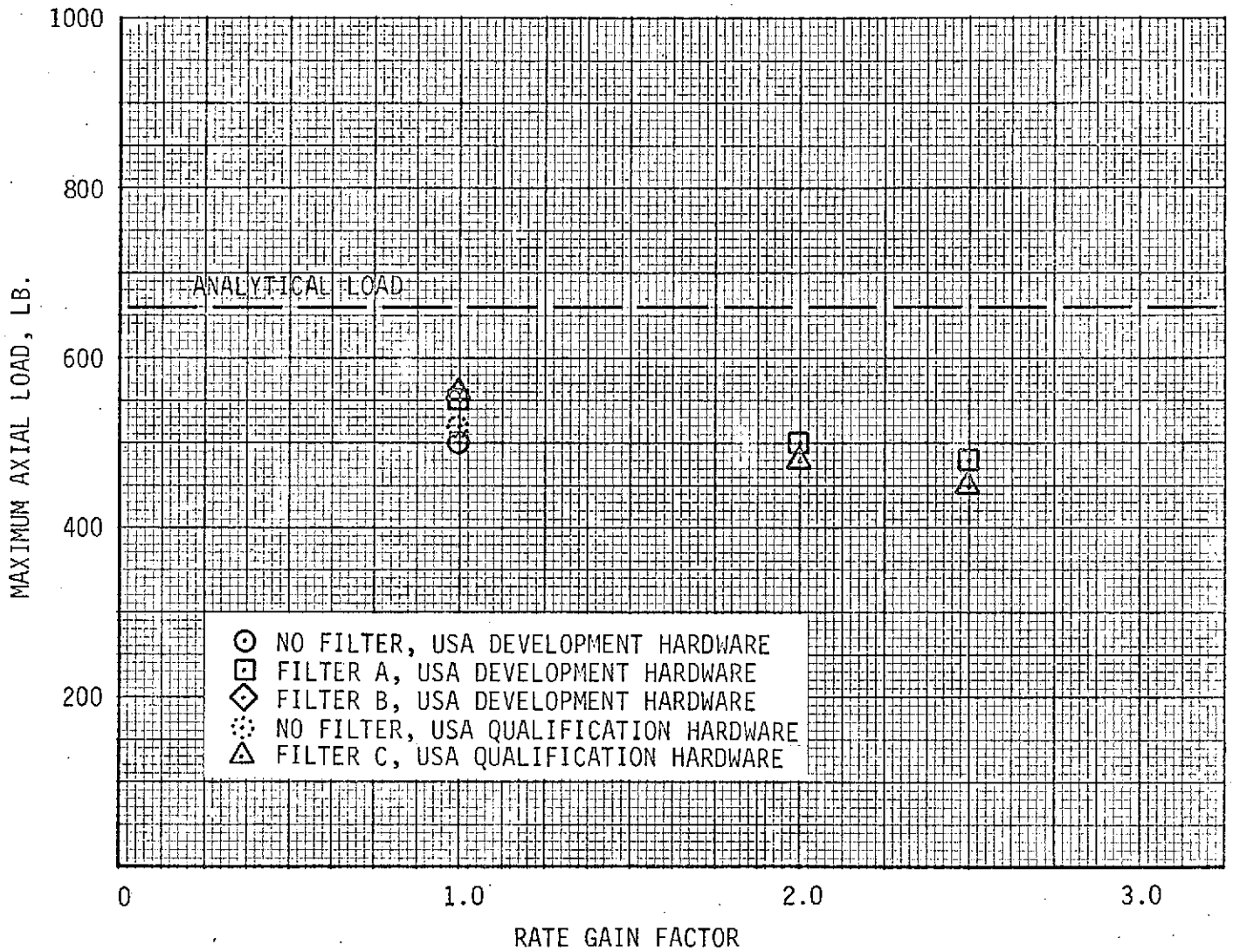


Figure 5-8. Effect of Rate Gain on Peak Load, Case 16

CASE 3 (US/US), STRAIGHT-IN, HIGH ENERGY

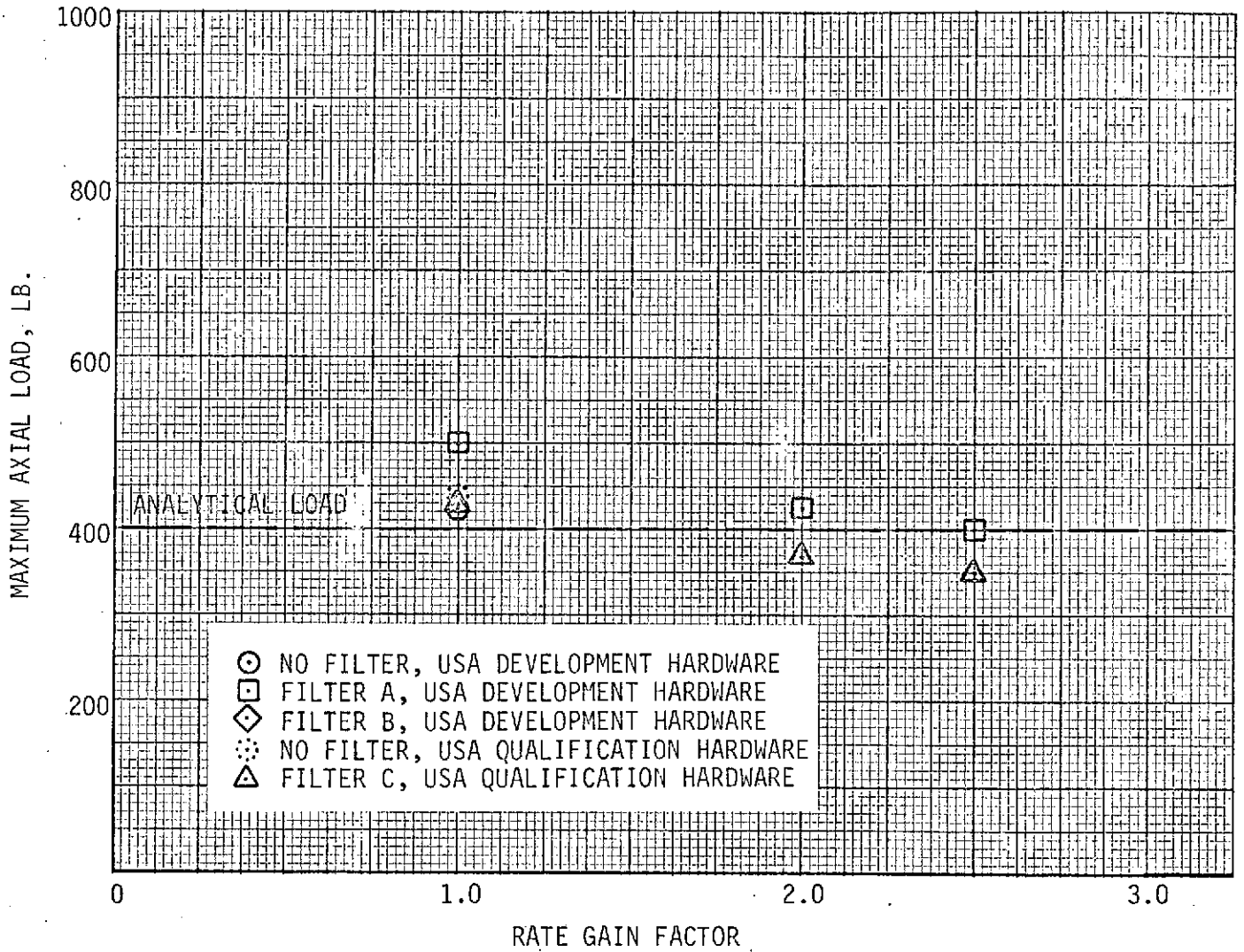


Figure 5-9. Effect of Rate Gain on Peak Load, Case 3

CASE 5, (US/US), -Y MISS, NOMINAL ENERGY

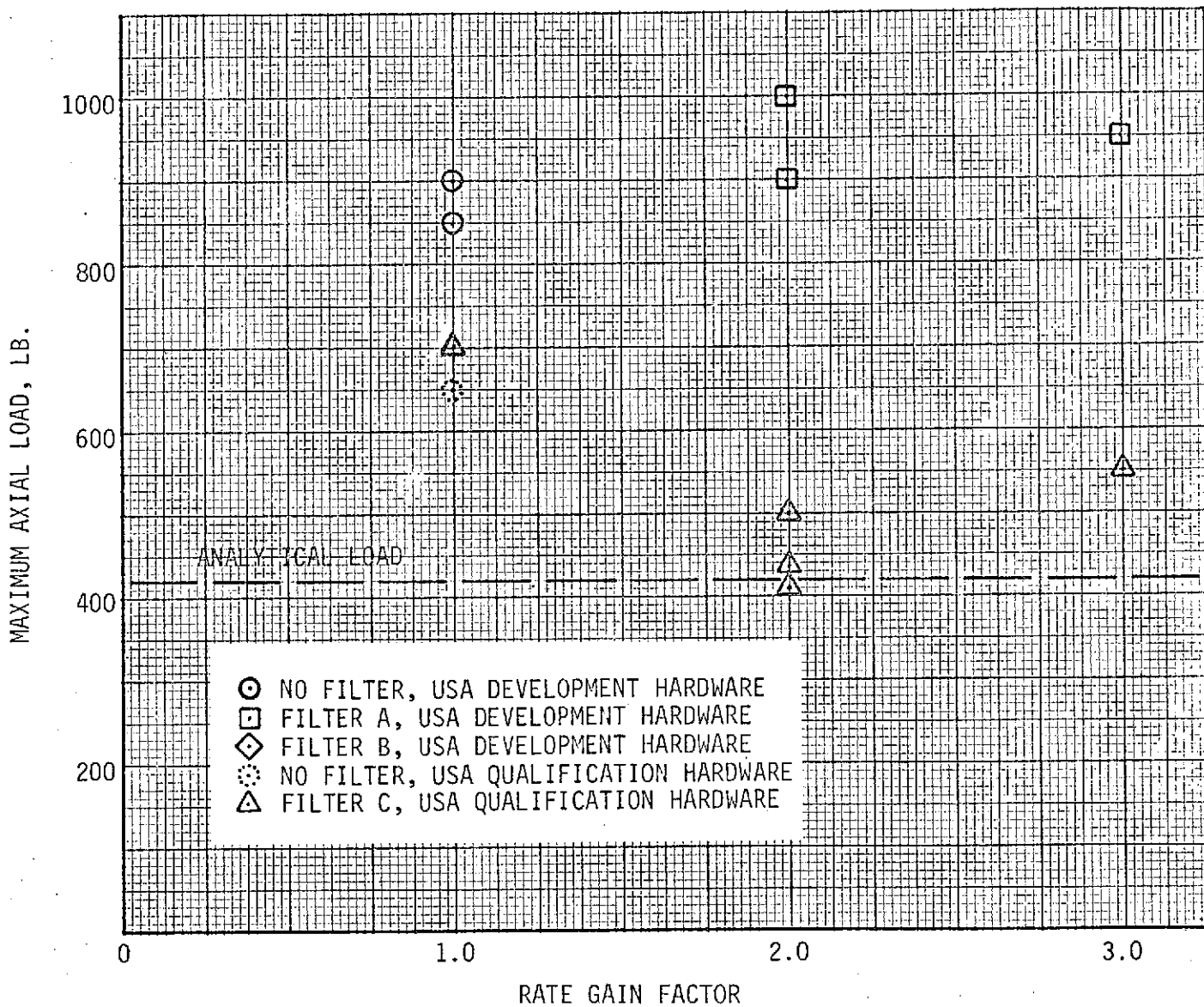


Figure 5-10. Effect of Rate Gain on Peak Load, Case 5



## 5.2 (Continued)

Figures 5-11 and 5-12 show typical load traces without and with the filter, respectively. This particular case happens to be the roll miss, high energy case. Twice the nominal rate command gain is used with the notch filter in Figure 5-12. Note the absence of the 10 Hz oscillations when the filter is used.

Based upon the results of this study, it was recommended that the qualification test program be conducted with a 9.5 Hz notch filter (filter C) in the rate command line. The value of the rate command gain was recommended as twice the nominal value previously used in the development test program.

## 5.3 US/US QUALIFICATION TEST

The US/US qualification tests were conducted using the notch filter with twice the nominal rate command gain. [Following the US/US qualification tests, a check case was run without the filter to verify the validity of the notch filter. These results are shown in Figures 5-13 (a) and (b). Identical load results were obtained with and without the filter; however, instability resulted immediately after peak load when no filter was used.] Table 5-6 shows the cases tested. The raw test data and correlation plots of all test cases were published in the NASA test agency report for the US/US qualification test program. A summary of peak loads is shown in Table 5-7.

In general, the correlation between test data and pretest analytical results was not as good as for the development tests. In most cases, the analytical load results were higher than test results. After a thorough assessment of the data available, the major difference between test and analysis appears to be due to a slight difference in the phasing of attenuator maximum loads. The analytical data show the peak loads phasing together while the test results have the attenuators slightly out of phase; hence, producing lower loads. The feeling at the present time is that the discrepancy between test

REPRODUCIBILITY OF THE ORIGINAL PAGE IS GOOD

US-US DEVELOPMENT TEST (10 M7) 032741100161

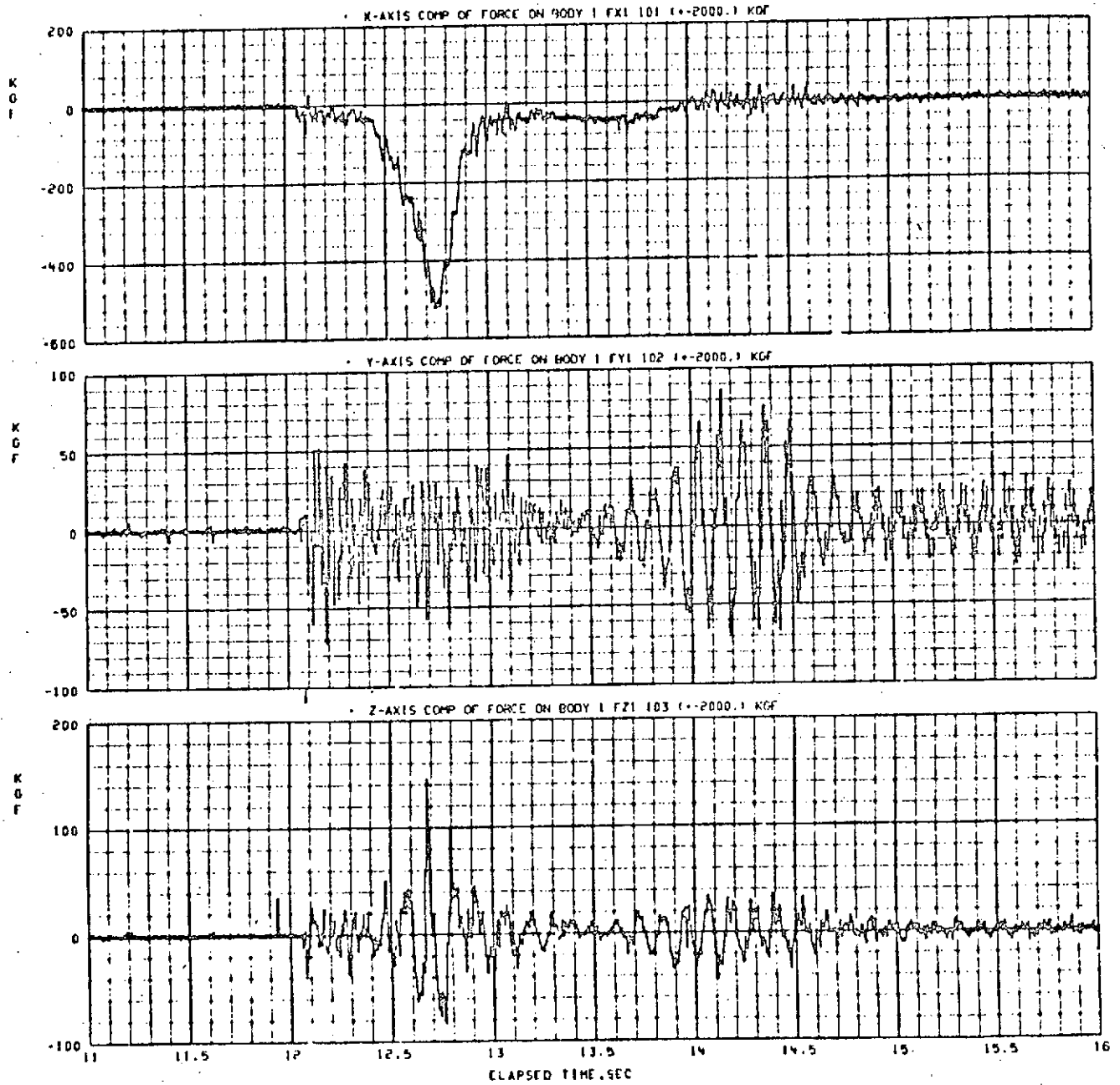


Figure 5-11. Typical Test Results Without Rate Command Filter

REPRODUCIBILITY OF THE ORIGINAL PAGE IS POOR

US-US DEVELOPMENT TEST (10 HZ) 032741100162

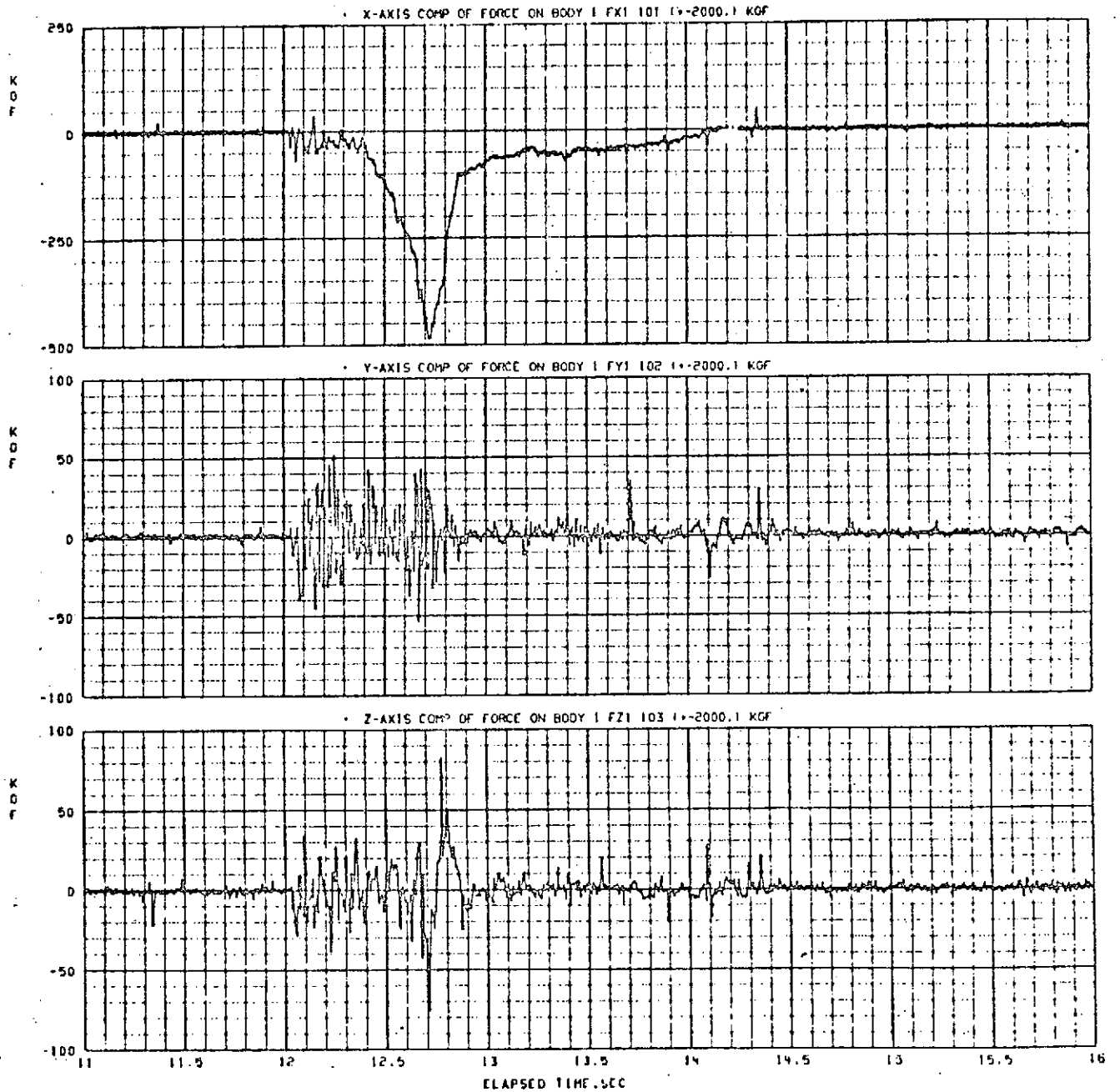


Figure 5-12. Typical Test Results with Notch Filter in Rate Command Line

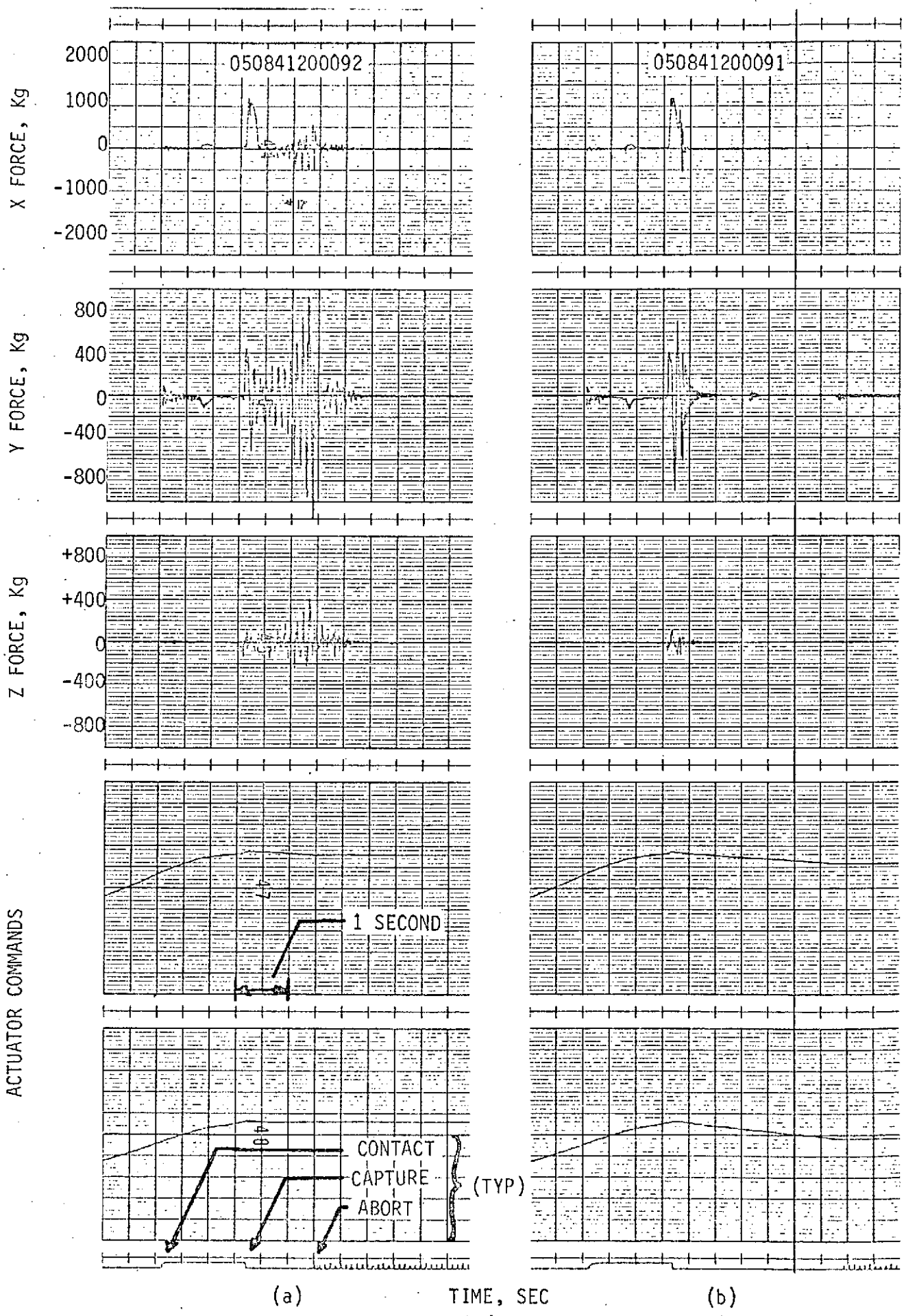


Figure 5-13. US-US Qual Case 9 (-Y Miss, High Energy) Without Rate Command Filter (a) and With Notch Filter (b)

REPRODUCIBILITY OF THE ORIGINAL PAGE IS POOR

TABLE 5-6 US/US QUALIFICATION TEST CONDITIONS

CASE	CLOSING VELOCITY			LATERAL VELOCITY			MISS DISTANCE		ANGULAR RATE			ANGULAR ATTITUDE			TEMPERATURE	REMARKS
	X (mps)	Y (mps)	Z (mps)	Ym (m)	Zm (m)	Roll (deg/sec)	Pitch (deg/sec)	Yaw (deg/sec)	Roll (deg)	Pitch (deg)	Yaw (deg)					
1	0.3	0.0	0.0	0.0	0.0	0.0	0.0	0.0	0.0	0.0	0.0	0.0	0.0	0.0	ambient, hot	Straight-in high energy
2	0.3	-0.1	0.0	-0.3	0.0	0.0	-1.0	0.0	0.0	0.0	-7.0	0.0	0.0	0.0	ambient, hot	-Y miss high energy
3	0.3	-0.1	0.0	-0.212	-0.212	-1.0	-1.0	0.0	0.0	0.0	-7.0	0.0	0.0	0.0	ambient, hot	-Y; -Z miss high energy
4	0.3	-0.1	0.0	-0.3	0.0	0.0	-1.0	0.0	0.0	0.0	7.0	0.0	0.0	0.0	ambient, hot	-Y miss Jack knife, high energy
5	0.05	0.0	0.0	0.0	0.0	0.0	0.0	0.0	0.0	0.0	0.0	0.0	0.0	0.0	cold	Straight-in low energy
6	0.05	-0.05	0.0	-0.3	0.0	0.0	-1.0	0.0	0.0	0.0	-3.0	0.0	0.0	0.0	cold	-Y miss low energy
7	0.05	-0.05	0.0	-0.212	-0.212	-1.0	-1.0	0.0	0.0	0.0	-3.0	0.0	0.0	0.0	cold	-Y; -Z miss low energy
8	.11	.02	0.0	.03	0.0	.02	.04	.07	-.9	.9	-1.5				ambient	Mean condition
9	0.3	-0.067	0.0	-0.3	0.0	0.0	-0.67	0.0	0.0	0.0	-5.0	0.0	0.0	0.0	ambient, hot	-Y miss high energy
10	0.3	+0.067	+0.067	+0.212	+0.212	0.0	+0.67	-0.67	0.0	+3.54	-3.54				ambient, hot	+Y; +Z miss high energy

- The spacecraft with the active and passive docking systems are designated as body 1 and body 2, respectively.
- Spacecraft control system operations are defined in IED50016.
- Closing and Lateral Velocities (X, Y, Z)  
Translational velocity components (expressed in the body 2 system) of the body 1 c.g. with respect to the body 2 c.g.
- Miss Distance (Ym, Zm)  
Coordinates (expressed in the body 2 system) of the point defined by the intersection of the X<sub>1</sub> axis and the plane passing through the forwardmost part of the body 1 docking system guides.
- Angular Rates (Roll, Pitch, Yaw)  
Relative rotational velocity components of body 1 relative to body 2 (expressed in the body 1 system) using the right-hand rule for direction of rotations about the X<sub>1</sub>, Z<sub>1</sub>, and Y<sub>1</sub> axes, respectively.
- Angular Attitude (Roll, Pitch, Yaw)  
Roll attitude is the included angle (measured in the Y-Z plane of the body 2 system) from the X-Y plane of body 2 to the X-Y plane of body 1, using the right-hand rule for direction of rotation about the X<sub>2</sub> axis. Pitch and yaw attitudes are the components of the included angle (expressed in the body 2 system) from the body 2 X-axis to the body 1 X-axis, using the right-hand rule for pitch attitude about the Z<sub>2</sub> axis and yaw attitude about the Y<sub>2</sub> axis.

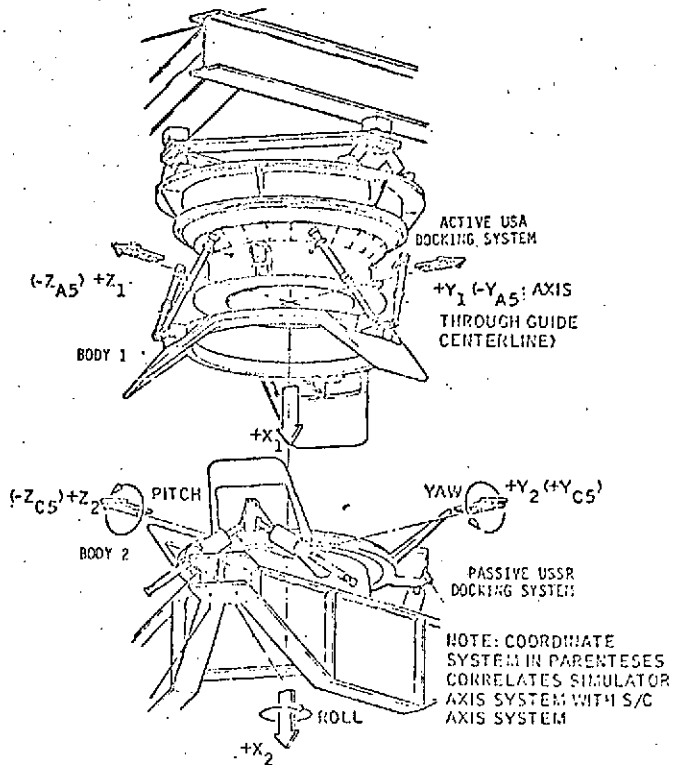


TABLE 5-7  
US/US QUALIFICATION TEST DATA MATH MODEL COMPARISON

CASE	TYPE CONDITION	TEMP (°C)	AXIAL LOAD		LATERAL LOAD		ATTENUATOR LOAD		LATCH LOAD		CAPTURE TIME	
			TEST	MODEL	TEST	MODEL	TEST	MODEL	TEST	MODEL	TEST	MODEL
1	STRAIGHT-IN HIGH ENERGY	+21	360.	400.	± 50.	3.0	100.	91.5	30.	1	.03	0.0
		+70	355.	400.	± 47.	3.0	90.	91.5	40.	1	.021	0.0
2	-Y MISS	+21	1500.(A)	1400.	750.(A)	+480 -750	880.(A)	870.	12.	766	NO CAP.	NO CAP.
	HIGH ENERGY	+70	1600.(A)	1400.	750.(A)	+480 -750	920.(A)	870.	16.5	766	NO CAP.	NO CAP.
3	-Y -Z MISS	+21	980.	820.	±500.	+380 -689	685.	680.	345.	596	NO CAP.	NO CAP.
	HIGH ENERGY	+70	1200.(A)	820.	1400.(A)	+380 -689	1562.(A)	680.	1440.(A)	596	NO CAP.	NO CAP.
9	-Y MISS MODIFIED	+21	1200.	1770.	±780.	+775 -330	615.	890.	510.	241	1.6	1.57
	HIGH ENERGY	+70	1200.	1770.	-900.	+775 -330	650.	890.	40.	241	NO CAP.	1.57
10	+Y +Z MISS	+21	1000.	1710.	±320.	+310 -160	630.	1100.	384.	168	3.96	3.97
	HIGH ENERGY	+70	1050.	1710.	±280.	+310 -160	760.	1100.	143.	168	NO CAP.	3.97

NOTES: 1. LOADS ARE IN KILOGRAMS. TIME IS IN SECONDS.  
2. LOADS FOLLOWED BY (A) ARE RESULTS OF ABORTS.

## 5.3 (Continued)

and analysis is mainly due to inadequacies in math model attenuator data. Attenuator parameters that could possibly be refined are attenuator preload, attenuator friction characteristics, and stroke versus area data.

## 6.0 CONCLUSIONS AND RECOMMENDATIONS

The DDTS provides an accurate simulation of the dynamics and loads which occur during docking. In particular, the following conclusions can be made concerning DDTS performance:

- a. Initial contact conditions are accurately obtained.
- b. Docking hardware capture performance is in good agreement with analytical results.
- c. Peak loads are in good agreement with analytical predictions.
- d. Load and motion time-histories are in good agreement with analytical predictions.

Although simulator performance is adequate for the simulation of docking dynamics, it is recommended that further study be conducted to understand the cause of higher than predicted dynamics during the table frequency response tests. This knowledge is desirable so that the feasibility of utilizing the DDTS to perform other dynamic motion simulations and dynamic tests can be assessed.